Spring 2001

Ground movement associated with microtunneling

Zhenyang Duan

INFORMATION TO USERS

This manuscript has been reproduced from the microfilm master. UMI films the text directly from the original or copy submitted. Thus, some thesis and dissertation copies are in typewriter face, while others may be from any type of computer printer.

The quality of this reproduction is dependent upon the quality of the copy submitted. Broken or indistinct print, colored or poor quality illustrations and photographs, print bleedthrough, substandard margins, and improper alignment can adversely affect reproduction.

In the unlikely event that the author did not send UMI a complete manuscript and there are missing pages, these will be noted. Also, if unauthorized copyright material had to be removed, a note will indicate the deletion.

Oversize materials (e.g., maps, drawings, charts) are reproduced by sectioning the original, beginning at the upper left-hand corner and continuing from left to right in equal sections with small overlaps.

Photographs included in the original manuscript have been reproduced xerographically in this copy. Higher quality 6" x 9" black and white photographic prints are available for any photographs or illustrations appearing in this copy for an additional charge. Contact UMI directly to order.

Bell & Howell Information and Learning
300 North Zeeb Road, Ann Arbor, MI 48106-1346 USA
800-521-0600

NOTE TO USERS

This reproduction is the best copy available.

UMI

GROUND MOVEMENT ASSOCIATED WITH MICROTUNNELING

by

Zhenyang Duan, M.S.

A Dissertation Presented in Partial Fulfillment
of the Requirement for the Degree of
Doctor of Philosophy

COLLEGE OF ENGINEERING AND SCIENCE
LOUISIANA TECH UNIVERSITY

MAY 2001

Bell & Howell Information and Learning Company
300 North Zeeb Road
P.O. Box 1346
Ann Arbor, MI 48106-1346

LOUISIANA TECH UNIVERSITY

THE GRADUATE SCHOOL

May, 17 , 2001
Date

We hereby recommend that the dissertation prepared under our supervision by Zhenyang Duan entitled Ground Movement Associated with Microtunneling be accepted in partial fulfillment of the requirements for the Degree of Doctor of Philosophy in Engineering

Supervisor of Thesis Research

Head of Department

Department

Recommendation concurred in:

Advisory Committee

Approved:

Director of Graduate Studies

Dean of the College

Approved:

Dean of the Graduate School

GS Form 13
(1/00)

ABSTRACT

Microtunneling is a trenchless technology for construction of pipelines. Its process is a cyclic pipe jacking operation. Microtunneling has been typically used for gravity sewer systems in urban areas. Despite its good success record overall, several large ground settlement cases caused by microtunneling have been reported. Also, in contrast with large diameter urban tunneling, there are few research projects about the ground settlement caused by microtunneling.

In this dissertation, the ground settlement caused by microtunneling is studied using a theoretical approach, empirical approach, numerical simulation approach, and artificial intelligence approach.

In the theoretical approach, the equivalent ground loss and settlement caused by concentrated ground loss have been used to drive the ground settlement profile. In the empirical approach, the ground settlement caused by large diameter tunneling case histories is used. In the numerical approach, FLAC^{3D} software, a commercially available finite difference code, is used to simulate the ground settlement caused by microtunneling. In the artificial intelligence approach, a three-layer back propagation neural network is developed to predict the ground settlement caused by microtunneling using the numerical simulation results.

It is found that the neural network developed as part of this thesis work provides a means of rapid prediction of the surface ground settlement curve based on the soil

parameters, project geometry and estimated ground loss. This prediction matches FLAC^{3D} results very well over the full range of parameters studied and has a reasonable correspondence to the field results with which it was compared.

APPROVAL FOR SCHOLARLY DISSEMINATION

The author grants to the Prescott Memorial Library of Louisiana Tech University the right to reproduce, by appropriate methods, upon request, any or all portions of this Thesis. It is understood that "proper request" consists of the agreement, on the part of the requesting party, that said reproduction is for his personal use and that subsequent reproduction will not occur without written approval of the author of this Thesis. Further, any portions of the Thesis used in books, papers, and other works must be appropriately referenced to this Thesis.

Finally, the author of this Thesis reserves the right to publish freely, in the literature, at any time, any or all portions of this Thesis.

Author 

Date 5/11/2001

GS Form 14
2/97

DEDICATION

To my wonderful wife Qiaoyu

TABLE OF CONTENTS

LIST OF TABLES

LIST OF FIGURES

ACKNOWLEDGMENTS

I would like to express my sincere appreciation to all those individuals who provided me with guidance and assistance in the preparation of this thesis. Heartfelt thanks are extended to Dr. Raymond Sterling for serving as the major advisor on this thesis. His guidance and assistance in the advice, time, and support will forever be remembered and appreciated. I would also like to thank Dr. Robert McKim, Dr. Paul Hadala, Dr. David Hall, and Dr. William Jordan for serving as advisory committee members of this thesis. Their willingness to assist in reviewing this thesis is sincerely appreciated. Further acknowledgment is extended to Dr. Mckim and Dr. Hadala for their additional advice and assistance in my research work.

I would like to thank College of Engineering and Science of Louisiana Tech University and Trenchless Technology Center for providing financial support throughout my research.

Finally, special thanks go to my wife, Qiaoyu Lu, whose love, understanding, and support encouraged me to complete this thesis.

CHAPTER 1

INTRODUCTION

1.1 General Description of Microtuneling

Microtunneling is a trenchless technology for construction of pipelines to close tolerances for line and grade. Microtunneling installations are typically for gravity sewers, although other specialized projects have been constructed using this method. The method was developed in the 1970s in Japan, refined in Germany and the United Kingdom, and made its debut in the United States in 1984 [Bennett 1995].

No universally accepted definition of microtunneling exists, but it can be described as a remotely controlled, guided pipe-jacking that provides continuous support to the excavation face. The guidance system usually consists of a laser mounted in the jacking pit as a reference with a target mounted inside the microtunneling machine's articulated steering head.

The microtunneling process is a cyclic pipe jacking operation. The microtunneling machine is pushed into the earth by means of hydraulic jacks carefully mounted and aligned in the jacking shaft. As the jacks are fully extended, the machine is pushed out of the pit, and the jacks are then retracted. A product pipe or casing is then inserted between the jacking ring and the microtunneling machine or previously jacked pipe, necessary connections are made, and the pipe and machine are advanced another

drive stroke. This cycle is repeated until the completion point (a reception shaft) is reached.

There are two primary types of microtunneling system - auger and slurry - defined by the method of spoil removal. These operation systems differ in their degree of control of ground conditions at the face. The slurry system is generally capable of a more precise control. The slurry system can handle higher groundwater and unstable ground conditions, but there is the disadvantage of added mechanical complexity and cost. In addition, production rates may be slightly lower for slurry machines. Auger machines have limitations on the length and diameter of installed pipelines due to the power requirements for turning the auger and head. Both auger and slurry systems consists of five independent subsystems: (1) Mechanized excavation system; (2) Propulsion or jacking system; (3) Spoil removal system; (4) Guidance and control system; and (5) Pipe lubrication system. Figure 1.1 shows a typical microtunneling system.

1.2 Ground Settlement Associated with Microtunneling

The ground movement associated with microtunneling is mainly a result of loss of ground during tunneling and consolidating compressible soils due to dewatering. During microtunneling, loss of ground may be associated with soil squeezing, running, or flowing into the heading; losses due to the size of overexcavation; and losses due to steering adjustments. The actual magnitude of these losses is largely dependent on the type and strength of the ground, groundwater conditions, size and depth of the pipe, equipment capabilities, and the skill of the contractor in operating and steering the machine. Sophisticated microtunneling equipment that has the capability to exert a

stabilizing pressure at the tunnel face, equal to that of the in-situ soil and groundwater pressures, will minimize loss of ground and surface settlement without the need of dewatering.

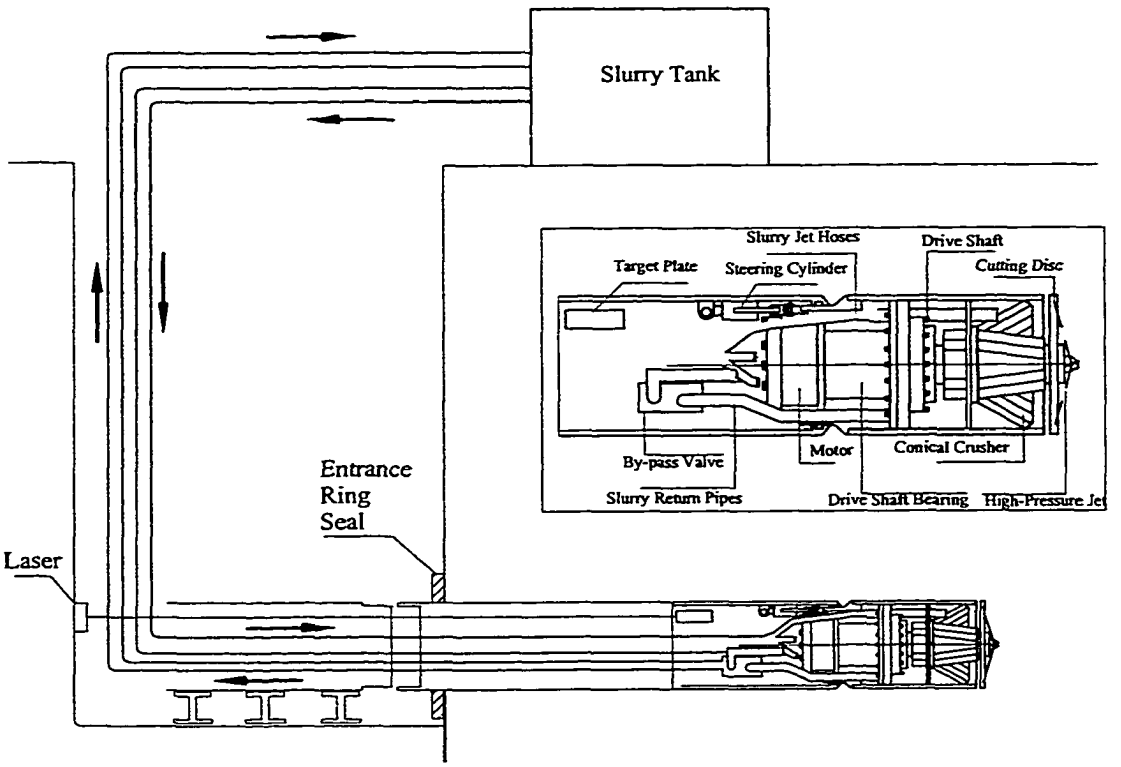

Figure 1.1 Microtunneling System

During microtunneling through soft water-bearing ground, the excavation face becomes unstable when the soil lacks sufficient cohesion. A temporary support is required to maintain ground stability in the working area, and a slurry microtunneling system is widely used to provide this support. In a slurry shield, the temporary support is provided by a pressurized mixture of bentonite clay and water. Because of the high viscosity of the slurry, the risk of an uncontrolled escape of fluid by leakage is generally reduced. As the slurry is only slightly heavier than water, the excess fluid pressure in the invert is small. The risk of an upheaval of ground, therefore, is eliminated as well. In the

last decade, slurry-shield tunneling has been applied successfully worldwide on a large number of projects.

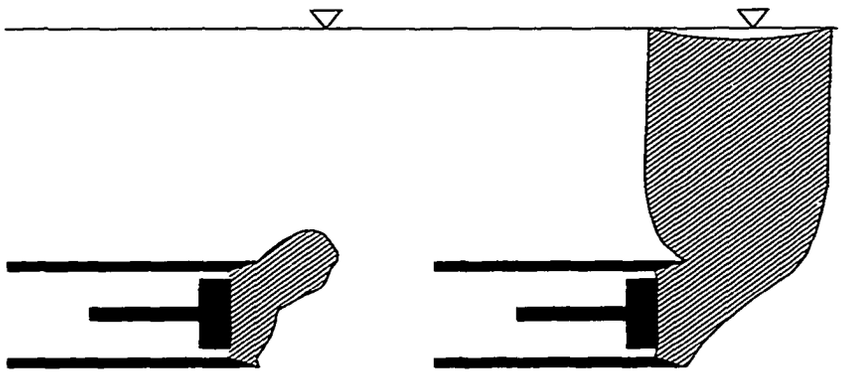

Figure 1.2 Two Typical Patterns of Failure

Figure 1.2 shows schematically two typical patterns of failure. In the first case, major soil movements are restricted to a zone close to the heading. The cave-in of the ground may form a cavity above the pipe permanently, or it may cause a collapse later. In the second case, the collapse propagates towards the surface creating a chimney, and sometimes a crater, on the ground surface. The heading failure then results in excessive subsidence and possible damage to overlying structures.

1.3 Research Need

More cost effective and less disruptive methods of installing underground utilities are key components in creating better utility systems, and they are the first step in the life cycle of a new underground utility service. Although a number of methods for installing underground utilities exist, there are several crosscutting technology improvements needed that would impact all such systems. The underground construction industry has changed radically in the past 20 years, adopting a number of advanced technology excavation and guidance systems. Microtunneling is one of such new technology. This

change in the nature of the industry (available hardware and receptivity to advanced methods) provides the path through which further radical changes in utility installation can be deployed in the industry. There are many research papers about ground settlement caused by larger diameter tunnel and underground space excavation, but few about ground settlement caused by microtunneling. Although some aspects of microtunneling are similar to large diameter tunneling, microtunneling is a significantly different technique.

CHAPTER 2

THEORETICAL APPROACH

In the past 20 years, significant advances have been made in procedures for evaluating and controlling ground movements around tunnels in soil. Ground movements are routinely measured on tunnel projects in order to pinpoint the cause of ground loss around the advancing tunnel heading and to determine the magnitude of ground movements that will develop at nearby structures. Such observations have resulted in better control of the tunneling process and have led to an improved understanding of ground behavior.

Despite improvements in tunneling and ground control procedures such as those previously noted, control of ground movements during tunneling is often difficult to achieve, particularly when variable ground conditions result in sudden changes along the length of the tunnel or across the tunnel face. Improvements are being made in tunnel shields (microtunneling machine), but a universal machine does not exist. In fact, many current machines and shields are very sensitive to variations in ground conditions. Therefore, it is important to obtain as complete a picture of the ground settlement as possible prior to selecting and installing the microtunneling machine.

2.1 Excavation Face Stability

Face stability in homogeneous ground can be assessed by considering the simple mechanism illustrated in Figure 2.1. This three-dimensional model, which was first proposed by Horn [1961], is based on the silo-theory of Janssen.

The circular cross-section of the face of microtunneling machine is approximated by a square whose sides are as long as the diameter D of the tunnel. The collapse mechanism consists of a wedge and right-angled prism that extends from the tunnel crown to the surface. The soil is idealized as a rigid-plastic material obeying the Mohr-Coulomb failure condition. Then the mobilized shearing resistance τ at each point on the slip surface is given by

$$\tau = \frac{c}{F} + \sigma \frac{\tan\phi}{F} \tag{2.1}$$

Where c is cohesion, ϕ is angle of internal friction, σ is the normal stress, and F is the factor of safety.

The wedge is acted upon by the following: (a) its own weight; (b) the resultant normal forces and shear forces along the failure surfaces ADE, BCF, and ABEF; (c) the resulting support forces of the slurry; and (d) the resultant vertical force of the prism at the interface DEFC.

Solving the limit-equilibrium equation of the wedge yields the support force for a specific collapse mechanism and for a specific inclination ω of the slip surface ABEF. The critical inclination ω_{cr} is determined by maximizing the necessary support force, i.e. for a given support force by iteratively minimizing the safety factor. All computation is carried out in terms of effective stresses, and a hydrostatic distribution of pore water pressure along the slip surfaces is assumed.

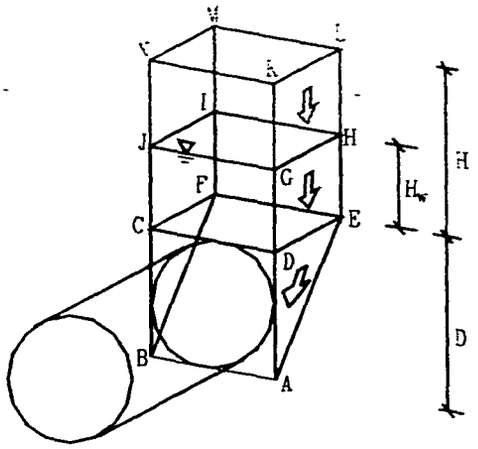

Figure 2.1 Face Stability Model

The shear stresses depend essentially on the horizontal stresses acting normal to the vertical slip surface. However, the horizontal stresses can't be computed without consideration of the deformation characteristics of the ground. Following Jassen's silo theory, a constant ratio λ of horizontal to vertical stress will be assumed here.

The vertical force at the interface CDEF is computed by applying the Janssen silo-formulae first to the prismatic body above the water table, and afterwards to the part between water table and crown. Thus, the different unit weights above and below the water table are taken into account. The mean effective vertical stress σ_v is given by:

$$\sigma_v = \frac{\gamma r - c}{\lambda \tan\phi}(1 - e^{-\lambda(\tan\phi)H_w/r}) + \frac{\gamma_d r - c}{\lambda \tan\phi}(e^{-\lambda(\tan\phi)H_w/r} - e^{-\lambda(\tan\phi)H/r}) \qquad (2.2)$$

Where H, H_w, γ_d, and γ denote the overburden, the elevation of the water table above the crown (Figure 2.1), the dry unit weight, and the submerged unit weight, respectively, The parameter r denotes the ratio of the volume to the circumference of the prism [$r=0.5D\tan\omega/(1+\tan\omega)$], where D is the diameter of the tunnel. Equation 2.2 is valid for a safety factor of F=1. Other values of F can be taken into account by replacing c and $\tan\phi$ by c/F and $\tan\phi/F$, respectively.

With regard to the σ_z, stress distribution along the slip surface ADE and BCF of the wedge, a linear approximation, is used in this report. The vertical stress σ_z increases linearly with depth due to the weight of soil, whereas the contribution of the interface stress σ_v to the vertical stress decreases. The mean frictional resistance τ_f is then obtained by integrating $\lambda\sigma_v tan\phi$ over the slip surfaces ADE and BCF:

$$\tau_\phi = \lambda(\frac{1}{3}\gamma D + \frac{2}{3}\sigma_v)\frac{\tan\phi}{F} \tag{2.3}$$

2.2 Equivalent Ground Loss

A method for the prediction of settlements at the surface has been suggested by Lo and Rowe [1982] and Rowe et al. [1983]. An important aspect of this approach is the introduction of a parameter, called the gap parameter, which takes into account the ground loss as a function of strength and deformation behavior in the elastic and plastic state, physical clearance between the excavated diameter and lining, and workmanship.

Excavation of the tunnel provides an opening into which the soil can deform, and the constraint to soil movements is primarily a function of the machine characteristics, workmanship, lining geometry, and lining flexibility. The movement of the soil into the opening can be related to the concept of "loss of ground," which is defined as volume of material (whether through the face or radial encroachment over and around or behind the shield) that has been excavated in excess of the theoretical design volume of excavation. Field studies [Peck, 1969] have highlighted the 3D nature of the problem and the effect of 3D-ground loss on the subsequent surface deformations. Based on field case histories, the loss of ground can be considered to occur in three stages as the tunnel advances in the soil mass: (1) ahead of the face; (2) over the shield; (3) tail void. It is further considered

that additional loss of ground may result from creep-consolidation, and/or long-term change in hydraulic conditions.

Three-dimensional finite element analysis, such as that described by Lee and Rowe [1990a, 1990b] can be used to predict the spatial 3D ground-displacement within the soil mass. However, because of the processing time associated with this analysis, simplified 2D procedures are usually adopted. For the purpose of performing a two-dimensional plane strain analysis, the components of loss of ground discussed above may be represented quantitatively in terms of the gap parameter. Thus the gap parameter is a measure of various components of lost ground into the tunnel as illustrated in Figure 2.2. Under idealized construction conditions (in which the microtunneling machine is kept hard against the face, and the slurry is used to minimize stress changes and deformations into the face, and the microtunneling machine is advanced under perfect alignment), the gap parameter is equivalent to the physical gap (G_p), which is defined as the vertical distance between the crown of the pipe and the crown of the excavated surface prior to removal of the microtunneling machine. If the slurry pressure is too small to balance the soil pressure at the microtunneling face, 3D movements ahead of the tunnel heading may be significant. Similarly, construction difficulties such as steering and alignment problems with the microtunneling shield can cause over-excavation and remolding of the soil adjacent to the pipe. These movements can be approximately incorporated in the 2D plane strain model by assuming a slightly larger excavated tunnel diameter, with an additional volume corresponding to the volume of ground lost through the heading and over the shield. Thus, a gap parameter (GAP) can be considered as the maximum settlement at the pipe crown, and it may be expressed as

$$GAP = G_p + u_{3D} + w \tag{2.4}$$

where G_p represents the geometric clearance between the outer skin of the shield and the pipe, u_{3D} represents the equivalent 3D elastoplastic deformation at the microtunneling machine face, and w takes into account the quality of workmanship.

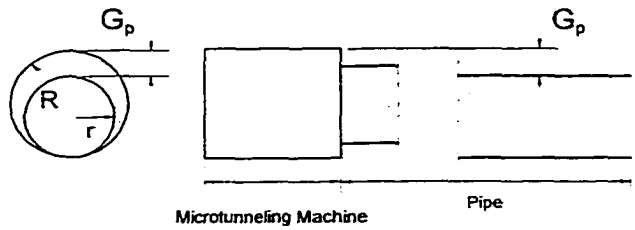

(a) Ground loss due to tail void

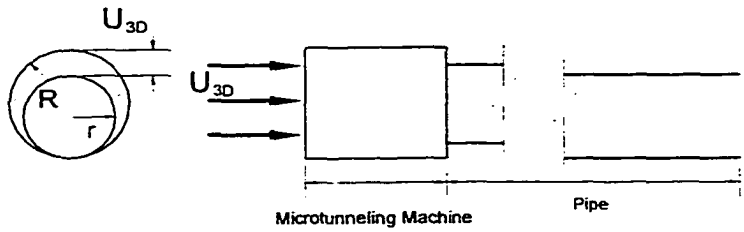

(b) Ground loss ahead of the microtunneling face

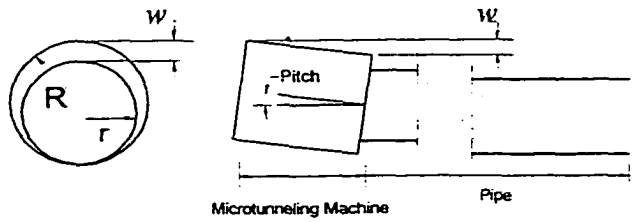

(c) Ground loss due to workmanship

Figure 2.2 Simulation of Loss of Ground (The Total Gap Parameter)

2.2.1 Ground Loss Ahead of the Microtunneling Face

Removal of the in situ stresses ahead of the tunnel face resulting from the excavation of the tunnel will cause the soil to intrude into the tunnel face. Therefore, a volume of lost ground is developed equal to the amount of over-excavated or displaced material at the face. Based on the results of 3D finite element analyses [Lee, 1989], it is

found that the progressive development of 3D face loss owing to the continuous advance of a tunneling shield can be approximately simulated in a plane strain finite element analysis (at a transverse section) by increasing the maximum allowable radial displacement at the tunnel crown. This 3D effect can be then be incorporated in the gap parameter in terms of u_{3D}. By representing a 3D configuration into an equivalent 2D approximation, u_{3d} can be given by

$$u_{3d} = \frac{1}{2}\delta_x \tag{2.5}$$

where δ_x is the magnitude of uniform axial intrusion at the tunnel face. Thus the 3D soil movement ahead of the microtunneling face can be represented by u_{3D}, provided that the values δ_x is determined.

The displacement δ_x can be represented in a non-dimensional form:

$$\Omega = \frac{\delta_x E}{rP_o} \tag{2.6}$$

where $P_o = (K_o P_v + P_w) - P_i$ where E is the Young's modulus of the soil at the tunnel spring line, r is the tunnel radius, P_o is the total stress removal at the tunnel face, K_o is the effective coefficient of earth pressure at rest, P_v is the vertical effective stress at the tunnel spring line, P_w is the pore pressure at the tunnel spring line (prior to microtunneling process), and P_i is the microtunneling slurry pressure.

Another non-dimensional parameter used is the stability ratio N, which can be considered as a measure of the available shear strength to the average boundary stress removed, and is defined as:

$$N = \frac{\gamma H - P_i}{c_u} \tag{2.7}$$

where c_u is the undrained shear strength, H is the depth of pipe spring line and γ is the soil density.

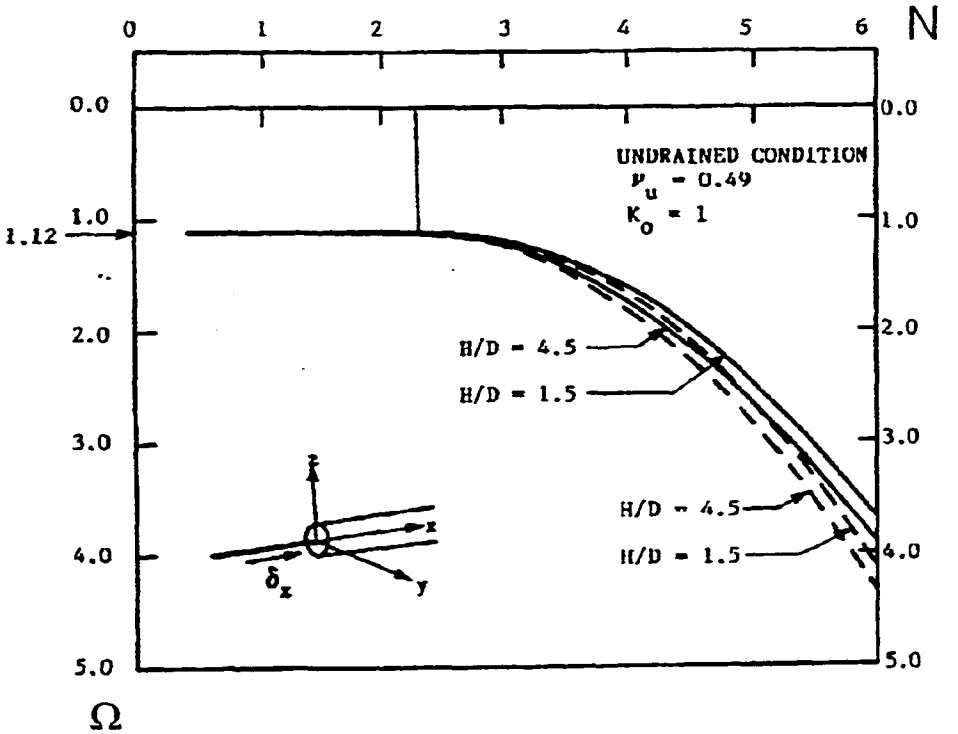

Figure 2.3 Dimensionless Axial Displacement Ω. (After Lee, 1992)

Based on the result of 3D elastoplastic finite element analyses, the development of axial displacement ahead of the tunnel face (in terms of the dimensionless parameter Ω) with stability ratio N is shown in Figure 2.3 for H/D of 1.5 and 4.5. Two soil profiles were considered: (1) the undrained modulus and shear strength (E_u, c_u) are assumed to be constant with depth; and (2) the undrained strength is assumed to increase linearly with depth. The elastic modulus is assumed to be proportional to the undrained strength. In both cases, the vertical initial stresses increase linearly with depth because of the weight of the overburden. As shown in Figure 2.3 (for the case of K_o = 1), the behavior of axial displacement δ_x is quite insensitive to the tunnel depth (H/D) or the distribution of soil properties. For stability ratio N less than about 2.5, a constant dimensionless

displacement Ω of 1.12 is obtained for all the variables considered, and the soil mass ahead of the face remains largely elastic. It may be seen that deformation increases rapidly as N exceeds a value of about 3. This increase in displacement is due to an increase in the extent of the plastic zone.

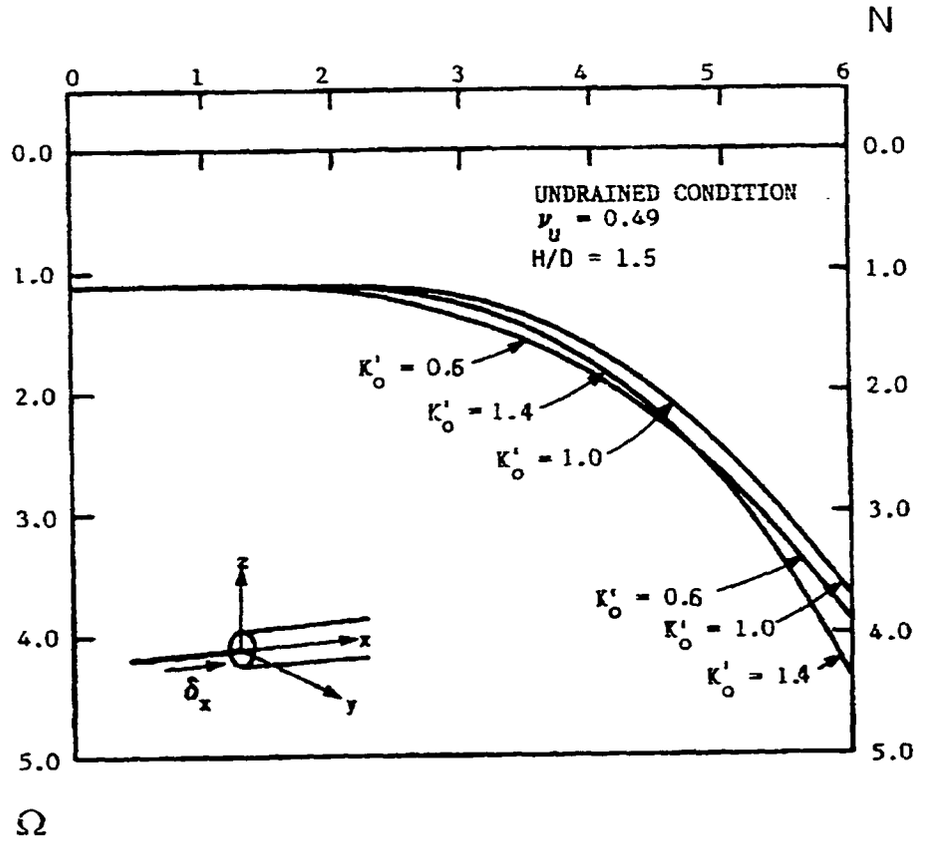

Figure 2.4 Dimensionless Axial Displacement Ahead of the Microtunneling Face with Various K_o Conditions. (after Lee, 1992)

The effect of K_o' not equal to unity is shown in Figure 2.4 for the case of K_o' of 0.6, 1.0, and 1.4. The results shown in Figure 2.4 are plotted in terms of Ω as defined by Equation 2.6. It is found that the dimensionless displacement (Ω) is quite insensitive to various K_o'. Equation 2.6 can be used to estimate the equivalent soil movement at the crown (u_{3D}) due to 3D movements ahead of the face. The parameter δ_x can be determined

by estimating the non-dimensional displacement Ω from Figure 2.3 for a given stability ratio N and back-calculating δ_x from the Equation 2.6.

2.2.2 Ground Loss Over the Shield

The loss of ground that occurs over the shield corresponds to the volume of soil that is excavated in excess of the diameter of the cutting shield. Causes of such loss in ground are primarily due to alignment problems encountered when steering the microtunneling machine. One of the common alignment problems is due to the fact that it is a common practice for the tunnel operator to advance the shield at a slightly upward pitch relative to the actual design grade thereby avoiding the diving tendency of the shield. This excessive pitch will cause overexcavation of the ground near the crown of the microtunneling machine. The volume of ground loss (V_{shield}) over the microtunneling machine can be estimated as:

$$V_{shield} = \frac{2\pi RL}{2} \times \theta \tag{2.8}$$

where R is the microtunneling machine radius, L is the length of the steerable portion of microtunneling machine, and θ is the excess pitch. An equivalent amount of ground loss at the transverse section in terms of the workmanship parameter w can be obtained by equating V_{shield} with the volume as defined in Figure 2.2:

$$V_{shield} = \frac{2\pi rL}{L} \times \theta = \pi\left[\left(r + \frac{w}{2}\right)^2 - r^2\right] \tag{2.9}$$

where r is the radius of microtunneling machine.Ignoring the secondary term,

$$w = L \times \theta \tag{2.10a}$$

This equation can be used as a guide to estimate the possible value of workmanship parameter w.

Additional ground loss can arise due to the irregular upward or downward pitching motion of the shield at an inclination other than the microtunneling design grade. Ground loss in a similar way occurs owing to yawing, when the microtunneling machine is allowed to move irregularly from side to side. The occurrence of the irregular motion is generally intermittent and highly dependent on experience of the workman controlling the advance of the shield. This irregular motion will cause the shield to over-excavate additional material. This over-excavation problem is primarily related to workmanship and cannot be precisely determined prior to construction.

2.2.3 Ground Loss Due to the Tail Void

The ground loss, which occurs from the tail void, results because the diameter of the pipes behind the microtunneling machine is usually less than the diameter of microtunneling machine. As the microtunneling machine moves forward, the change in stress state induced in the ground by the excavation causes the ground to squeeze into the void. This source of lost ground is represented by the physical gap G_p which is:

$$G_p = 2\Delta t \tag{2.10}$$

where $\Delta t = D - d$, D is the outer diameter of the microtunneling machine, and d is outer diameter of the pipe.

Once the soil comes in contact with the pipe, the lining will deflect under the applied loading. It has been observed that the crown of the pipe usually will compress under this loading, whereas the springline will expand [Ward, 1969; Peck et al., 1972].

However, for most cases, the magnitude of this component will not be as significant as the other sources described.

2.3 Ground Movement Due to Concentrated Ground Loss

All the solutions described in the above approach refer to deep problems, i.e; to cases in which the effect of the ground surface can be neglected. The purpose of next approach is to use a 'strain approach' for the analysis of the strains in an incompressible soil caused by ground losses at moderate depth below the ground surface.

It is well known in continuum mechanics that a free surface adds additional complexity to a problem. If the irrotationality and the stress-free condition are imposed at the surface, it leads to trivial solutions, except for perfect (invisicid) fluids. Therefore, a different approach is needed. The method presented herein tries to solve the problem by combining the fluid approach with elastic solutions, taking advantage of their relative merits. In the first step, the continuum mechanics approach is used, taking the absolute displacements instead of velocities as variables. The analysis of a problem such as that depicted in Figure 2.5 involves several steps, as listed follows [Sagaseta, 1988].

(a) The effect of the soil surface is neglected and the strains are computed as though the ground loss was in an infinite medium (step1);

(b) These strains will produce some stresses at the top surface, thus violating the stress-free condition. These stresses can be partially cancelled by one of the following methods:

(i) Considering a virtual source, a negative mirror image of the actual sink with respect to the top surface will produce opposite normal stresses and the same shear stresses as the actual sink.

(ii) As in (i), but taking a positive image (i.e., as image sink) will produce the same normal stresses and opposite shear stresses.

In any case, the strains due to the image are added to those calculated in step 1 (step 2); and

(c) The remaining shear or normal stresses at the surface are then evaluated and subsequently removed. The resulting strains are again added to those obtained in steps 1 and 2 (step 3).

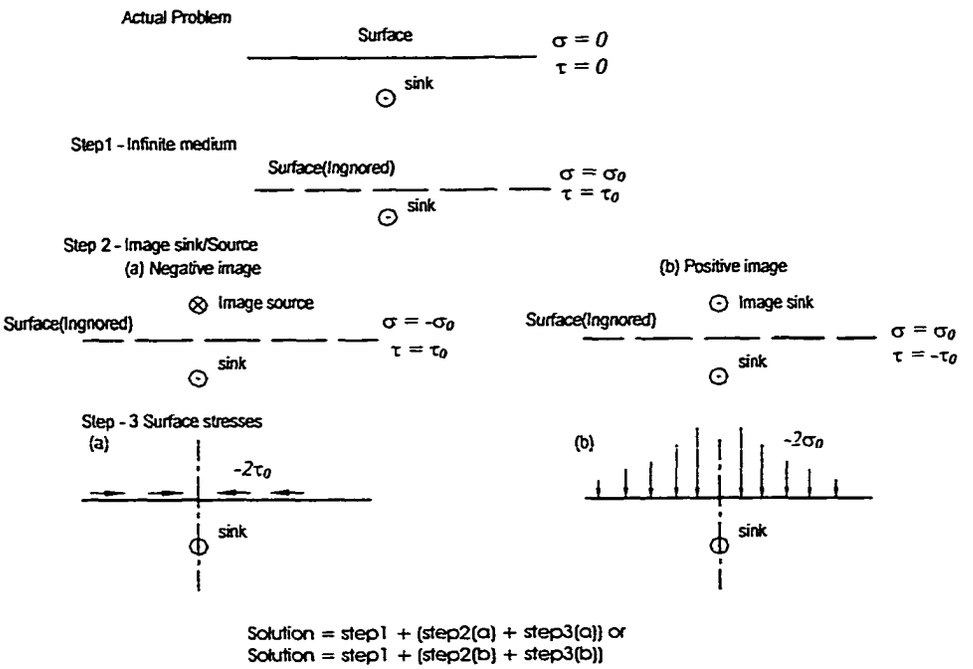

Figure 2.5 Steps in Analysis

Steps 1 and 2 involve no consideration of soil stresses. The stresses at the soil surface are not evaluated. Instead, the procedure takes advantage of the fact that the sink and its image will produce zero shear or normal stresses at their plane of symmetry. However,

step 3 does require the evaluation of surface shear or normal stresses which are doubled by the image sink. Therefore, steps1 and 2 mean an actual 'direct strain analysis' while step 3 implies the introduction of stresses and hence the adoption of a particular soil model.

Of the two possibilities in step 2, the first is more useful. This arises from the fact that surface shear stresses will produce displacements in a dominant horizontal direction, while surface normal stresses will cause greater vertical movement. So, the use of the first method provides the possibility of omitting step 3 of the analysis, with no stress evaluation, giving a reasonably accurate solution for the vertical movements which are generally of a greater concern than the horizontal movements. This point will be discussed later, and the relative merits of both methods will be further analyzed.

If the free-surface condition is to be completely taken in account, then step 3 is necessary to eliminate the effect of the surface stresses implied by steps 1 and 2. To accomplish this, the applied methods derived from the continuum mechanics approach is needed using the method and techniques of soil mechanics. The following procedure can be used for step 3:

(a) Evaluate the strains at the surface by differentiation of the displacement field obtained in steps 1 and 2 (step 3.1);

(b) From these strains, calculate the corresponding surface stresses (step 3.2); and

(c) Obtain the strain field in a half-space subjected to a system of forces acting on its surface equal and opposite to those calculated in step 3.2 (step 3.3).

The first step is straightforward because the equations arising from the sink in an infinite medium are simple, as will be shown later. Step 3.2 is also easy, even for a

relatively complex soil model, because it is used in a direct way for the evaluation of the stresses from a known strain field. However, step 3.3 is only possible for the simplest model, i.e., a homogeneous isotropic linear elastic half-space, unless a numerical method is used.

The assumption of linear elasticity in step 3.2 is fully justified because the soil elements at the top surface are generally well away from the sink, and so their plastic strains will be negligible. The accuracy of this assumption is not so clear for step 3.3, but in any case, the difference with respect to a better soil model must be small. The movements associated with step 3 are small compared with those resulting from steps 1 and 2, particularly if method (i) (negative image sink) is used for the reasons given earlier.

The basic case considered is the action of a point sink that extracts a finite volume of soil at some depth H below the top surface. The extracted soil has a volume V if the case is in three dimensions, or if a volume per unit length l is in plane strain. For convenience, in both cases, the amount of ground loss is defined by the radius a of the equivalent sphere or cylinder. The analysis is carried out in steps as shown earlier.

2.3.1 Infinite Medium

If the topsoil is ignored, the problem is symmetric about the sink, and so the displacement of any point is only radial, the other components being zero. The condition of no volume change implies that the points located at a distance r from the sink must have an inward radial displacement (Figure 2.6).

$$S_r(r) = \frac{a}{n}\left(\frac{a}{r}\right)^{n-1} \tag{2.11}$$

where n=2 in plane strain, n=3 in three dimensions, and πa^2 represents the ground loss volume over a unit length. Equation 2.11 has been derived on the basis of assumption of small displacements, neglecting the change in geometry. This assumption will be kept in the following. For large strains, the equivalent to Equation 2.11 would be

$$S_r(r_o) = r_o - (r_o^n - a^n)^{1/n} \tag{2.12a}$$

where r is the undeformed (material) co-ordinate for a Lagrangian formulation, or

$$S_r(r) = (r^n + a^n)^{1/n} - r \tag{2.12b}$$

where r is the deformed (spatial) co-ordinate for an Eulerian formulation.

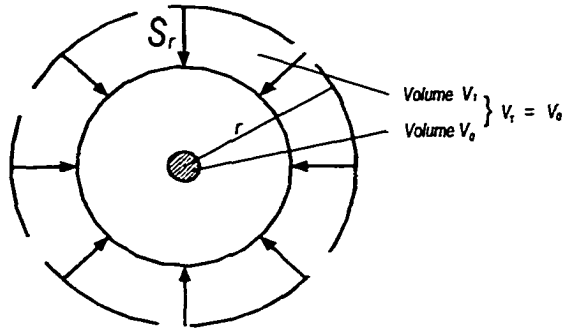

Figure 2.6 Point Sink: Infinite Medium

In a Cartesian reference frame, the displacement components at a point P(x,y,z), if the sink is at $C(x_o,y_o,z_o)$ (Figure 2.6), are:

$$S_x = -\frac{a^n}{n}\frac{x - x_o}{r^n} \tag{2.13a}$$

$$S_y = -\frac{a^n}{n}\frac{y - y_o}{r^n} \tag{2.13b}$$

in three dimensions and

$$S_y = 0 \tag{2.13c}$$

in plane strain

$$S_z = -\frac{a^n}{n}\frac{z-z_o}{r^n} \tag{2.13d}$$

where

$$r = [(x-x_o)^2 + (y-y_o)^2 + (z-z_o)^2]^{1/2}$$

in three dimensions and

$$r = [(x-x_o)^2 + (z-z_o)^2]^{1/2}$$

in plane strain.

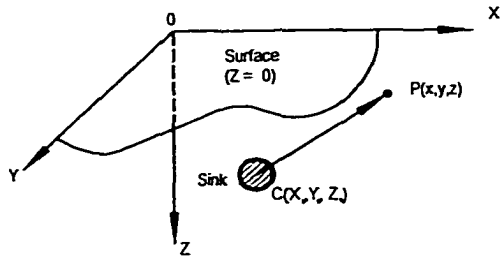

Figure 2.7 Point Sink: Cartesian Co-ordinates

2.3.2 Image Sink: Paved Half-Space

The displacements in Equation 2.12 will produce a certain stress field, depending on the soil stress-strain properties. At the top surface, normal and shear stresses will result so violating the imposed boundary condition of a free surface.

These surface stresses can be partially removed by the use of image sinks or sources as described in the preceding section. If a negative image is used, then the surface normal stresses are eliminated, while a positive image will cancel the shear stresses.

Following the first possibility (method (ii)), the result is a half-space whose top surface has no normal vertical stress but is totally constrained in the horizontal direction. The situation is as though the soil surface was covered by a flexible but not extensible membrane. This situation will be referred to by the term 'paved' half-space.

This condition is not too far from reality. A relatively stiff pavement is common above underground utility in urban areas. Where soil movements caused by nearby excavations are of interest. It is common practice when surface movements are measured in urban areas to refer the observation points to a given depth to avoid the influence of the pavement. Under these conditions, the paved solution may be at least as good as the assumption of a completely free surface. This consideration is especially valid for the vertical component of the displacement.

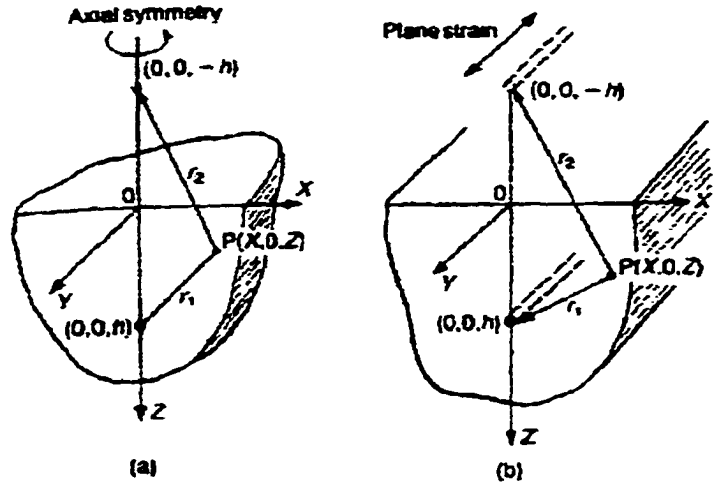

Figure 2.8 Point Sink-Negative Image: (a) Three Dimensions and (b)Two Dimensions

Adding the displacements caused by the sink and its negative image, the following result is obtained for the points on the plane XZ (other points are defined either by the plane strain or the axial symmetry condition) (Figure 2.8):

$$S_x = -\frac{a^n}{n}\left(\frac{x}{r_1^n} - \frac{x}{r_2^n}\right) \tag{2.14a}$$

$$S_y = 0 \tag{2.14b}$$

$$S_z = -\frac{a^n}{n}\left(\frac{z-h}{r_1^n} - \frac{z+h}{r_2^n}\right) \tag{2.14c}$$

Where

$$r_1 = [x^2 + (z-h)^2]^{1/2}$$

$$r_2 = [x^2 + (z+h)^2]^{1/2}$$

If a positive image were to be used (method (ii)), the result would be a half-space whose surface is free in the horizontal direction but which can not undergo any vertical movement as though it were suspended from a system of inextensible wires. This condition is completely unrealistic. The only reason for keeping this method in mind is that it will be used in a later stage as a tool for theoretical reasoning regarding the movements of the top surface.

2.3.3 Free Surface

For the complete elimination of the surface stresses, the procedure described earlier must follow steps 3.1-3.3.

$$\gamma = \left(\frac{\partial S_x}{\partial z} + \frac{\partial S_z}{\partial x}\right)_{z=0} = -4a^n \frac{hx}{(x^2+h^2)^{1+n/2}} \tag{2.15}$$

For a linear elastic material, the associated shear stresses are (step 3.2)

$$\tau = G\gamma = -4Ga^n \frac{hx}{(x^2+h^2)^{1+n/2}} \tag{2.16}$$

The shear stress distribution is shown in Figure 2.9, for both the plane strain and plane stress cases.

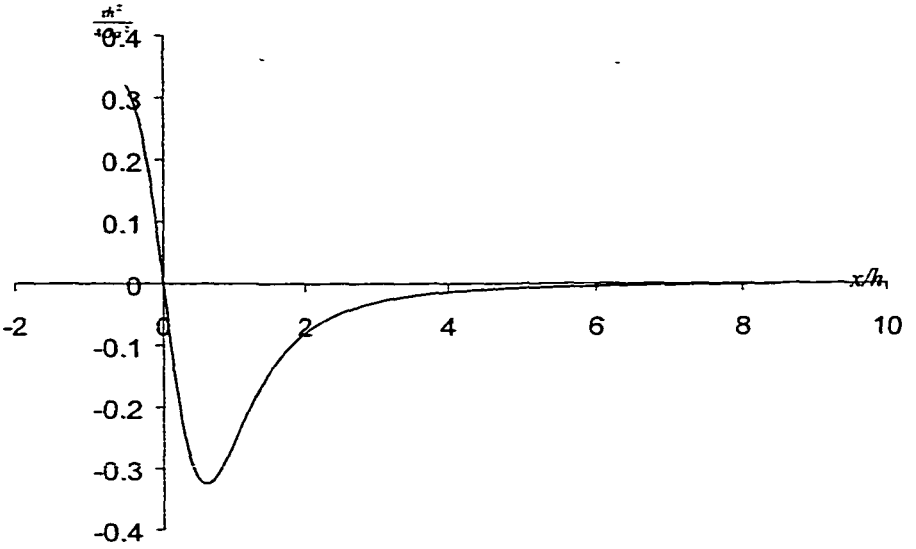

Figure 2.9 Point Sink: Surface Shear Stresses

Step 3.3 of the analysis involves the evaluation of the displacement in a homogeneous linear elastic half-space subjected to a system of horizontal forces at its surface acting oppositely to the shear stresses (Equation 2.16). This can be performed by direct integration of the known solution for a horizontal point load. The results, for the plane strain case, are:

$$S_{x_r} = -a^2 \frac{x}{r_2^2}[1 - 2\frac{z(z+h)}{r_2^2}] \tag{2.17a}$$

$$S_{z_r} = a^2 \frac{z}{r_2^2}(1 - 2\frac{x^2}{r_2^2}) \tag{2.17b}$$

where

$$r_2 = [x^2 + (z+h)^2]^{1/2}$$

In the three dimensional case.

$$S_{x_r} = \frac{2}{\pi} a^3 \frac{h}{x} \int_0^\infty r_b \frac{\alpha}{(h^2+\alpha^2)^{5/2}} \times [I_E E(k) + I_F F(k)] d\alpha \tag{2.18a}$$

$$S_{z_r} = \frac{2}{\pi} a^3 hz \int_0^{\infty} \frac{1}{r_b} \frac{\alpha}{(h^2+\alpha^2)^{5/2}} \times [J_E E(k) + F(k)] d\alpha \qquad (2.18b)$$

where

$$I_E = 1 + \frac{1}{2} z^2 \left(\frac{1}{r_a^2} + \frac{1}{r_b^2}\right)$$

$$I_F = -(\alpha^2 + x^2 + 2z^2)$$

$$J_E = -1 + 2\frac{\alpha(\alpha - x)}{r_a^2}$$

$$r_a = [(\alpha - x)^2 + z^2]^{1/2}$$

$$r_b = [(\alpha + x)^2 + z^2]^{1/2}$$

F(k) and *E(k)* are complete elliptic functions of the first and second kind respectively, with

$$k = \left(1 - \frac{r_a^2}{r_b^2}\right)^{1/2}$$

The integrals of Equation 2.18 must be evaluated numerically.

2.3.4 Surface Movements

The addition of the displacement in Equations 2.17 or 2.18 to the values in Equation 2.14 defines the final value of the soil movements at any point. In most cases, attention is mainly focused on the displacements of the soil surface. Determination of stresses (step 3 of the general procedure) is not necessary.

The simplicity comes from the fact that, for an incompressible material (Poisson's ratio of 0.5), the application of a vertical point load at the soil surface produces zero

horizontal movements at surface points, and the surface vertical displacement due to a horizontal load are also zero [Sagaseta,1988].

With this in mind, if the vertical movements are considered, the superposition of the negative image will cancel the surface normal stresses and the relief of the remaining surface shear stresses will not mean any additional vertical movement, and hence it can be omitted.

To obtain the horizontal surface displacement, the alternative possibility of method (ii) can be followed. In this case, the surface shear stresses will be cancelled, and then subsequent removal of the remaining normal stresses will produce no additional horizontal movement and so can be avoided.

As the vertical movements of the soil surface are doubled by the negative image and the horizontal displacements are also doubled by the positive image, the conclusion is that the surface movements can be directly obtained simply by multiplying the movements due to the sink in an infinite medium by a factor of 2 ignoring the presence of the soil surface.

In this way, the final exact displacements of the soil surface due to the point sink are:

$$S_{x0} = S_{x(z=0)} = -2\frac{a^n}{n}\frac{x}{(x^2+h^2)^{n/2}} \tag{2.19a}$$

$$S_{z0} = S_{z(z=0)} = 2\frac{a^n}{n}\frac{h}{(x^2+h^2)^{n/2}} \tag{2.19b}$$

where h is the depth of the tunnel spring line. For two dimenal case, these values are shown in Figure 2.10. In Figure 2.10 the unit of y axis is S/a^2, the unit of x axis is x/h.

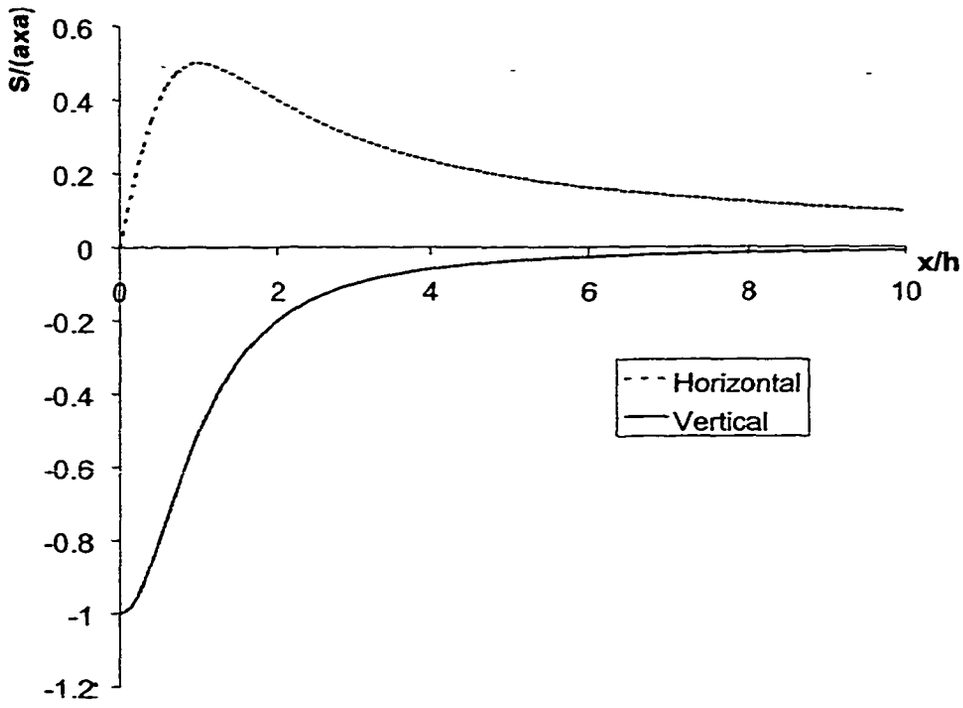

Figure 2.10 Point Sink: Final Surface Displacement

2.4 Ground Movement Associated with Microtunneling

The equivalent ground loss parameter obtained in Equation 2.4 can be further modified to incorporate the non-uniform radial movement of the soil (due to the oval-shaped gap) around the tunnel, which basically influences the deformation pattern of the surrounding soil. The component of the equivalent ground loss parameter $\varepsilon_{x,z=0}$ which causeS the surface settlement may be derived by adopting an exponential function to the equivalent ground loss parameter ε_0 that models the non-uniform movement of the soil around the tunneling as shown in Figure 2.11.

$$\varepsilon_{x,z=0} = \varepsilon_0 B e^{-Ax^2} \tag{2.20}$$

where A, B are constants, and ε_0 = equivalent ground loss and is defined as:

$$\varepsilon_0 = \frac{\pi\left(r+\frac{g}{2}\right)^2 - \pi r^2}{\pi r^2} \times 100\% = \frac{4gr+g^2}{4r^2} \times 100\%$$

Constants g is gap parameter, r is radius of microtunneling face, A and B are derived based on the boundary conditions described next.

When the portion of the soil above the tunnel crown touches the tunnel lining, the soil at the side of the tunnel displaces towards the bottom of the tunnel. Therefore, the upward movement of soil below the tunnel is limited. Centrifuge model tests carried out by Stallebrass et al. [1996] revealed similar results. When the tunnel lining settles on the bottom of the annulus gap (due to the self-weight), the distance between the crown of the tunnel lining and crown of the excavated surface becomes twice the thickness of the annulus gap. Based on simple geometry, the void area above the tunnel spring line is about 75% of the total void area. Therefore, 75% percent of vertical ground movement occurs within the upper annulus of the gap around the tunnel. Figure 2.11 shows the vertical ground movement influence zone where most of the soil displacements occur. The relationship between settlement trough width, which is an indirect measure of the ground movement influence zone, and the tunnel depth can be expressed as a horizontal angle β, drawn from the spring line of the tunnel to the width of the settlement trough at the surface. From the observations made by Cording and Hansmire [1975], the β value is about 45° for soft to stiff clays. The ground movement occurs predominantly within the 45° wedge in between the ground surface and the tunnel. Therefore, it may be considered that the surface settlement above the tunnel axis is the resultant of the complete cumulative equivalent ground loss ($100\%\varepsilon_0$) around the tunnel, and the surface settlement

at a horizontal distance (h+r) is the resultant of partial cumulative equivalent ground loss ($25\%\varepsilon_0$). These boundary conditions are shown in Figure 2.11 (Loganathan 1998).

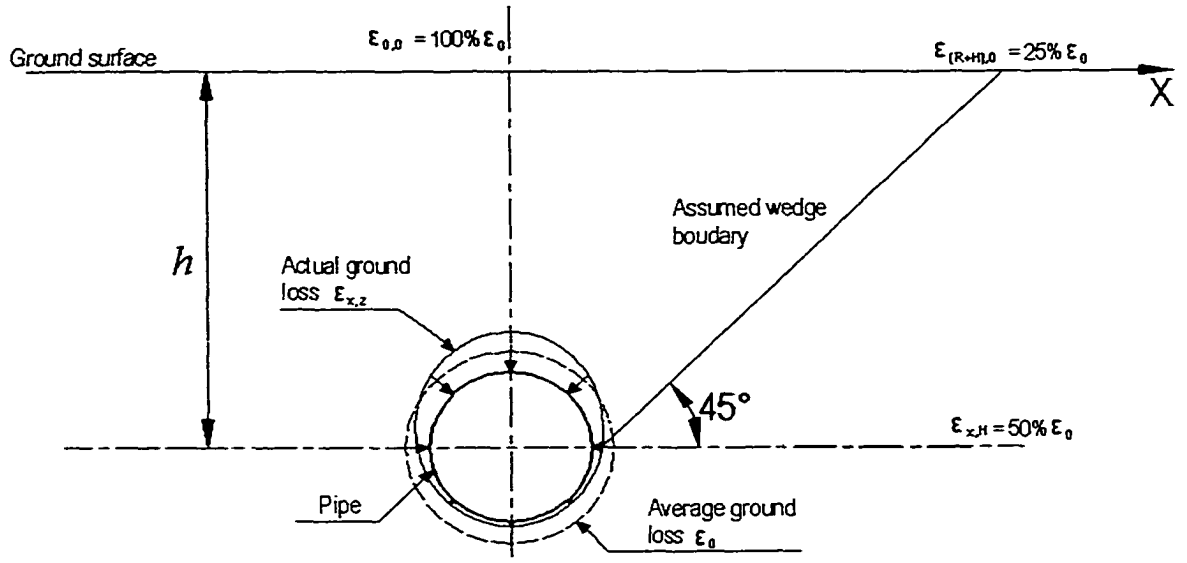

Figure 2.11 Ground Deformation Pattern and Ground Loss Boundary Conditions

By applying these boundary conditions, the equivalent ground loss component those models the nonuniform vertical movement is derived as:

$$\varepsilon_{x,z=0} = \varepsilon_o \exp\left[\frac{-1.38x^2}{(h+r)^2}\right] \tag{2.21}$$

Observation made by Deane and Bassett [1995] and Tallebrass et al. [1996] show that the horizontal ground movement into the tail void or gap is at a maximum at the spring line of the tunnel and is zero at the crown and the invert of the tunnel. Therefore, the lateral ground movement is symmetrical about the tunnel axis. The lateral movement component is incorporated into the ground loss as shown:

$$\varepsilon_{x,z} = \varepsilon_{x,z=0} C e^{-Dz^2} \tag{2.22}$$

where C and D are constants that are derived based on the boundary conditions.

Based on the oval-shaped gap geometry, the magnitude of the horizontal movement at the tunnel spring line is approximately half of the vertical movement at the tunnel crown, which causes 75% of the ground movement into the upper annulus of the oval-shaped gap around the tunnel. Therefore, the equivalent ground loss component due to the horizontal movement at horizontal distance x and depth h is 50% of the equivalent ground loss causing surface settlement at horizontal distance x. By applying these boundary conditions and substituting Equation 2.21 in Equation 2.22, the modified equivalent ground loss parameter, incorporating the nonlinear ground movement around the tunnel soil interface, may be defined as

$$\varepsilon_{x,z} = \frac{4gr+g^2}{4r^2}\exp\left(-\left(\frac{1.38x^2}{(h+r)^2}+\frac{0.69z^2}{h^2}\right)\right) \tag{2.23}$$

where h is the depth of the pipe, r is the radius of pipe, and g is gap parameter.

Substituting Equation 2.23 in Equation 2.19, we get:

$$S_{x_r} = -\frac{\varepsilon_{x,z}}{\pi}\frac{x}{(x^2+h^2)} \tag{2.24a}$$

$$S_{z_r} = \frac{\varepsilon_{x,z}}{\pi}\frac{h}{(x^2+h^2)} \tag{2.24b}$$

and the ground movement at the surface can be defined by:

$$S_{x0} = S_{x(z=0)} = \frac{4gr+g^2}{4r^2}\exp\left(-\frac{1.38x^2}{(h+r)^2}\right)\frac{x}{\pi(x^2+h^2)} \tag{2.25a}$$

$$S_{z0} = S_{z(z=0)} = \frac{4gr+g^2}{4r^2}\exp\left(-\frac{1.38x^2}{(h+r)^2}\right)\frac{h}{\pi(x^2+h^2)} \tag{2.25b}$$

The S_z value is shown in Figure 2.12. Figure 2.12 shows that the deeper microtunneling is the wider the trough is and smaller the maximum ground settlement is

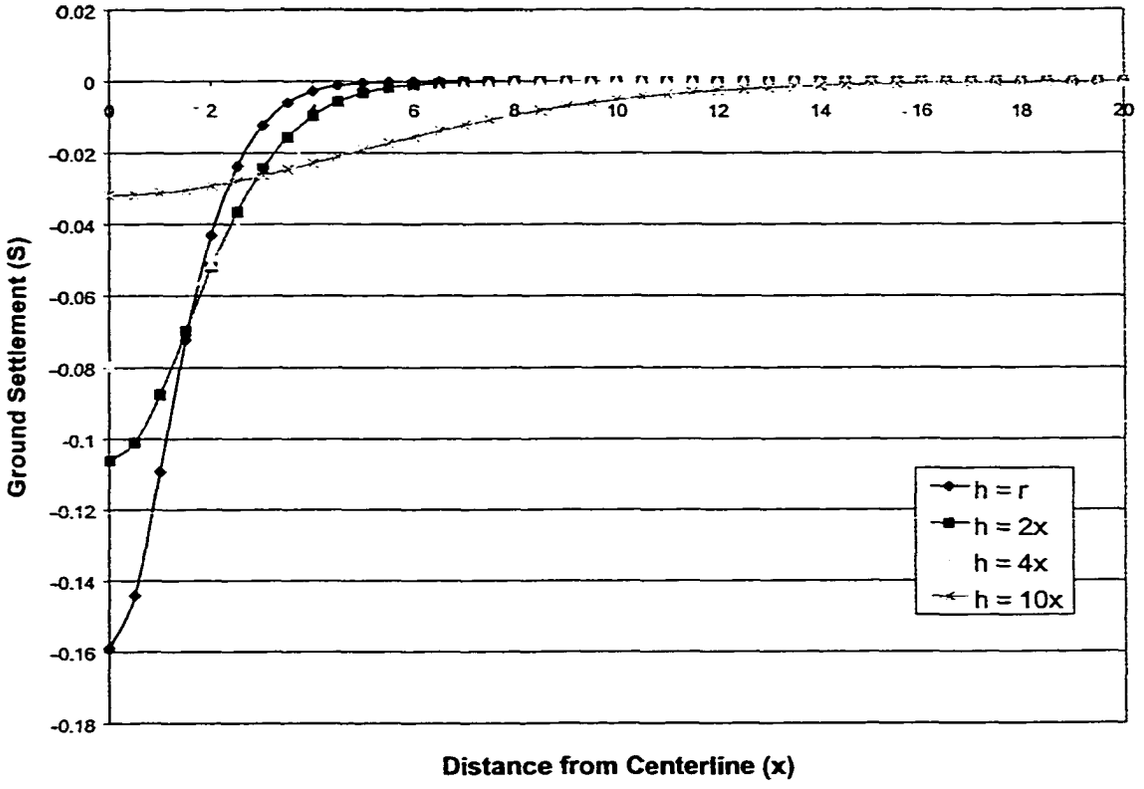

Figure 2.12 Vertical Ground Movement

CHAPTER 3

EMPIRICAL APPROACH

A quite extensive survey of tunnel-induced (large diameter) ground movements has been compiled and tabulated [Attewell, 1989]. The settlement caused by tunnels in granular soils shows considerable scatter in a significant number of cases. Settlement often is greater than 100mm. The majority of tunnels in cohesive soils show settlements below 50 mm, and further investigation has shown that these settlements can be foreseen quite reliably in most cases.

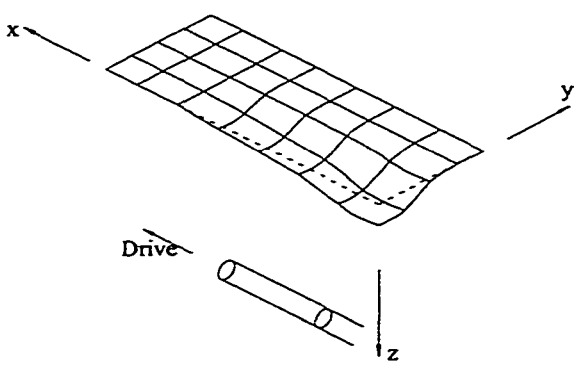

Figure 3.1 Surface Settlement Trough

The free ground settlement w has been conveniently approximated by normal and cumulative probability functions as:

$$w = \frac{V_s}{\sqrt{2\pi i}} \exp[\frac{-y^2}{2i^2}] \{G(\frac{x - x_i}{i}) - G(\frac{x - x_f}{i})\} \tag{3.1}$$

where V_s is the soil-loss-induced surface settlement volume per meter of tunneling machine advance, i is a parameter which is equivalent to the standard deviation of a statistical normal distribution, x,y are the ground coordinates along and transverse to the tunnel center line respectively, x_i is the tunnel starting point, and x_f is the microtunneling machine face position.

For a position remote from the start, and at a distance of at least three times the tunnel depth behind the microtunneling machine face, the transverse soil-loss-induced surface settlement profile can be defined by:

$$w_s(y) = \frac{V_{ss}}{\sqrt{2\pi i_s}} \exp\left[\frac{-y^2}{2i_s^2}\right] \tag{3.2}$$

and the center maximum settlement is:

$$w_{\max} = \frac{V_{ss}}{\sqrt{2\pi i_s}} \tag{3.3}$$

In the above two equations, the s subscript is used to denote short-term (i.e., from ground loss rather than long-term consolidation). The surface settlement volume is appropriately double-subscripted.

Settlement volume V_{ss} can be estimated from the proposed tunneling rate and method, deduced rate of soil relaxation [Attewell, 1978], or by the choice of an appropriate percentage of face area base on similar tunneling case histories, usually in the range 0.5% to 2.5% of the face area for clay soils. O'Reilly and New [1982] have proposed the empirical expressions for evaluation of the parameter i_s for U.K. conditions as:

$$i_s = 0.43(z_0 - z) + 1.1m \text{ for clay soil } (3<z_0<34\text{m}) \tag{3.4}$$

when consolidation effects are significant. In the above equations, z_0 is the tunnel axis depth, and z is depth to the settlement reference surface (zero for surface).

In addition to an increased maximum settlement, the width of the zone of influence may also be increased by the consolidation mechanism. It has been proposed by Hurrell [1985] that the long-term transverse settlement profile comprises the superposition of the short-term settlement and of two discrete consolidation settlement profiles. The long-term profile is then defined as:

$$w_c = w_{max\,s} \exp[\frac{-y^2}{2i_s^2}] + w_{max\,c}(\exp[\frac{-(y+D)^2}{2i_s^2}] + \exp[\frac{-(y-D)^2}{2i_s^2}]) \qquad (3.5)$$

where w_c is the consolidation element of transverse settlement. As shoen in Figure 3.12, this is a relatively smooth profile, but not necessarily a pure normal probability curve. In practice, however, a curve close to this is obtained.

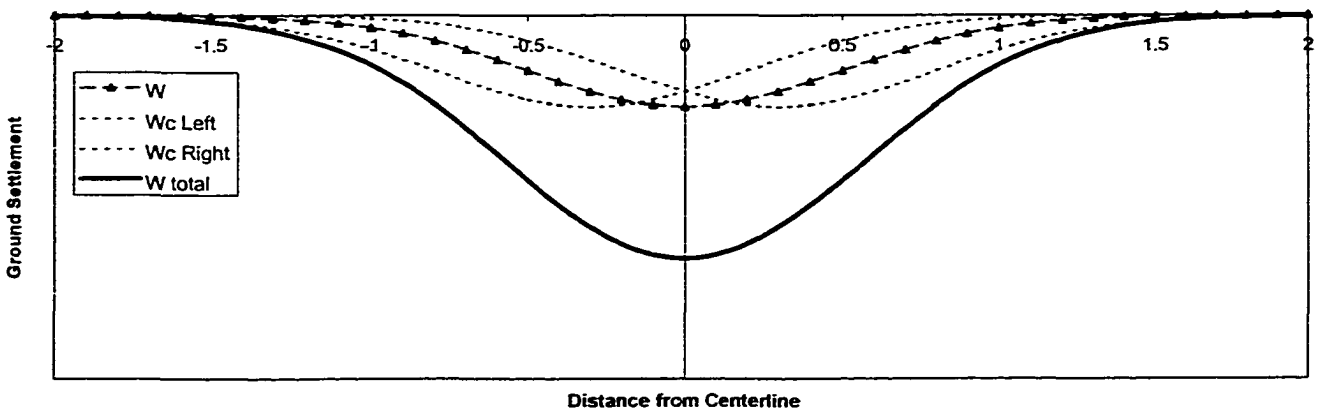

Figure 3.2 Short-Term and Long-Term (Consolidation) Settlements at Ground Surface

Use of empirical Equation 3.5 can be reasonably justified in ground having permeability isotropy. However, there are examples in the U.K. of long-term settlement measurements in which the character of the ultimate settlement trough cannot be satisfied by this equation. Non-compliance may be attributed to several factors, and particularly to

a state of ground permeability anisotropy. Take, for example, the case of stratified ground in which the horizontal permeability k_h is greater than the vertical permeability k_v. Then, following flow net procedure, the scaling factor is:

$$s = \sqrt{K_h / K_v} \tag{3.6}$$

After Hurrell [1987], let the potential spread of the long-term transverse settlement trough, y_t be:

$$y_t = 2Sz_0 \tag{3.7}$$

In the case of anisotropic permeability, the standard deviation $i_{t(a)}$ for the long-term surface settlement trough is estimated as:

$$i_{t(a)} = y_t / 3 \tag{3.8}$$

Thus, Equation (3.5) may be generalized for both anisotropic permeability and long-term settlement:

$$w_{\max t} = \frac{V_{st}}{\sqrt{2\pi} i_{t(a)}} \tag{3.9}$$

Definition of the complete form of the long-term transverse settlement trough is then:

$$w(y)_t = w_{\max t} \exp[-y^2 / 2i_t^2] \text{ --- permeability isotropy} \tag{3.10}$$

$$w(y)_t = w_{\max t} \exp[-y^2 / 2i_{t(a)}^2] \text{ --- permeability anisotropy} \tag{3.11}$$

There were two microtunneling experiment carried out at Waterways Experiment Station (WES) in Vicksburg, MS [Bennett, 1993; Bennett, 1997]. The microtunneling demonstrations and evaluations were performed during 1992, and 1995 at a specially constructed test facility built at WES [Bennett, 1993]. Some of the results and calculated

ground settlement of these two experiments are listed and compared with numerical method and neural network method in this dissertaion.

CHAPTER 4

NUMERICAL APPROACH

4.1 FLAC^{3D} Software

Flac^{3D} is an explicit finite difference program for numerical study of the mechanical behavior of a continuous three-dimensional medium as it reaches equilibrium or steady-state flow. Materials are represented by polyhedral elements within a three-dimensional grid adjusted by the user to fit the shape of the object to be modeled. Each element behaves according to a prescribed linear or non-linear stress/strain law in response to applied forces or boundary restraints. The material can yield and flow, and the grid can deform (in large-strain mode) and move with the material represented.

Flac^{3D} offers a wide range of capabilities to solve complex problems in mechanics and especially in geomechanics. The Flac^{3D} version 2.0 has ten built-in material models:

1. null;
2 elastic, isotropic;
3. elastic, orthotropic;
4. elastic, transversely isotropic;
5. Drucker-Prager plasticity;
6. Mohr-Coulomb plasticity;
7. strain-hardening/softening Mohr-Coulomb plasticity;
8. ubiquitous-joint plasticity;

9. bilinear strain-hardening/softening ubiquitous-joint plasticity; and
10. modified cam-clay plasticity.

Each model is developed to represent a specific type of constitutive behavior commonly associated with geologic materials. The *null* model is used to represent material that is removed from the model but with the associated zones left in place. The *elastic, isotropic* model is valid for homogeneous, isotropic, continuous materials that exhibit linear stress-strain behavior. The *elastic, orthotropic* model and the *elastic, transversely isotropic* model are appropriate for elastic materials that exhibit well-defined elastic anisotropy. The *Drucker-Prager plasticity* model is a simple failure criterion in which the shear yield stress is a function of isotropic stress. The *Mohr-Coulomb plasticity* model is used for materials that yield when subjected to shear loading, but the yield stress depends on the major and minor principal stresses only; the intermediate principal stress has no effect on yield. The *strain-softening Mohr-Coulomb* model is based upon the Mohr-Coulomb model, but is appropriate for materials that show degradation or increase in shear strength when loaded beyond the initial failure limit. The *ubiquitous-joint* model applies for a Mohr-Coulomb material that exhibits a well-defined strength anisotropy. The *bilinear strain-softening ubiquitous-joint* model combines the strain-softening Mohr-Coulomb model with the ubiquitous-joint model. This model includes a bilinear failure envelope for both the matrix and the ubiquitous joints. The *modified Cam-clay* model accounts for the influence of volume change on deformability and on resistance to failure.

Table 4.1 FLAC3D Constitutive Models (after FLAC^{3D} Menu)

Model	Representative Material	Example Application
null	void	holes, excavations, regions in which material will be added at later stage
elastic	homogeneous, isotropic continuum;linear stress-strain behavior	manufactured materials (e.g., steel) loaded below strength limit; factor-of-safety calculation
orthotropic elastic	elastic materials with three mutually perpendicular axis of elastic symmetry	columar basalt loaded below strength limit
transversely isotropic elastic	thinly laminated material exhibiting elastic anisotropy (e.g., slate)	laminated material loaded below strength limit
Drucker-Prager plasticity	limited application; soft clays with low friction	common model for comparison to implicit finite-element programs
Mohr-Coulomb plasticity	loose and cemented granular materials; soils, rock, concrete	general soil or rock mechanics (e.g. slope stability and underground excavation)
strain-hardening / softening Mohr-Couloomb	granular materials that exhibit non-linear material hardening or softening	studies in post-failure (e.g., progressive collapse, yielding pillar, caving)
unbiquitous-joint	thinly laminated material exhibiting strength anisotropy (e.g., slate)	excavation in closely bedded strata
bilinear strain-hardening / softening ubiquitous-joint	laminated materials that exhibit non-linear material hardening or softening	studies in post-failure of laminated materials
modified Cam-Clay	materials for which deformability and shear strength are a function of volume change	geotechnical construction on clay

In addition, three optional features are available in Flac3D for dynamic analysis, thermal analysis, and modeling creep material behavior:

1. The dynamic analysis option permits three-dimensional, fully dynamic analysis. The calculation is based on the explicit finite difference scheme to solve the full equations of motion. The dynamic option extends Flac3D's analysis capability to a wide range

of dynamic problems in disciplines such as earthquake engineering, seismology, and mine rockbursts.

2. The thermal analysis option allows simulation of transient heat conduction in materials and the subsequent development of thermally induced stresses.
3. The creep analysis option can be used to simulate the behavior of materials that exhibit creep, i.e., time-dependent material behavior. There are five creep models in this option: the classical viscoelastic (Maxwell) model, a two-component power law, a reference creep formulation implemented for nuclear waste isolation studies, a viscoplastic model that combines the reference creep formulation with the Drucker-Prager plasticity model, and a "crushed-salt" model that simulates both volumetric and deviatoric creep compaction.

Flac3D also contains a powerful built-in programming language, FISH, which enables the user to define new variables and functions. FISH offers a unique capability to users who wish to tailor analyses to suit their specific needs.

4.2 Basic Definitions of Flac^{3D} Terms (after Flac^{3D} Menu)

Flac^{3D} Model – The Flac3D model is created by the user to simulate a physical problem. When referring to a Flac3D model, the model implies a sequence of Flac3D commands that define the problem conditions for numerical solution.

Zone – The finite difference zone is the smallest geometric domain within which the change in a phenomenon (e.g., stress versus strain) is evaluated. Polyhedral zones of different shapes (e.g., brick, wedge, pyramid, and tetrahedral shaped zones) are used to create models.

Gridpoint – Gridpoints are associated with the corners of the finite difference zones. There are five, six, seven, or eight gridpoints associated with each polyhedral zone, depending on the zone shape.

Finite Difference Grid – The finite difference grid is an assemblage of one or more finite difference zones across the physical region being analyzed.

Boundary Conditions – A boundary condition is the prescription of a constraint or controlled condition along a model boundary.

Constitutive Model – The constitutive model represents the deformation and strength behavior prescribed to the zones in a Flac3D model.

Step – Because Flac3D is an explicit code, the solution to a problem requires a number of computational steps. During computational stepping, the information associated with the phenomenon under investigation is propagated across the zones in the finite difference grid. A certain number of steps are required to arrive at an equilibrium state for a static solution. When using the dynamic analysis option, Step refers to the actual time step for the dynamic problem.

Unbalanced Force – The unbalanced force indicates when a mechanical equilibrium state (or the onset of plastic flow) is reached for a static analysis. The maximum unbalanced force will never exactly reach zero for a numerical analysis. The model is considered to be in equilibrium when the maximum unbalanced force is small compared with the total applied forces in the problem.

Large Strain/Small Strain – By default, Flac^{3D} operates in small-strain mode; that is, gridpoint coordinates are not changed even if computed displacements are large. In the

large-strain mode, gridpoint coordinates are updated at each step according to computed displacements. In the large-strain mode, geometric nonlinearity is possible.

4.3 Intrinsic Deformability Properties

All material models in FLAC,[3D] except for the transversely isotropic elastic and orthotropic elastic models, assume an isotropic material behavior in the elastic range described by two elastic constants, bulk modulus (K) and shear modulus (G). The elastic constants, K and G, are used in FLAC rather than Young's modulus, E, and Poisson's ratio, ν, because it is believed that bulk and shear moduli correspond to more fundamental aspects of material behavior than do Young's modulus and Poisson's ratio. The equations to convert from (E, ν) to (K, G) are:

$$K = \frac{E}{3(1-2\nu)} \tag{4.1}$$

$$G = \frac{E}{2(1+\nu)} \tag{4.2}$$

Equation 4.1 should not be used blindly when ν is near 0.5 since the computed value of K will be unrealistically high and convergence to the solution will be very slow. It is better to fix the value of K at its known physical value (estimated from an isotropic compression test or from the P-wave speed), and then compute G from K and ν.

The basic criterion for material failure in FLAC3D is the Mohr-Coulomb relation, which is a linear failure surface corresponding to shear failure:

$$f_s = \sigma_1 - \sigma_3 N_\phi + 2c\sqrt{N_\phi} \tag{4.3}$$

where $N_\phi = (1+\sin\phi)/(1-\sin\phi)$,

σ_1 = major principal stress,

σ_3 = minor principal stress,

ϕ = friction angle, and

c = cohesion.

Shear yield is detected if $f_s < 0$. The two strength constants, ϕ and c, are conventionally derived from laboratory triaxial tests.

4.4 Modeling Procedure

For modeling purposes, the problem is defined by the domain sketched in Figure 4.1 where advantage has been taken of the half-symmetry geometry and plain strain condition. A system of reference axes is selected with the origin located at the intersection of the cavity axis with the front face of the domain and the z-axis pointing upward. The boundary conditions applied to this domain are

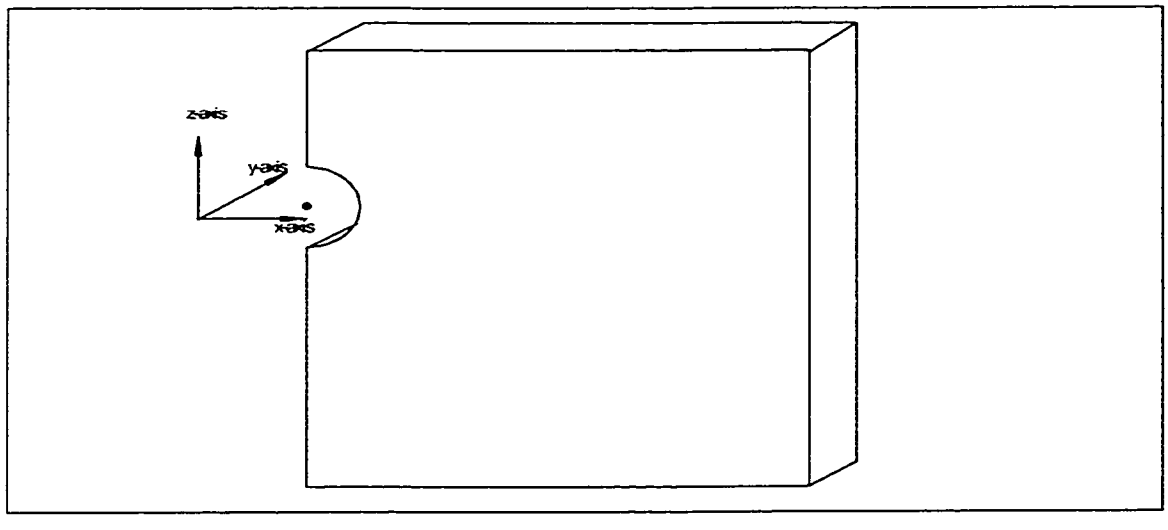

Figure 4.1 Domain for Flac3D Simulation – Half Symmetry

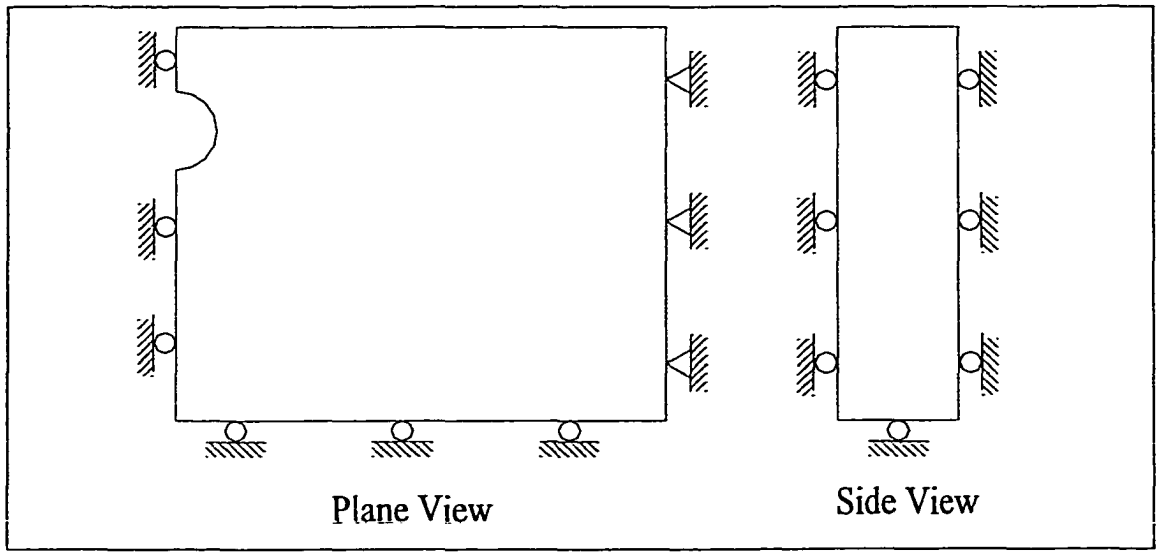

Figure 4.2 Boundary Conditions for Flac3D Analysis – Half Symmetry

sketched in Figure 4.2. The displacements of the x, y, and z direction at far right and boundary are restricted in all directions.. The displacements of the symmetry boundary corresponding to the plane at x = 0 is restricted in the x-direction. Plain strain is assumed along the y-plane. The thickness of the domain is selected as 4m. The domain is discretized into one layer of zones organized in a pattern shown in Figure 4.3.

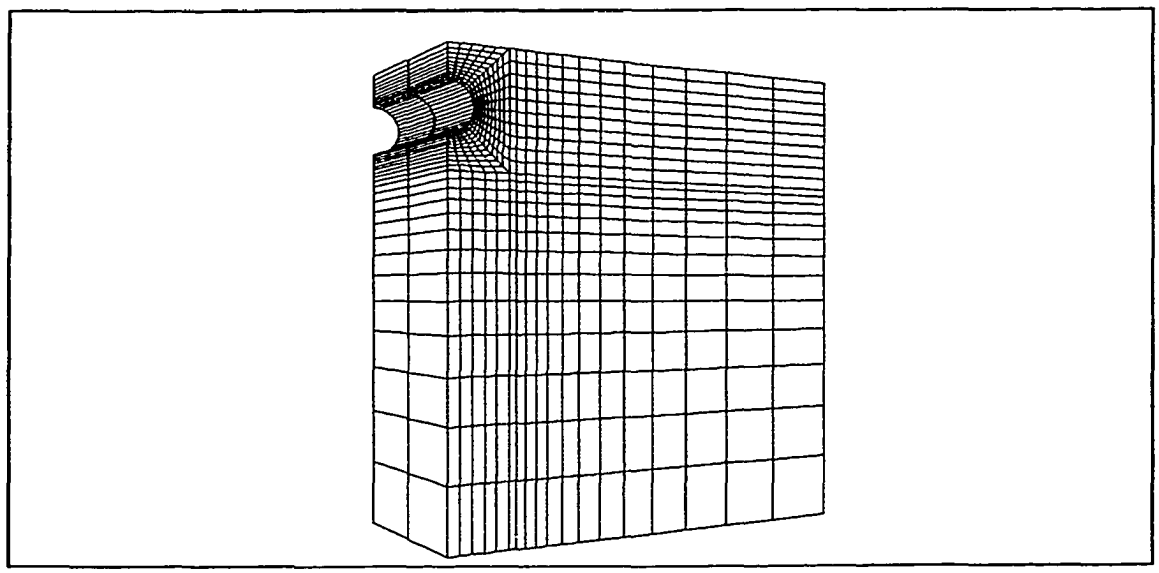

Figure 4.3 Flac3d Grid – Half Symmetry

The Flac3D model is initialized by first simulating gravity loading to develop the in-situ state of stress in the soil. Initial internal stresses that satisfy both equilibrium and gravitational gradient are applied to the domain. The initialized stresses will cut the number of time steps taken for the model to reach equilibrium due to gravity. The displacements of the soil due to the gravitational forces are then initialized to zero. The microtunneling machine and following pipe are modeled at a depth from the ground surface. The soil surrounding the microtunneling machine is assumed to deform under plane strain conditions. To simulate the microtunneling process, a cavity around the pipe is created. Then the soil will fall onto the pipe's outside surface. Once the soil contacts the pipe surface, the pipe will stop the soil's further movement. The pipe and soil will interact until the equilibrium condition is reached. The soil is assumed to be homogeneous and is assigned a Mohr-Coulomb material model.

4.5 Selection of Boundary and Zones

Two important points of concern in building any model are:

1. How the location of the grid boundaries influence model results; and
2. The density of zoning required for an accurate solution in the region of interest

4.5.1 Selection of Boundary Condition

Artificial boundaries are introduced to enclose the chosen number of zones. In the test for selecting an artificial boundary for the semi-infinite soil media as shown in Figure 4.1, the far-right boundary and the far boundary in the negative z-direction were evaluated. The distance between far boundary global axis (D) is 5 × H to 8 × H. The

vertical soil displacements on the ground surface were compared. Figure 4.4 shows the location of the points where the vertical soil displacements are measured.

Figures 4.5, 4.6, 4.7, and 4.8 show the ground settlement trough at D = 5H, D = 6H, D = 7H, and D = 8H respectively. Figure 4.9 shows a comparison of the result for surface settlement at point A-F. Table 4.2 shows the comparison in table format. All ground settlement troughs are similar, but the magnitude of ground settlement increases with the D to H ratio. The ground settlement at D = 7H is almost same as D = 8H. This indicates that to simulate the ground settlement associated with microtunneling with FLAC,^{3D} the far boundary distance equal to seven times the microtunneling machine depth is sufficient to obtain accurate results.

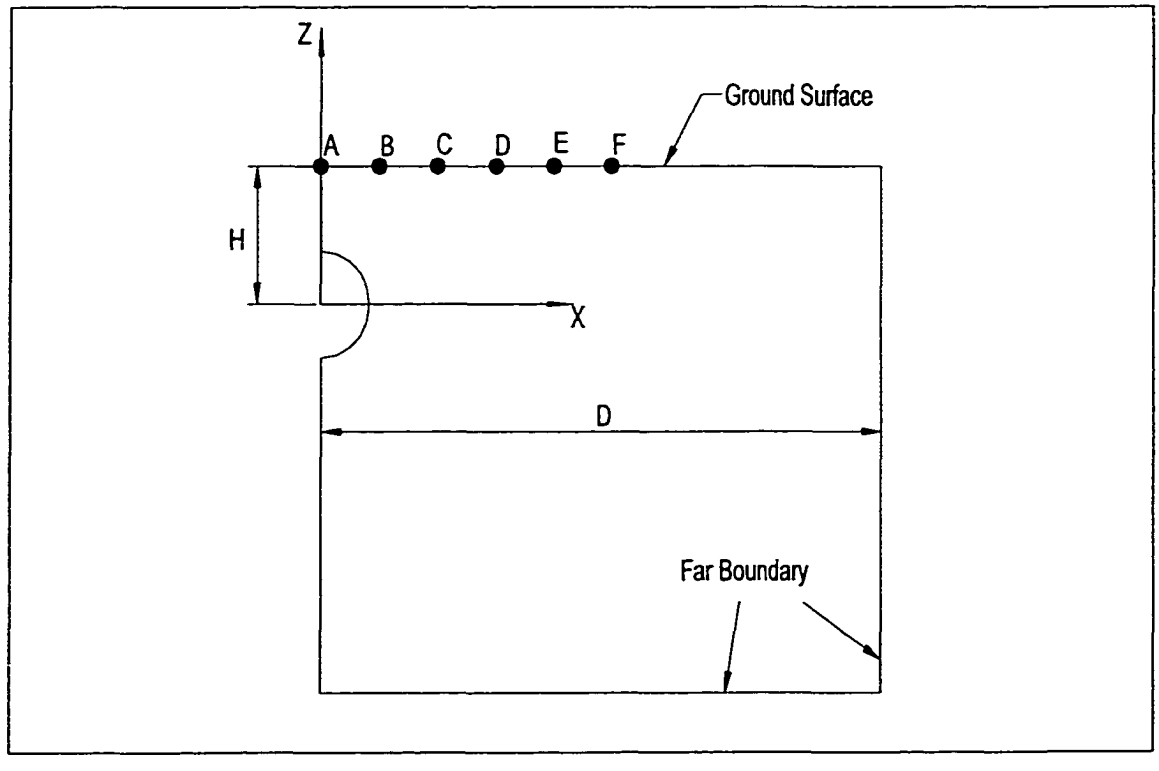

Figure 4.4 Model Showing Locations of Ground Surface Points

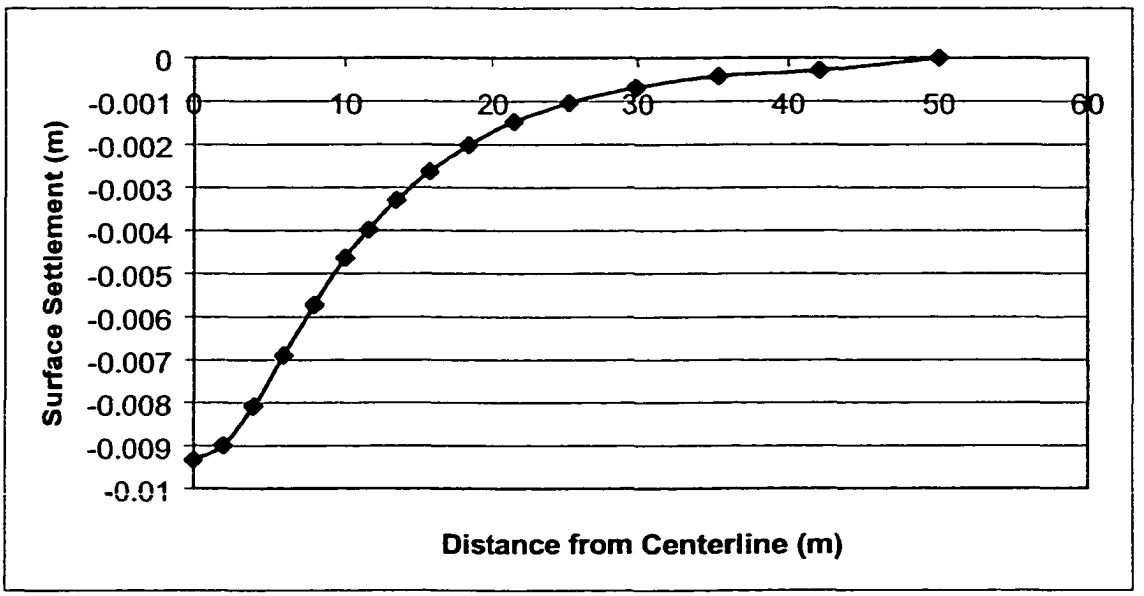

Figure 4.5 Ground Settlement Trough at D = 5H

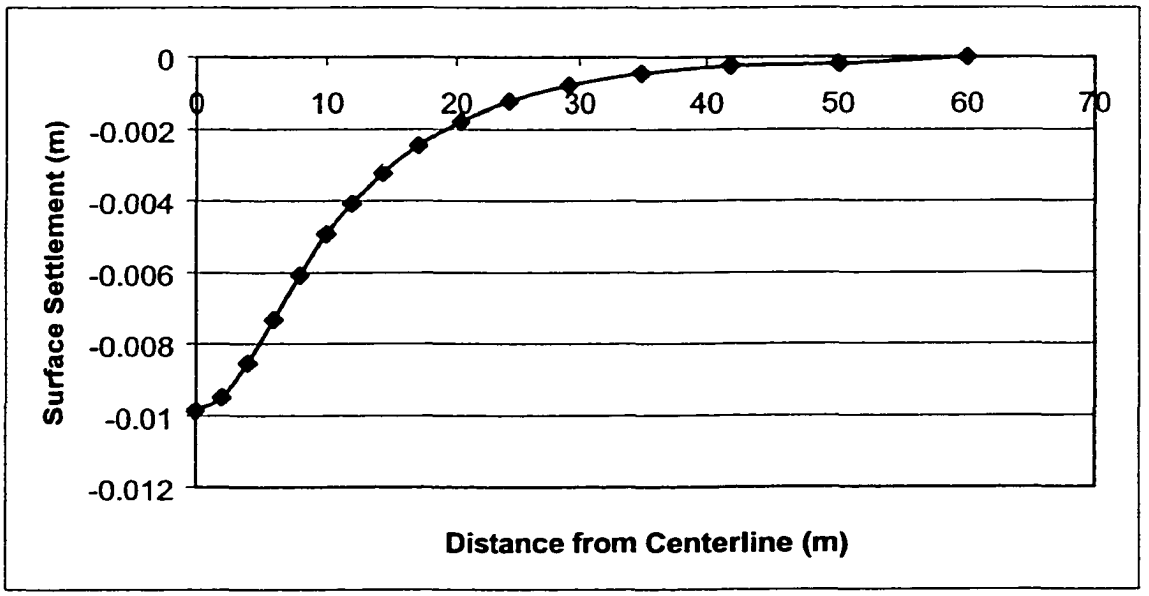

Figure 4.6 Ground Settlement Trough at D = 6H

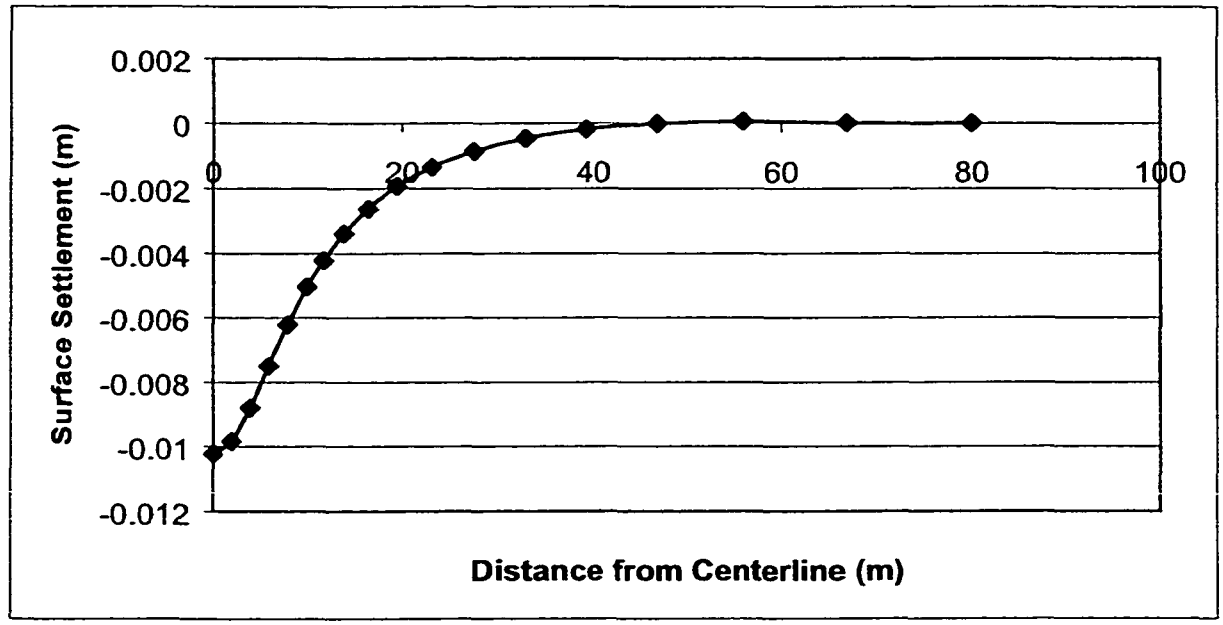

Figure 4.7 Ground Settlement Trough at D = 7H

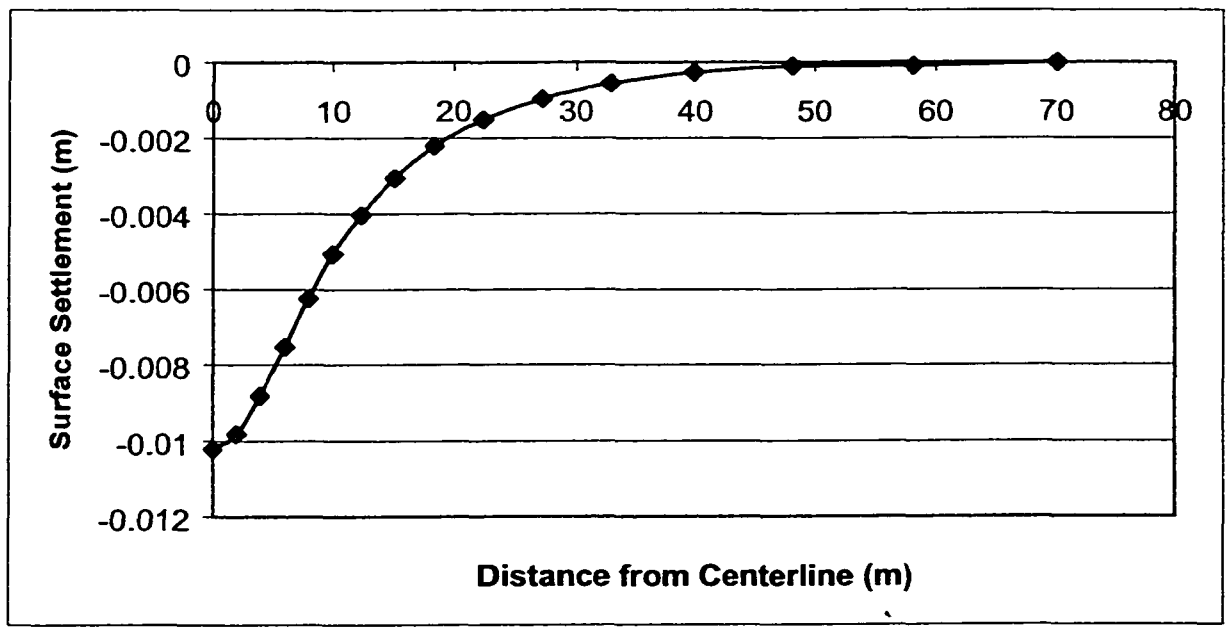

Figure 4.8 Ground Settlement Trough at D = 8H

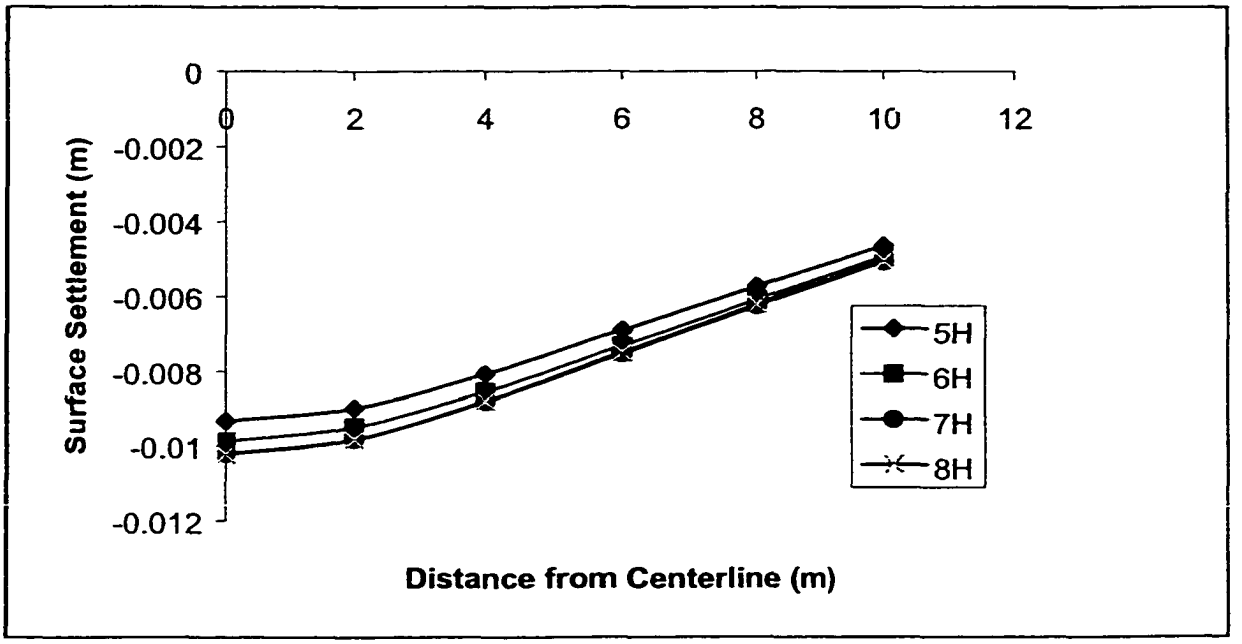

Figure 4.9 Comparison of Soil Displacement for Different Boundary Conditions

Table 4.2 Vertical Soil Displacements on the Ground Surface

Points	Distance along the horizontal axis x (m)	Vertical Soil Displacements in mm			
		5H	6H	7H	8H
A	0.0	-9.33	-9.87	-10.2	-10.2
B	2	-8.99	-9.49	-9.83	-9.83
C	4	-8.08	-8.54	-8.81	-8.80
D	6	-6.90	-7.32	-7.53	-7.50
E	8	-5.73	-6.08	-6.25	-6.22
F	10	-4.64	-4.94	-5.07	-5.04

4.5.2 Selection of Pipe Material

In this test, two different pipe materials were examined, Steel and HDPE (elastic behavior only). The mechanical property of A36 Steel and HDPE is listed in Table 4.3.

The pipe is considered using an elastic model in FLAC^{3D} analysis. The result of ground movement is shown in Figure 4.10. The shape of the two settlement troughs is very similar, and the maximum vertical displacement is almost same. This shows that the pipe properties do not significantly affect the vertical displacement. In the following numerical analysis, the A36 steel pipe is used.

Table 4.3 Mechanical Property of A36 Steel and HDPE

	A36 Steel	HDPE
Elastic Modulus KPa (psi)	2.0×10^{8} (2.90×10^{7})	896×10^{3} (1.30×10^{5})
Tensile Yield Strength Kpa (psi)	248×10^{3} (36000)	22×10^{3} (3200)
Compressive Yield Strength Kpa (psi)	248×10^{3} (36000)	11×10^{3} (1600)

The ground movements were studied in different type of soils due to microtunneling. The soil parameters were selected from the Flac^{3D} manual. Table 4.4 gives the types of soils selected and their respective strength properties.

Figure 4.11 shows the graphs for vertical displacement of soil at the ground surface for the selected soils. The figure indicates that the ground movement for gravel, sandy gravel, and sand were smaller compared to the silt and clay soils. The maximum surface displacement of soil for silt and clay was higher than the maximum surface displacement of soil for gravel and sand. The reason for the movement for gravel and sand soil being smaller than the movement for clay and silt is that the elastic modulus of gravel and sand is much higher than the elastic modulus of silt and clay. However, it should be noted that sand and gravel are still at risk of significant face stability problems leading to large ground movements.

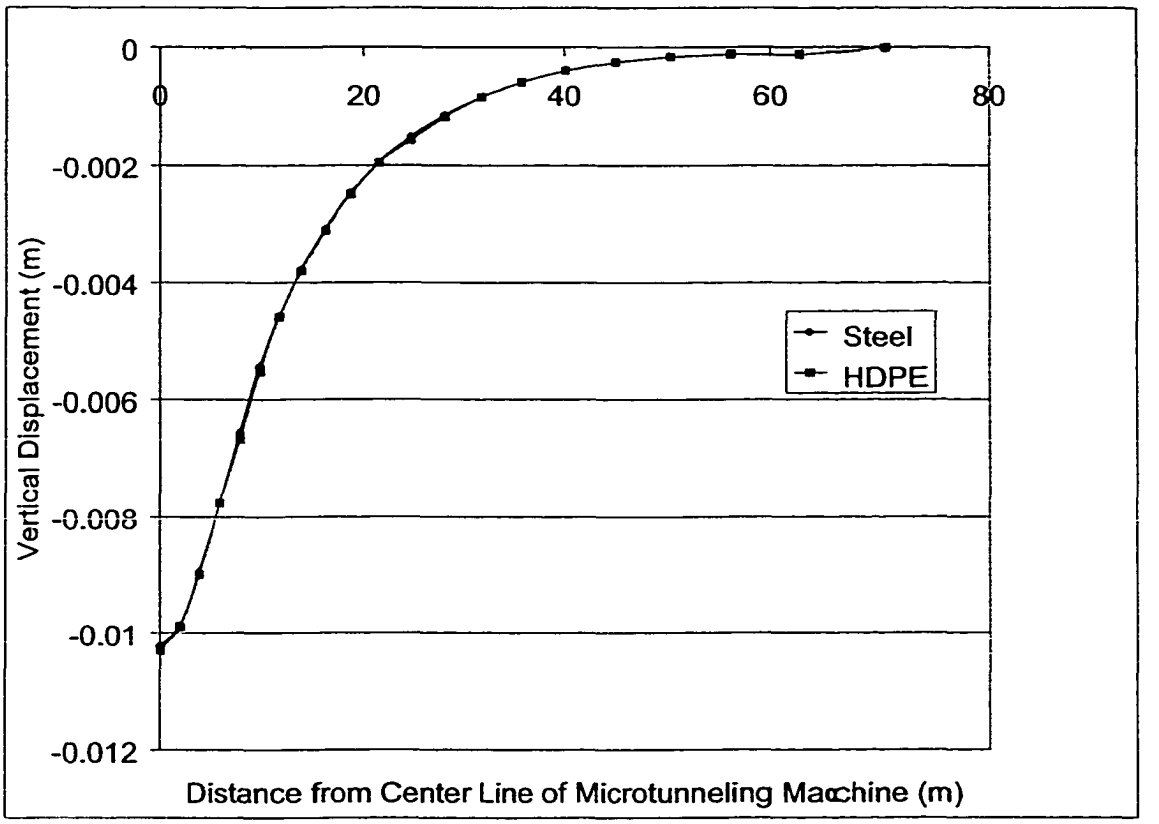

Figure 4.10 Vertical Displacement at Ground Surface For Different Pipe Materials

Table 4.4 Selected Elastic Constants and Strength Properties for Soils [Oritz et al., 1986]

Soil	Dry Density (kg/m^3)	Elastic Modulus (Mpa)	Cohesion (Kpa)	Friction Angle (degree)
Gravel	1600	40		34-32
Sandy Gravel with few fines	2100	40		35-32
Sandy Gravel with silty or Clayey fines	2100	40	1	35-33
Mixture of Gravel and sand with fines	2000	15	3	28-22
Uniform sand – fine	1600	15		32-30
Uniform sand – coarse	1600	25		34-30
Well-graded sand	1800	20		33-32
Low plasticity silt	1750	4	2	28-25
Medium to high plasticity silt	1700	3	3	25-22
Low plasticity clay	1900	2	6	24-20
Medium plasticity clay	1800	1	8	20-10
High plasticity clay	1650	0.6	10	17-6
Organic silt or clay	1550	0.5	7	20-15

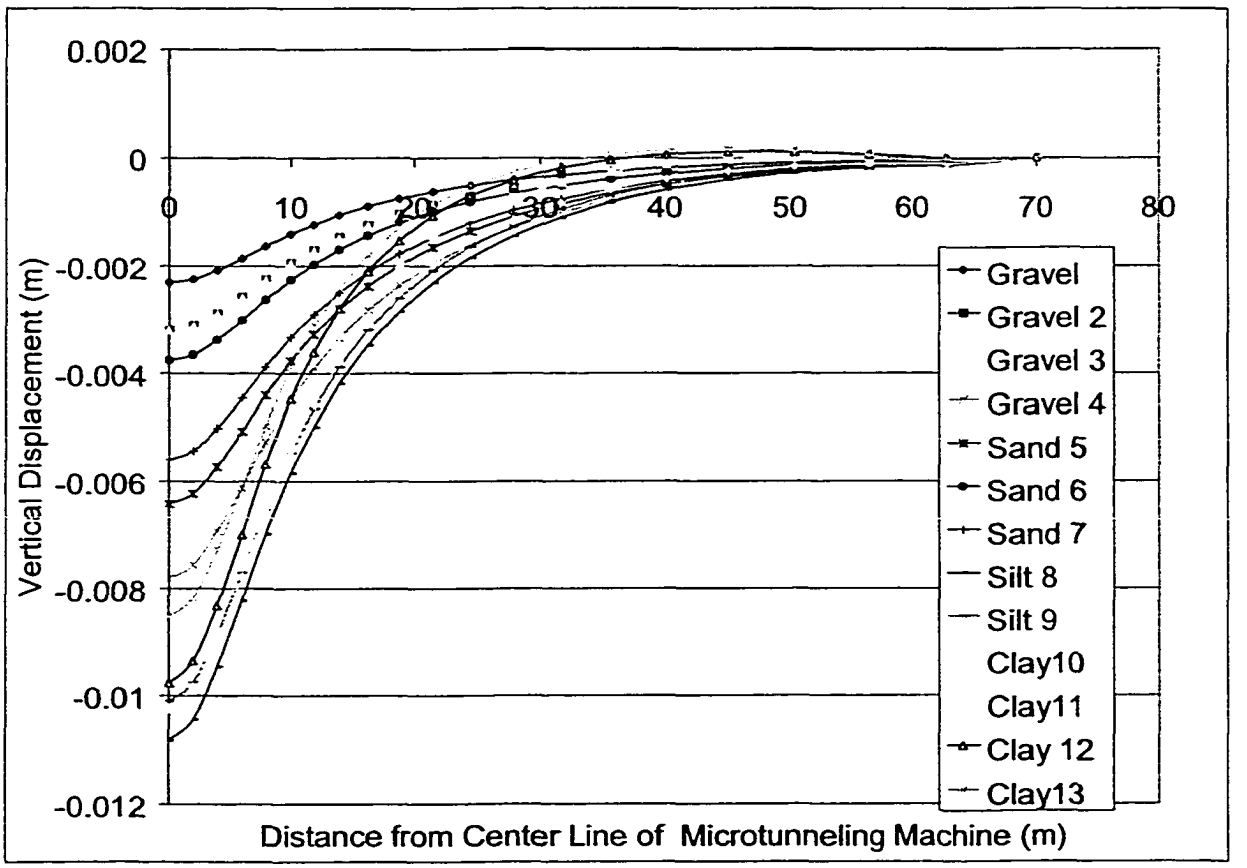

Figure 4.11 Simulated Ground Movement with Different Soil Type (See Table 4.4 for soil type description)

Table 4.5 Ground Displacement (meter) for Different Types of Soil

Distance	Gravel	Gravel 2	Gravel 3	Gravel 4	Sand 5	Sand 6	Sand 7	Silt 8	Silt 9	Clay10	Clay11	Clay 12	Caly13
0.00E+00	-2.31E-03	-3.20E-03	-3.20E-03	-7.80E-03	-6.43E-03	-3.76E-03	-5.60E-03	-1.08E-02	-1.01E-02	-1.02E-02	-1.03E-02	-9.77E-03	-8.52E-03
2.00E+00	-2.24E-03	-3.11E-03	-3.11E-03	-7.56E-03	-6.23E-03	-3.66E-03	-5.44E-03	-1.04E-02	-9.76E-03	-9.87E-03	-9.85E-03	-9.36E-03	-8.16E-03
4.00E+00	-2.08E-03	-2.88E-03	-2.88E-03	-6.92E-03	-5.73E-03	-3.38E-03	-5.02E-03	-9.46E-03	-8.86E-03	-8.95E-03	-8.82E-03	-8.32E-03	-7.27E-03
6.00E+00	-1.86E-03	-2.58E-03	-2.58E-03	-6.10E-03	-5.08E-03	-3.01E-03	-4.46E-03	-8.22E-03	-7.71E-03	-7.76E-03	-7.52E-03	-7.00E-03	-6.14E-03
8.00E+00	-1.63E-03	-2.26E-03	-2.26E-03	-5.27E-03	-4.40E-03	-2.63E-03	-3.88E-03	-6.99E-03	-6.54E-03	-6.55E-03	-6.21E-03	-5.68E-03	-4.96E-03
1.00E+01	-1.41E-03	-1.95E-03	-1.95E-03	-4.49E-03	-3.77E-03	-2.26E-03	-3.34E-03	-5.85E-03	-5.46E-03	-5.43E-03	-5.00E-03	-4.47E-03	-3.88E-03
1.19E+01	-1.23E-03	-1.70E-03	-1.70E-03	-3.90E-03	-3.28E-03	-1.97E-03	-2.91E-03	-4.99E-03	-4.64E-03	-4.58E-03	-4.11E-03	-3.61E-03	-3.11E-03
1.40E+01	-1.06E-03	-1.46E-03	-1.46E-03	-3.33E-03	-2.81E-03	-1.69E-03	-2.49E-03	-4.19E-03	-3.88E-03	-3.79E-03	-3.29E-03	-2.80E-03	-2.41E-03
1.63E+01	-8.97E-04	-1.24E-03	-1.24E-03	-2.82E-03	-2.38E-03	-1.43E-03	-2.11E-03	-3.48E-03	-3.20E-03	-3.08E-03	-2.59E-03	-2.10E-03	-1.80E-03
1.88E+01	-7.52E-04	-1.04E-03	-1.04E-03	-2.36E-03	-1.99E-03	-1.20E-03	-1.78E-03	-2.85E-03	-2.60E-03	-2.48E-03	-1.99E-03	-1.54E-03	-1.28E-03
2.15E+01	-6.22E-04	-8.66E-04	-8.66E-04	-1.96E-03	-1.65E-03	-9.95E-04	-1.47E-03	-2.31E-03	-2.09E-03	-1.95E-03	-1.48E-03	-1.07E-03	-8.64E-04
2.46E+01	-5.08E-04	-7.09E-04	-7.09E-04	-1.60E-03	-1.35E-03	-8.13E-04	-1.21E-03	-1.84E-03	-1.64E-03	-1.51E-03	-1.07E-03	-6.96E-04	-5.26E-04
2.79E+01	-4.08E-04	-5.71E-04	-5.71E-04	-1.29E-03	-1.09E-03	-6.52E-04	-9.70E-04	-1.44E-03	-1.27E-03	-1.14E-03	-7.38E-04	-4.15E-04	-2.61E-04
3.16E+01	-3.20E-04	-4.50E-04	-4.50E-04	-1.01E-03	-8.54E-04	-5.12E-04	-7.63E-04	-1.11E-03	-9.53E-04	-8.35E-04	-4.65E-04	-1.89E-04	-6.93E-05
3.56E+01	-2.44E-04	-3.45E-04	-3.45E-04	-7.76E-04	-6.52E-04	-3.91E-04	-5.84E-04	-8.19E-04	-6.93E-04	-5.82E-04	-2.64E-04	-3.68E-05	6.08E-05
4.01E+01	-1.80E-04	-2.55E-04	-2.55E-04	-5.73E-04	-4.81E-04	-2.88E-04	-4.30E-04	-5.85E-04	-4.84E-04	-3.87E-04	-1.17E-04	6.43E-05	1.41E-04
4.50E+01	-1.27E-04	-1.80E-04	-1.80E-04	-4.05E-04	-3.38E-04	-2.03E-04	-3.02E-04	-4.01E-04	-3.22E-04	-2.45E-04	-2.65E-05	1.07E-04	1.63E-04
5.04E+01	-8.59E-05	-1.21E-04	-1.21E-04	-2.72E-04	-2.26E-04	-1.36E-04	-2.02E-04	-2.66E-04	-2.08E-04	-1.54E-04	4.73E-06	1.03E-04	1.46E-04
5.63E+01	-5.54E-05	-7.73E-05	-7.73E-05	-1.72E-04	-1.43E-04	-8.71E-05	-1.27E-04	-1.76E-04	-1.38E-04	-1.10E-04	-7.33E-06	6.08E-05	9.36E-05
6.28E+01	-3.72E-05	-5.09E-05	-5.09E-05	-1.13E-04	-9.29E-05	-5.80E-05	-8.29E-05	-1.36E-04	-1.15E-04	-1.10E-04	-5.63E-05	-1.09E-05	1.00E-05
7.00E+01	0.00E+00	0.00E+00	0.00E+00	0.00E+00	0.00E+00	0.00E+00	0.00E+00	0.00E+00	0.00E+00	0.00E+00	0.00E+00	0.00E+00	0.00E+00

Note: See Table 4.4 for soil description

4.6 Effect of Bulk Modulus and Shear Modulus

The Flac3D models were used to simulate the effect of varying the shear modulus and bulk modulus

4.6.1 Effect of Bulk Modulus on Extent of Settlement

The models were simulated using a constant shear modulus (G) of 3.84×10^6 Pa (557 psi), varying the bulk modulus (K) from a value of 5×10^6 Pa (725 psi) to 35×10^6 Pa (5076 psi). The ground movement data are presented in Table 4.6.

Figure 4.12 shows the results for vertical soil displacements at the ground surface under the effect of a varying bulk modulus. Figure 4.13 shows the results for horizontal displacement at the ground surface under the effect of a varying bulk modulus. Overall, the results indicate that a higher bulk modulus corresponds to decrease in the extent of vertical surface displacement and horizontal surface displacement.

4.6.2 Effect of Shear Modulus on Extent of Settlement

The models were simulated using a constant bulk modulus (K) 3.84×10^6 Pa (577 psi), varying the shear modulus (G) from a value of 5×10^6 Pa (725 psi) to 35×10^6 Pa (5076 psi). The ground movement data are presented in Table 4.7.

Figure 4.14 shows the results for vertical soil displacements at the ground surface under the effect of a varying shear modulus (G). Figure 4.15 shows the results for the horizontal displacement at the ground surface under the effect of a varying shear modulus (G). The results indicate that a higher shear modulus corresponds to an increase in the extent of vertical surface displacement and horizontal surface displacement.

4.6.3 Effect of Bulk and Shear Modulus on Magnitude of Displacement

Figures 4.12 and 4.14 show that the maximum vertical displacement occurred at the ground surface directly above the centerline of microtunneling machine. Figures 4.13 and 4.15 indicate that the maximum horizontal displacement occurred at a horizontal distance equal to the depth of microtunneling.

Small horizontal and vertical displacements at the ground surface were seen for soils having a high bulk modulus. The vertical and horizontal displacement decreased as bulk modulus increased. High horizontal and vertical displacements at the ground surface were seen for soils having a low shear modulus.

Figure 4.16 shows the vertical displacement contour and displacement vector plot.

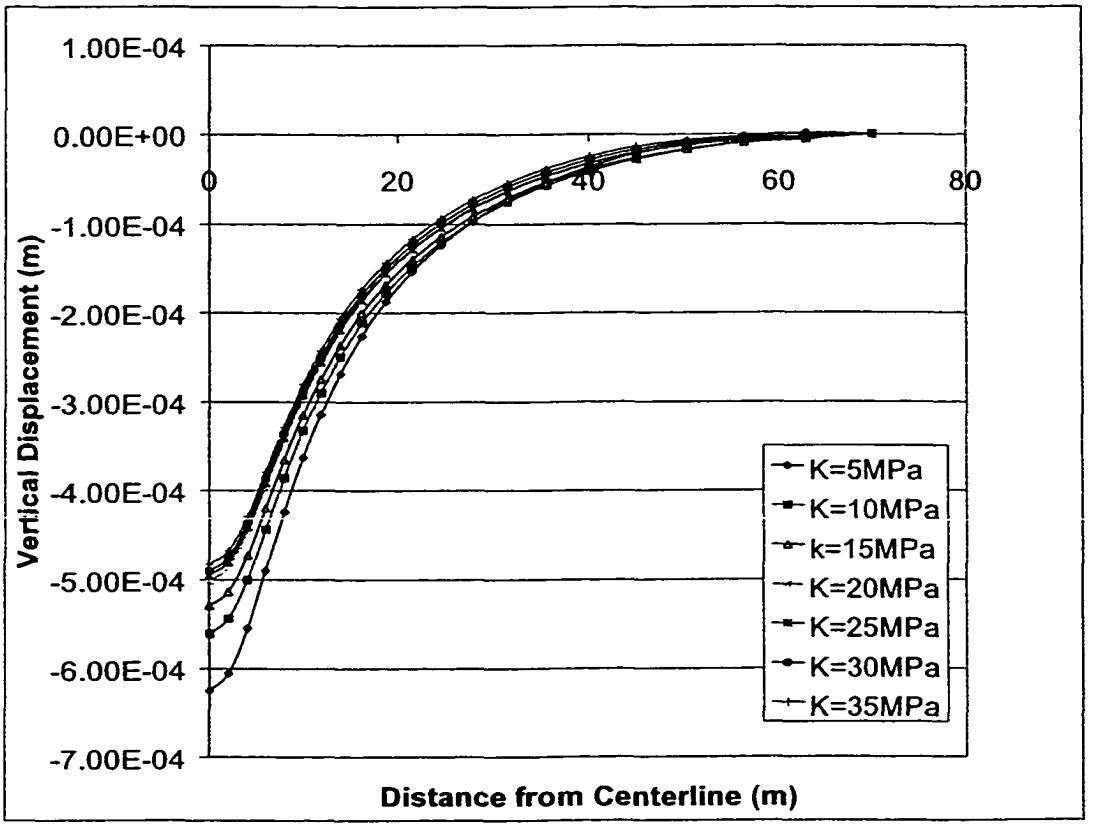

Figure 4.12 Variation of Ground Surface Settlement with Bulk Modulus

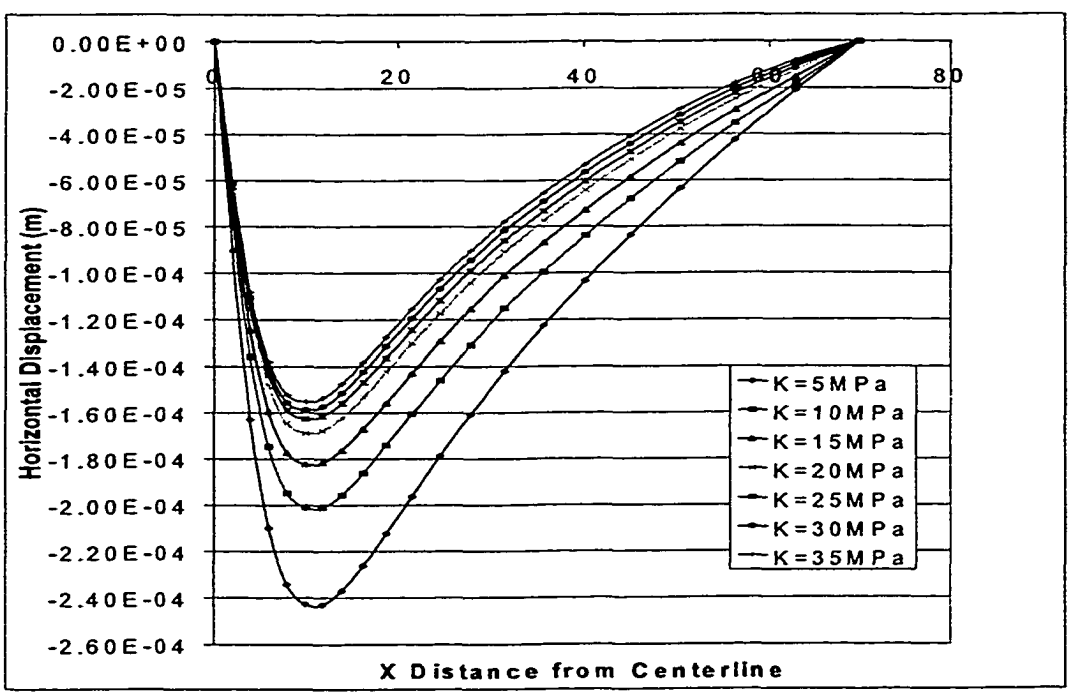

Figure 4.13 Variation of Ground Surface Horizontal Displacement with Bulk Modulus

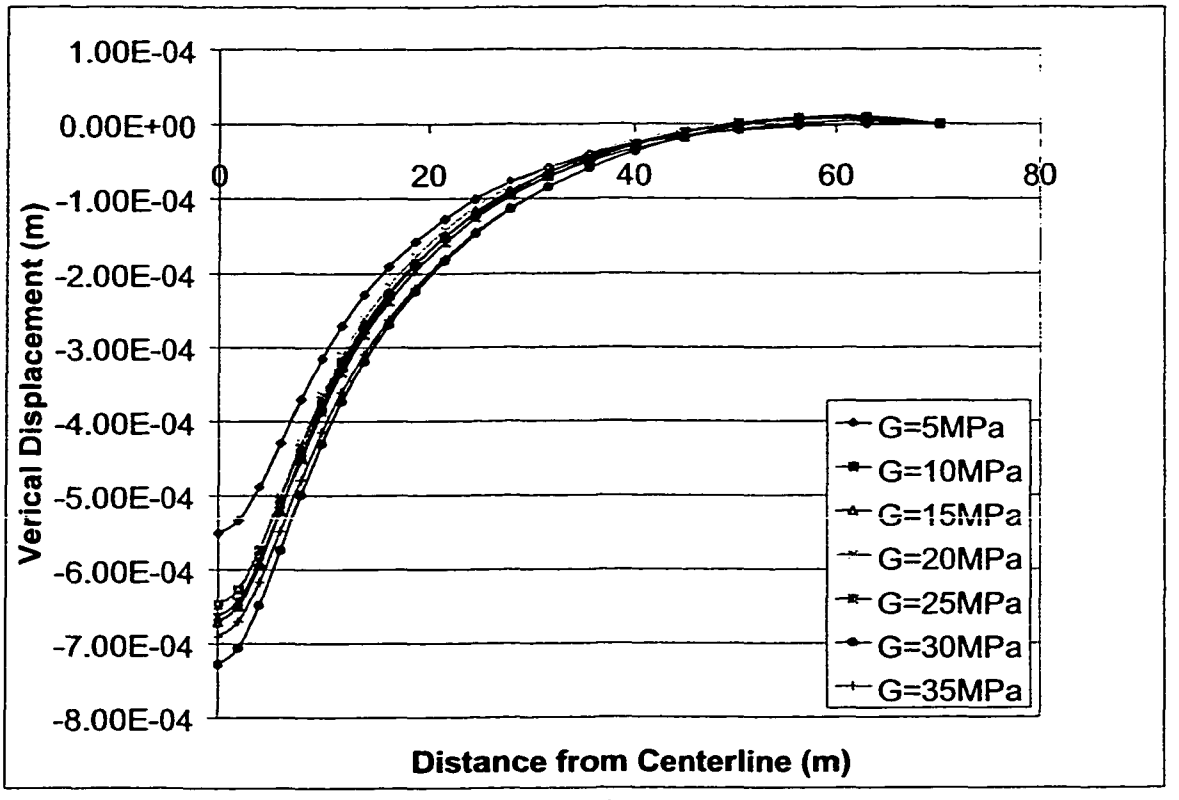

Figure 4.14 Variation of Ground Surface Settlement with Shear Modulus

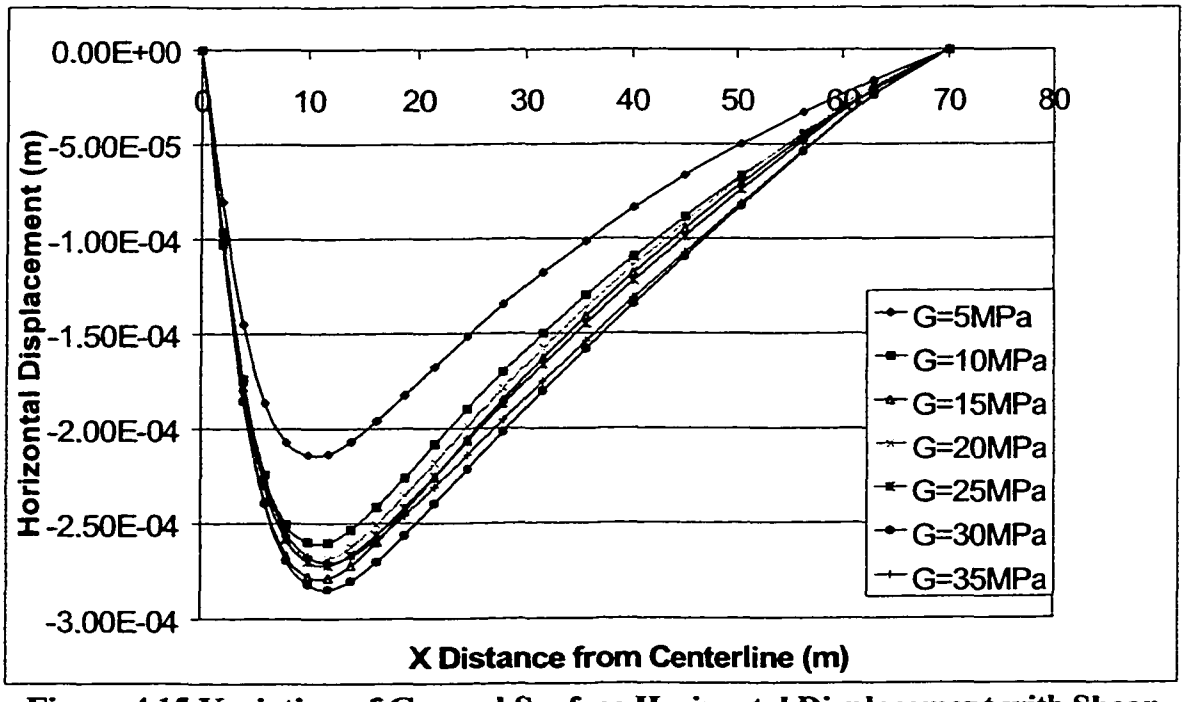

Figure 4.15 Variation of Ground Surface Horizontal Displacement with Shear Modulus

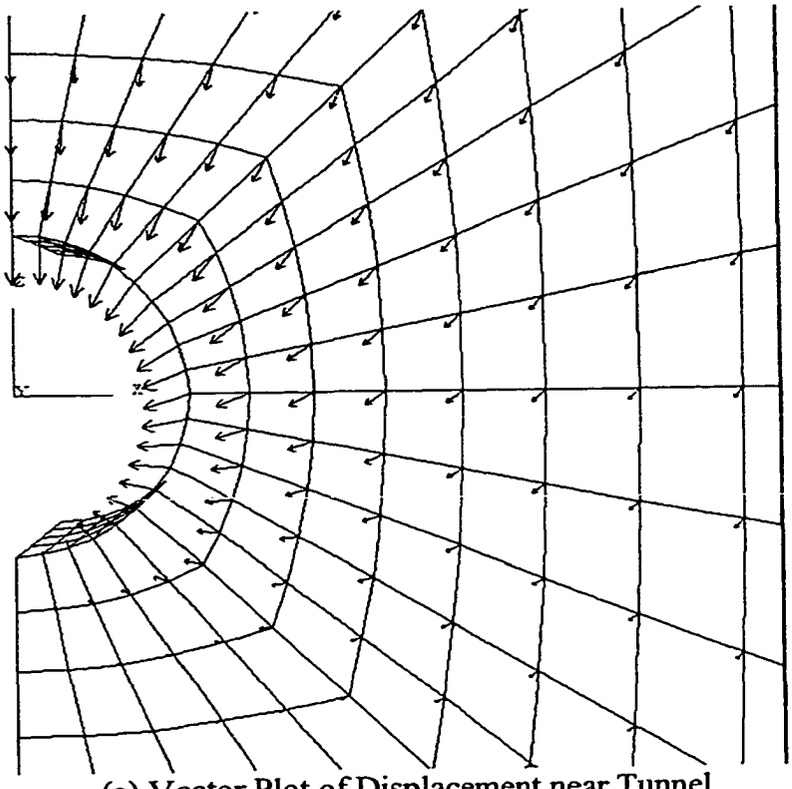

(a) Vector Plot of Displacement near Tunnel

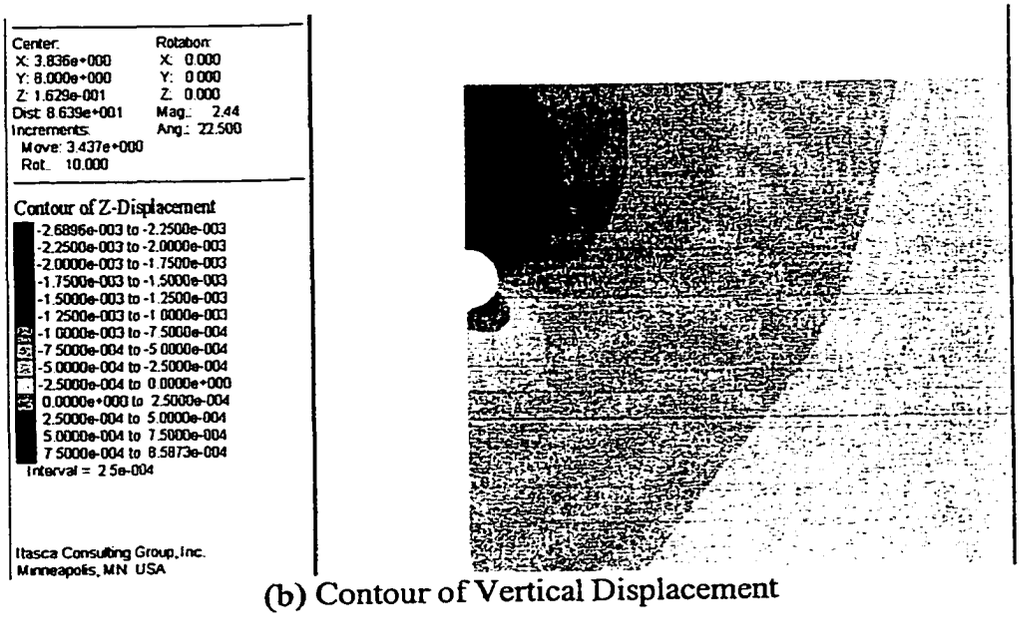

(b) Contour of Vertical Displacement

Figure 4.16 (a) Vector and (b) Contour Plot of Soil Displacement

Table 4.6 Vertical Gound Surface Displacement (meter) for Different Bulk Moduli

Distance from Centerline (m)	Bulk Modulus (MPa)						
	5	10	15	20	25	30	35
0.0	-6.25E-04	-5.61E-04	-5.30E-04	-5.01E-04	-4.95E-04	-4.90E-04	-4.83E-04
2.0	-6.06E-04	-5.44E-04	-5.14E-04	-4.86E-04	-4.80E-04	-4.76E-04	-4.68E-04
4.0	-5.55E-04	-5.01E-04	-4.73E-04	-4.47E-04	-4.41E-04	-4.37E-04	-4.29E-04
6.0	-4.90E-04	-4.44E-04	-4.20E-04	-3.97E-04	-3.92E-04	-3.87E-04	-3.80E-04
8.0	-4.24E-04	-3.86E-04	-3.66E-04	-3.45E-04	-3.41E-04	-3.35E-04	-3.29E-04
10.0	-3.63E-04	-3.32E-04	-3.15E-04	-2.96E-04	-2.92E-04	-2.86E-04	-2.80E-04
11.9	-3.14E-04	-2.90E-04	-2.74E-04	-2.57E-04	-2.55E-04	-2.49E-04	-2.43E-04
14.0	-2.68E-04	-2.49E-04	-2.36E-04	-2.20E-04	-2.18E-04	-2.13E-04	-2.06E-04
16.3	-2.26E-04	-2.12E-04	-2.00E-04	-1.87E-04	-1.85E-04	-1.80E-04	-1.74E-04
18.8	-1.87E-04	-1.78E-04	-1.68E-04	-1.57E-04	-1.55E-04	-1.50E-04	-1.44E-04
21.5	-1.54E-04	-1.48E-04	-1.40E-04	-1.29E-04	-1.28E-04	-1.23E-04	-1.17E-04
24.6	-1.23E-04	-1.21E-04	-1.14E-04	-1.05E-04	-1.04E-04	-9.90E-05	-9.37E-05
27.9	-9.70E-05	-9.65E-05	-9.15E-05	-8.36E-05	-8.20E-05	-7.77E-05	-7.25E-05
31.6	-7.36E-05	-7.57E-05	-7.12E-05	-6.44E-05	-6.29E-05	-5.86E-05	-5.43E-05
35.6	-5.36E-05	-5.71E-05	-5.38E-05	-4.76E-05	-4.63E-05	-4.24E-05	-3.82E-05
40.1	-3.64E-05	-4.14E-05	-3.89E-05	-3.35E-05	-3.18E-05	-2.83E-05	-2.46E-05
45.0	-2.18E-05	-2.78E-05	-2.64E-05	-2.16E-05	-2.04E-05	-1.71E-05	-1.39E-05
50.4	-1.04E-05	-1.73E-05	-1.66E-05	-1.30E-05	-1.15E-05	-9.20E-06	-6.71E-06
56.3	-2.55E-06	-9.13E-06	-9.38E-06	-7.26E-06	-6.22E-06	-4.52E-06	-2.81E-06
62.8	1.43E-06	-3.99E-06	-5.26E-06	-4.76E-06	-4.32E-06	-3.32E-06	-2.44E-06
70.0	0.00E+00	0.00E+00	0.00E+00	0.00E+00	0.00E+00	0.00E+00	0.00E+00

Table 4.7 Horizontal Ground Surface Displacement (meter) for Different Bulk Moduli

Distance from Centerline (m)	Bulk Modulus (MPa)						
	5	10	15	20	25	30	35
0.0	0.00E+00	0.00E+00	0.00E+00	0.00E+00	0.00E+00	0.00E+00	0.00E+00
2.0	-9.06E-05	-7.57E-05	-6.93E-05	-6.46E-05	-6.27E-05	-6.17E-05	-6.06E-05
4.0	-1.63E-04	-1.36E-04	-1.24E-04	-1.16E-04	-1.12E-04	-1.10E-04	-1.08E-04
6.0	-2.10E-04	-1.75E-04	-1.60E-04	-1.48E-04	-1.44E-04	-1.41E-04	-1.38E-04
8.0	-2.34E-04	-1.95E-04	-1.77E-04	-1.65E-04	-1.59E-04	-1.56E-04	-1.52E-04
10.0	-2.43E-04	-2.01E-04	-1.82E-04	-1.69E-04	-1.63E-04	-1.59E-04	-1.55E-04
11.9	-2.43E-04	-2.01E-04	-1.82E-04	-1.68E-04	-1.62E-04	-1.57E-04	-1.54E-04
14.0	-2.37E-04	-1.96E-04	-1.76E-04	-1.62E-04	-1.56E-04	-1.51E-04	-1.47E-04
16.3	-2.26E-04	-1.86E-04	-1.67E-04	-1.53E-04	-1.47E-04	-1.42E-04	-1.38E-04
18.8	-2.12E-04	-1.74E-04	-1.56E-04	-1.42E-04	-1.36E-04	-1.31E-04	-1.28E-04
21.5	-1.96E-04	-1.61E-04	-1.43E-04	-1.30E-04	-1.24E-04	-1.20E-04	-1.15E-04
24.6	-1.79E-04	-1.46E-04	-1.29E-04	-1.17E-04	-1.12E-04	-1.07E-04	-1.03E-04
27.9	-1.61E-04	-1.31E-04	-1.15E-04	-1.04E-04	-9.90E-05	-9.45E-05	-9.04E-05
31.6	-1.42E-04	-1.15E-04	-1.01E-04	-9.10E-05	-8.61E-05	-8.17E-05	-7.78E-05
35.6	-1.23E-04	-9.98E-05	-8.70E-05	-7.75E-05	-7.34E-05	-6.92E-05	-6.54E-05
40.1	-1.04E-04	-8.39E-05	-7.29E-05	-6.42E-05	-6.04E-05	-5.66E-05	-5.31E-05
45.0	-8.38E-05	-6.80E-05	-5.85E-05	-5.09E-05	-4.76E-05	-4.41E-05	-4.09E-05
50.4	-6.35E-05	-5.18E-05	-4.39E-05	-3.77E-05	-3.48E-05	-3.18E-05	-2.91E-05
56.3	-4.25E-05	-3.53E-05	-2.95E-05	-2.47E-05	-2.23E-05	-2.00E-05	-1.80E-05
62.8	-2.10E-05	-1.83E-05	-1.52E-05	-1.23E-05	-1.07E-05	-9.30E-06	-7.94E-06
70.0	0.00E+00	0.00E+00	0.00E+00	0.00E+00	0.00E+00	0.00E+00	0.00E+00

Table 4.8 Vertical Ground Surface Displacement (meter) for Different Shear Moduli

Distance from Centerline (m)	Shear Modulus (MPa)						
	5	10	15	20	25	30	35
0.0	-5.51E-04	-6.47E-04	-6.71E-04	-6.46E-04	-6.63E-04	-7.28E-04	-6.90E-04
2.0	-5.33E-04	-6.27E-04	-6.49E-04	-6.25E-04	-6.43E-04	-7.06E-04	-6.70E-04
4.0	-4.88E-04	-5.74E-04	-5.93E-04	-5.70E-04	-5.89E-04	-6.48E-04	-6.17E-04
6.0	-4.29E-04	-5.05E-04	-5.21E-04	-5.00E-04	-5.20E-04	-5.74E-04	-5.48E-04
8.0	-3.70E-04	-4.35E-04	-4.48E-04	-4.29E-04	-4.51E-04	-4.99E-04	-4.79E-04
10.0	-3.15E-04	-3.71E-04	-3.81E-04	-3.64E-04	-3.87E-04	-4.30E-04	-4.15E-04
11.9	-2.70E-04	-3.19E-04	-3.27E-04	-3.11E-04	-3.33E-04	-3.73E-04	-3.61E-04
14.0	-2.29E-04	-2.71E-04	-2.76E-04	-2.62E-04	-2.83E-04	-3.19E-04	-3.10E-04
16.3	-1.91E-04	-2.26E-04	-2.29E-04	-2.17E-04	-2.38E-04	-2.69E-04	-2.63E-04
18.8	-1.57E-04	-1.86E-04	-1.88E-04	-1.77E-04	-1.96E-04	-2.24E-04	-2.19E-04
21.5	-1.28E-04	-1.51E-04	-1.51E-04	-1.42E-04	-1.59E-04	-1.84E-04	-1.80E-04
24.6	-1.01E-04	-1.21E-04	-1.19E-04	-1.10E-04	-1.26E-04	-1.47E-04	-1.45E-04
27.9	-7.81E-05	-9.41E-05	-9.02E-05	-8.31E-05	-9.65E-05	-1.14E-04	-1.13E-04
31.6	-5.89E-05	-7.07E-05	-6.53E-05	-5.94E-05	-7.06E-05	-8.50E-05	-8.44E-05
35.6	-4.14E-05	-5.05E-05	-4.42E-05	-3.90E-05	-4.79E-05	-5.90E-05	-5.90E-05
40.1	-2.70E-05	-3.32E-05	-2.60E-05	-2.17E-05	-2.84E-05	-3.65E-05	-3.66E-05
45.0	-1.65E-05	-1.86E-05	-1.16E-05	-7.92E-06	-1.22E-05	-1.73E-05	-1.77E-05
50.4	-8.40E-06	-7.26E-06	-4.62E-07	2.51E-06	2.13E-07	-2.25E-06	-2.51E-06
56.3	-2.89E-06	7.38E-07	6.43E-06	8.46E-06	8.10E-06	7.67E-06	7.74E-06
62.8	-2.60E-07	3.89E-06	7.27E-06	8.40E-06	9.04E-06	9.77E-06	9.89E-06
70.0	0.00E+00	0.00E+00	0.00E+00	0.00E+00	0.00E+00	0.00E+00	0.00E+00

Table 4.9 Horizontal Ground Surface Displacement (meter) for Different Shear Moduli

Distance from Centerline (m)	Shear Modulus (MPa)						
	5	10	15	20	25	30	35
0.0	0.00E+00	0.00E+00	0.00E+00	0.00E+00	0.00E+00	0.00E+00	0.00E+00
2.0	-8.06E-05	-9.67E-05	-1.03E-04	-9.94E-05	-9.89E-05	-1.03E-04	-9.62E-05
4.0	-1.45E-04	-1.74E-04	-1.85E-04	-1.79E-04	-1.78E-04	-1.85E-04	-1.74E-04
6.0	-1.86E-04	-2.24E-04	-2.38E-04	-2.30E-04	-2.30E-04	-2.40E-04	-2.25E-04
8.0	-2.07E-04	-2.51E-04	-2.67E-04	-2.58E-04	-2.58E-04	-2.69E-04	-2.54E-04
10.0	-2.14E-04	-2.60E-04	-2.78E-04	-2.68E-04	-2.70E-04	-2.82E-04	-2.67E-04
11.9	-2.13E-04	-2.60E-04	-2.79E-04	-2.69E-04	-2.72E-04	-2.85E-04	-2.71E-04
14.0	-2.07E-04	-2.53E-04	-2.72E-04	-2.62E-04	-2.67E-04	-2.80E-04	-2.67E-04
16.3	-1.96E-04	-2.42E-04	-2.60E-04	-2.51E-04	-2.56E-04	-2.70E-04	-2.59E-04
18.8	-1.83E-04	-2.26E-04	-2.44E-04	-2.36E-04	-2.42E-04	-2.56E-04	-2.46E-04
21.5	-1.68E-04	-2.09E-04	-2.26E-04	-2.18E-04	-2.25E-04	-2.40E-04	-2.31E-04
24.6	-1.52E-04	-1.90E-04	-2.06E-04	-1.99E-04	-2.07E-04	-2.22E-04	-2.14E-04
27.9	-1.34E-04	-1.70E-04	-1.85E-04	-1.79E-04	-1.87E-04	-2.02E-04	-1.96E-04
31.6	-1.18E-04	-1.50E-04	-1.63E-04	-1.58E-04	-1.67E-04	-1.81E-04	-1.75E-04
35.6	-1.01E-04	-1.30E-04	-1.41E-04	-1.36E-04	-1.45E-04	-1.58E-04	-1.54E-04
40.1	-8.39E-05	-1.10E-04	-1.18E-04	-1.14E-04	-1.22E-04	-1.35E-04	-1.32E-04
45.0	-6.67E-05	-8.86E-05	-9.50E-05	-9.15E-05	-9.89E-05	-1.09E-04	-1.07E-04
50.4	-5.00E-05	-6.71E-05	-7.11E-05	-6.81E-05	-7.42E-05	-8.27E-05	-8.15E-05
56.3	-3.32E-05	-4.48E-05	-4.63E-05	-4.37E-05	-4.82E-05	-5.41E-05	-5.33E-05
62.8	-1.65E-05	-2.15E-05	-2.10E-05	-1.93E-05	-2.14E-05	-2.42E-05	-2.37E-05
70.0	0.00E+00	0.00E+00	0.00E+00	0.00E+00	0.00E+00	0.00E+00	0.00E+00

4.7 Effect of Elastic Modulus, Poisson's Ratio, Cohesion, Friction Angle and Dilation Angle

The common model parameters are as follows:

The depth of microtunneling is 10 m.

The product pipe radius is 0.5 m.

4.7.1 Effect of Young's modulus

A total of 7 models were test to check the effect of elastic modulus. The parameters used in the analysis are as follows:

Elastic modulus: 0.5 MPa, 1.0 MPa, 5.0MPa, 10,0MPa, 20.0MPa, 30MPa, and 40.0Mpa.

Poisson Ratio: 0.3

Cohesion: 2kPa

Friction angle: 15°

The results of vertical and horizontal displacements at the ground surface are shown in Figure 4.17 and 4.18. The displacement data are listed in Table 4.10 and 4.11. Both vertical and horizontal displacement decreases with the increase of the Young's modulus.

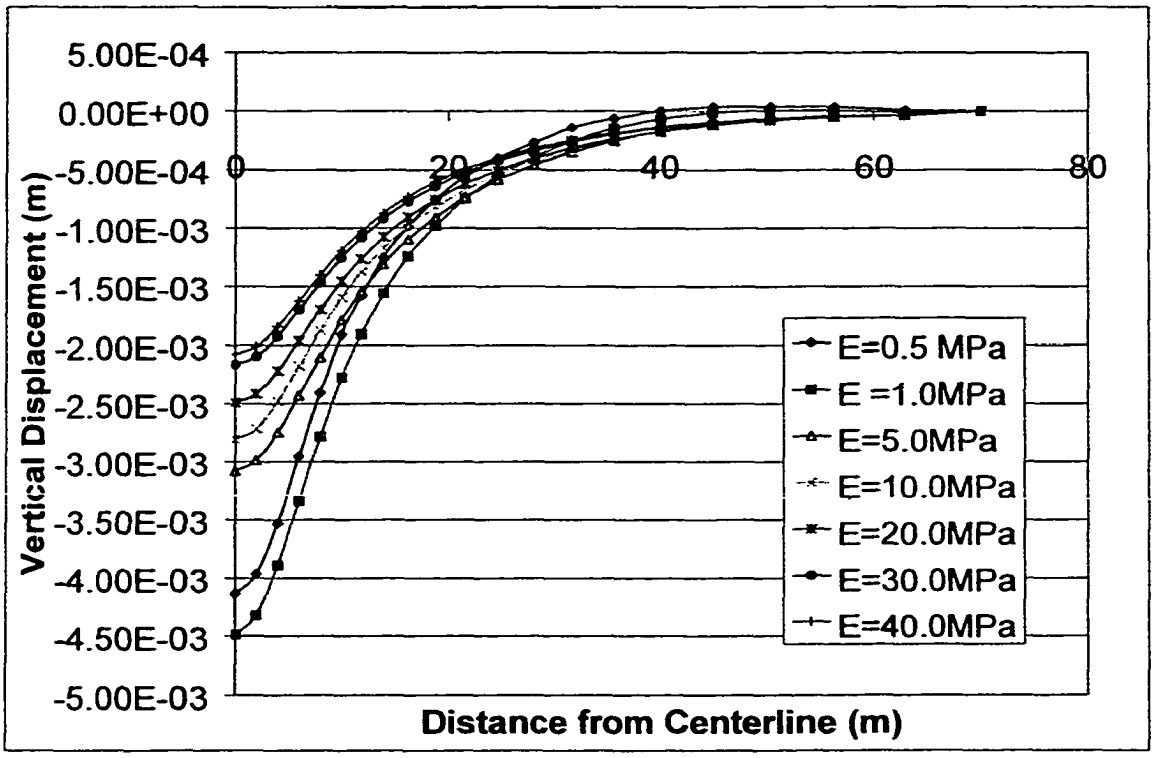

Figure 4.17 Variation of Ground Surface Vertical Displacement with Young's Modulus

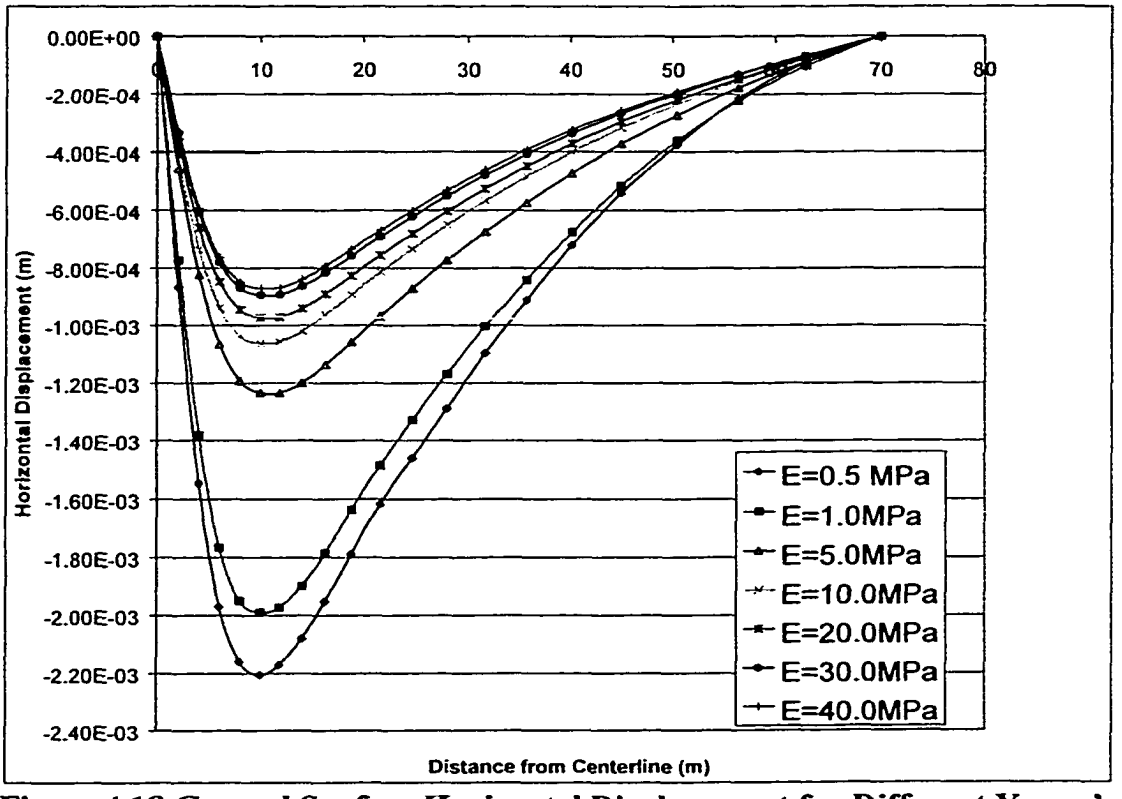

Figure 4.18 Ground Surface Horizontal Displacement for Different Young's Modulus

Table 4.10 Ground Surface Vertical Displacement (meter) for Different Young's Modulus

Distance from Centerline (m)	Young's Modulus (MPa)						
	0.5	1.0	5.0	10.0	20.0	30.0	40.0
0.0	-4.14E-03	-4.49E-03	-3.08E-03	-2.81E-03	-2.49E-03	-2.17E-03	-2.08E-03
2.0	-3.97E-03	-4.32E-03	-2.99E-03	-2.72E-03	-2.42E-03	-2.10E-03	-2.01E-03
4.0	-3.53E-03	-3.89E-03	-2.75E-03	-2.48E-03	-2.22E-03	-1.93E-03	-1.84E-03
6.0	-2.96E-03	-3.34E-03	-2.43E-03	-2.18E-03	-1.96E-03	-1.70E-03	-1.63E-03
8.0	-2.41E-03	-2.78E-03	-2.10E-03	-1.88E-03	-1.70E-03	-1.47E-03	-1.40E-03
10.0	-1.91E-03	-2.28E-03	-1.79E-03	-1.59E-03	-1.45E-03	-1.25E-03	-1.19E-03
11.9	-1.58E-03	-1.91E-03	-1.55E-03	-1.38E-03	-1.26E-03	-1.08E-03	-1.03E-03
14.0	-1.25E-03	-1.56E-03	-1.31E-03	-1.17E-03	-1.08E-03	-9.21E-04	-8.72E-04
16.3	-9.81E-04	-1.24E-03	-1.10E-03	-9.83E-04	-9.07E-04	-7.72E-04	-7.30E-04
18.8	-7.54E-04	-9.79E-04	-9.08E-04	-8.16E-04	-7.56E-04	-6.41E-04	-6.05E-04
21.5	-5.59E-04	-7.51E-04	-7.37E-04	-6.70E-04	-6.22E-04	-5.26E-04	-4.95E-04
24.6	-4.02E-04	-5.52E-04	-5.87E-04	-5.41E-04	-5.05E-04	-4.24E-04	-4.00E-04
27.9	-2.70E-04	-3.93E-04	-4.59E-04	-4.29E-04	-4.02E-04	-3.37E-04	-3.17E-04
31.6	-1.40E-04	-2.55E-04	-3.47E-04	-3.31E-04	-3.13E-04	-2.61E-04	-2.47E-04
35.6	-6.47E-05	-1.49E-04	-2.52E-04	-2.46E-04	-2.37E-04	-1.98E-04	-1.87E-04
40.1	-2.44E-07	-6.72E-05	-1.72E-04	-1.77E-04	-1.72E-04	-1.44E-04	-1.37E-04
45.0	3.68E-05	-1.29E-05	-1.11E-04	-1.20E-04	-1.20E-04	-1.01E-04	-9.63E-05
50.4	3.85E-05	6.27E-06	-6.87E-05	-7.89E-05	-8.03E-05	-6.85E-05	-6.59E-05
56.3	3.57E-05	7.98E-06	-4.32E-05	-5.03E-05	-5.21E-05	-4.57E-05	-4.46E-05
62.8	6.04E-06	-1.19E-05	-3.39E-05	-3.55E-05	-3.63E-05	-3.30E-05	-3.24E-05
70.0	0.00E+00	0.00E+00	0.00E+00	0.00E+00	0.00E+00	0.00E+00	0.00E+00

Table 4.11 Ground Surface Horizontal Displacement (meter) for Different Young's Modulus

Distance from Centerline (m)	Young's Modulus (MPa)						
	0.5	1.0	5.0	10.0	20.0	30.0	40.0
0.0	0.00E+00	0.00E+00	0.00E+00	0.00E+00	0.00E+00	0.00E+00	0.00E+00
2.0	-8.67E-04	-7.73E-04	-4.57E-04	-4.12E-04	-3.67E-04	-3.37E-04	-3.30E-04
4.0	-1.55E-03	-1.38E-03	-8.25E-04	-7.36E-04	-6.60E-04	-6.07E-04	-5.94E-04
6.0	-1.97E-03	-1.77E-03	-1.07E-03	-9.40E-04	-8.50E-04	-7.81E-04	-7.64E-04
8.0	-2.16E-03	-1.95E-03	-1.19E-03	-1.04E-03	-9.47E-04	-8.71E-04	-8.50E-04
10.0	-2.21E-03	-1.99E-03	-1.23E-03	-1.06E-03	-9.74E-04	-8.95E-04	-8.72E-04
11.9	-2.17E-03	-1.97E-03	-1.24E-03	-1.06E-03	-9.72E-04	-8.93E-04	-8.69E-04
14.0	-2.08E-03	-1.90E-03	-1.20E-03	-1.02E-03	-9.42E-04	-8.65E-04	-8.40E-04
16.3	-1.95E-03	-1.79E-03	-1.14E-03	-9.63E-04	-8.91E-04	-8.18E-04	-7.93E-04
18.8	-1.79E-03	-1.64E-03	-1.06E-03	-8.93E-04	-8.28E-04	-7.58E-04	-7.35E-04
21.5	-1.62E-03	-1.49E-03	-9.69E-04	-8.15E-04	-7.56E-04	-6.92E-04	-6.69E-04
24.6	-1.46E-03	-1.33E-03	-8.73E-04	-7.33E-04	-6.81E-04	-6.21E-04	-6.01E-04
27.9	-1.29E-03	-1.17E-03	-7.74E-04	-6.50E-04	-6.03E-04	-5.50E-04	-5.31E-04
31.6	-1.10E-03	-1.00E-03	-6.74E-04	-5.66E-04	-5.26E-04	-4.79E-04	-4.62E-04
35.6	-9.13E-04	-8.43E-04	-5.74E-04	-4.83E-04	-4.49E-04	-4.08E-04	-3.93E-04
40.1	-7.21E-04	-6.76E-04	-4.73E-04	-4.00E-04	-3.72E-04	-3.37E-04	-3.25E-04
45.0	-5.40E-04	-5.16E-04	-3.73E-04	-3.17E-04	-2.96E-04	-2.68E-04	-2.59E-04
50.4	-3.76E-04	-3.62E-04	-2.74E-04	-2.35E-04	-2.21E-04	-2.00E-04	-1.93E-04
56.3	-2.18E-04	-2.25E-04	-1.79E-04	-1.56E-04	-1.47E-04	-1.33E-04	-1.29E-04
62.8	-9.08E-05	-1.03E-04	-8.88E-05	-7.92E-05	-7.56E-05	-6.84E-05	-6.64E-05
70.0	0.00E+00	0.00E+00	0.00E+00	0.00E+00	0.00E+00	0.00E+00	0.00E+00

4.7.2 Effect of Poisson's Ratio

The parameters used for the analysis are as follows:

Poisson's ratio of 0.1, 0.2, 0.3, and 0.4

Elastic modulus is 5 MPa.

Friction angle: 15°

Dilation angle: 0°

Figures 4.19 and 4.20 show vertical and horizontal displacement at the ground surface. The displacement data is listed in Tables 4.12 and 4.13. Both vertical and horizontal displacement at ground surface increase with an increase in the Poisson's ratio. Compared to the Elastic modulus, the value of Poisson's ratio has a relatively small effect on the soil displacement.

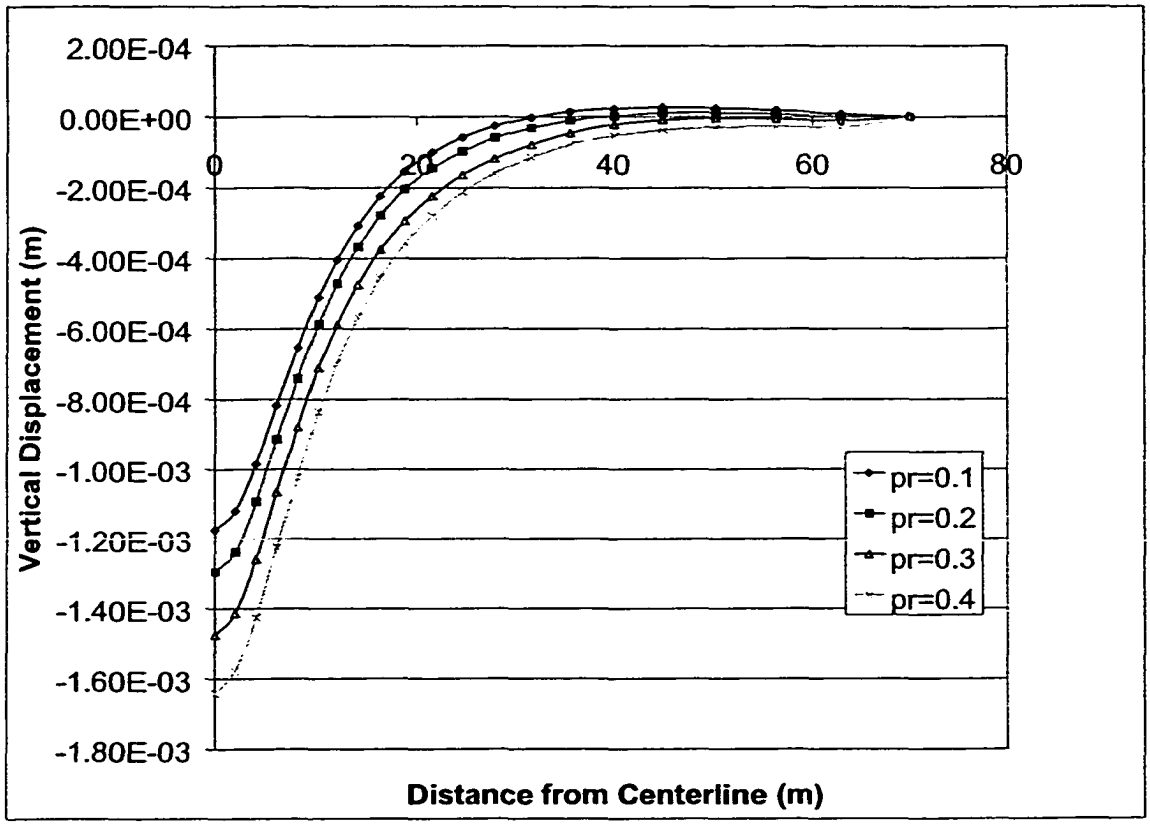

Figure 4.19 Variation of Ground Surface Vertical Displacement with Poisson's Ratio

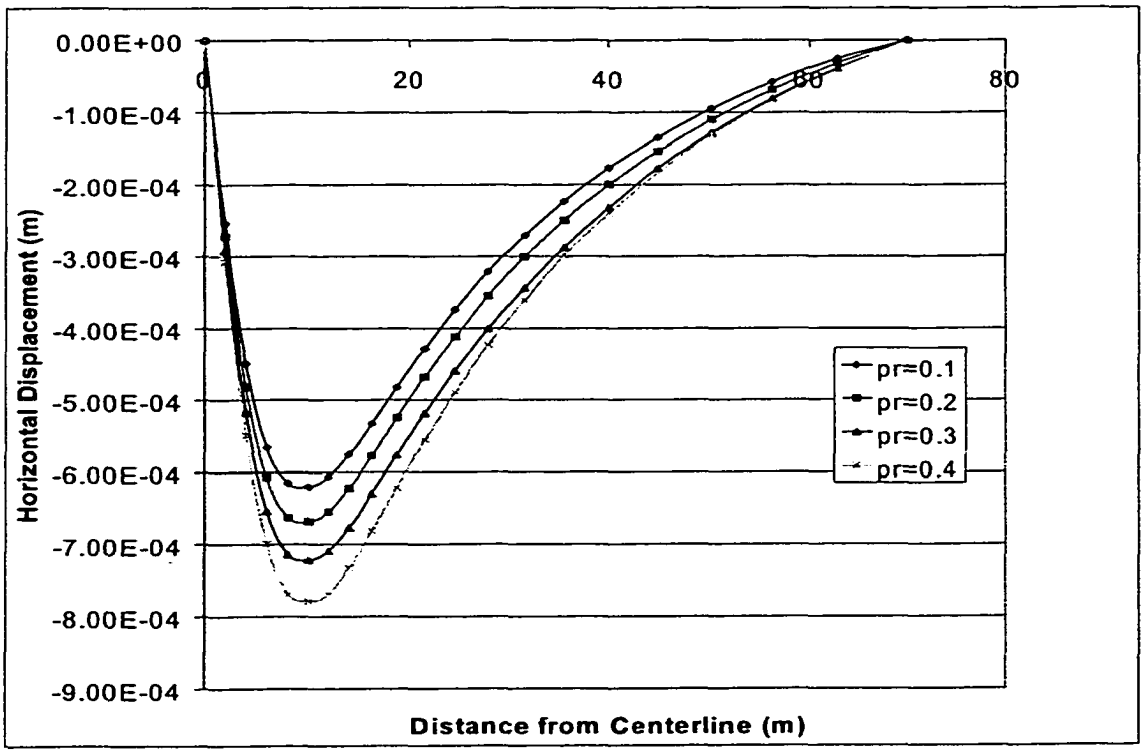

Figure 4.20 Variation of Ground Surface Horizontal Displacement with Poisson's Ratio

Table 4.12 Ground Surface Vertical Displacement (meter) for Different Poisson's Ratio

Distance from Centerline (m)	Poisson's Ratio			
	0.1	0.2	0.3	0.4
0.0	-1.17E-03	-1.30E-03	-1.48E-03	-1.64E-03
2.0	-1.12E-03	-1.24E-03	-1.41E-03	-1.58E-03
4.0	-9.86E-04	-1.09E-03	-1.26E-03	-1.43E-03
6.0	-8.18E-04	-9.16E-04	-1.07E-03	-1.22E-03
8.0	-6.54E-04	-7.42E-04	-8.81E-04	-1.02E-03
10.0	-5.12E-04	-5.87E-04	-7.11E-04	-8.37E-04
11.9	-4.05E-04	-4.73E-04	-5.89E-04	-6.99E-04
14.0	-3.08E-04	-3.68E-04	-4.76E-04	-5.68E-04
16.3	-2.25E-04	-2.80E-04	-3.76E-04	-4.56E-04
18.8	-1.55E-04	-2.05E-04	-2.95E-04	-3.58E-04
21.5	-1.01E-04	-1.46E-04	-2.24E-04	-2.79E-04
24.6	-5.87E-05	-9.86E-05	-1.65E-04	-2.13E-04
27.9	-2.60E-05	-5.97E-05	-1.20E-04	-1.59E-04
31.6	-2.92E-06	-3.22E-05	-7.90E-05	-1.15E-04
35.6	1.42E-05	-1.10E-05	-4.60E-05	-7.73E-05
40.1	2.32E-05	1.75E-06	-2.19E-05	-5.30E-05
45.0	2.68E-05	1.08E-05	-9.35E-06	-3.65E-05
50.4	2.51E-05	1.21E-05	-3.58E-06	-2.84E-05
56.3	1.86E-05	8.09E-06	-5.19E-06	-2.60E-05
62.8	8.11E-06	6.10E-07	-1.03E-05	-2.83E-05
70.0	0.00E+00	0.00E+00	0.00E+00	0.00E+00

Table 4.13 Ground Surface Horizontal Displacement (meter) for Different Poisson's Ratio

Distance from Centerline (m)	Poisson's Ratio			
	0.1	0.2	0.3	0.4
0.0	0.00E+00	0.00E+00	0.00E+00	0.00E+00
2.0	-2.54E-04	-2.72E-04	-2.92E-04	-3.07E-04
4.0	-4.49E-04	-4.82E-04	-5.17E-04	-5.49E-04
6.0	-5.65E-04	-6.07E-04	-6.54E-04	-6.99E-04
8.0	-6.15E-04	-6.63E-04	-7.14E-04	-7.69E-04
10.0	-6.20E-04	-6.68E-04	-7.22E-04	-7.79E-04
11.9	-6.07E-04	-6.55E-04	-7.09E-04	-7.69E-04
14.0	-5.75E-04	-6.22E-04	-6.77E-04	-7.33E-04
16.3	-5.33E-04	-5.78E-04	-6.30E-04	-6.81E-04
18.8	-4.83E-04	-5.25E-04	-5.76E-04	-6.21E-04
21.5	-4.28E-04	-4.68E-04	-5.19E-04	-5.55E-04
24.6	-3.74E-04	-4.12E-04	-4.59E-04	-4.90E-04
27.9	-3.21E-04	-3.55E-04	-4.01E-04	-4.23E-04
31.6	-2.71E-04	-3.01E-04	-3.44E-04	-3.61E-04
35.6	-2.23E-04	-2.50E-04	-2.88E-04	-2.99E-04
40.1	-1.77E-04	-2.00E-04	-2.32E-04	-2.40E-04
45.0	-1.35E-04	-1.54E-04	-1.78E-04	-1.84E-04
50.4	-9.46E-05	-1.10E-04	-1.28E-04	-1.31E-04
56.3	-5.78E-05	-6.87E-05	-8.07E-05	-8.28E-05
62.8	-2.56E-05	-3.21E-05	-3.91E-05	-3.97E-05
70.0	0.00E+00	0.00E+00	0.00E+00	0.00E+00

4.7.3 Effect of Cohesion

There are total 6 models used in the analysis of the effect of cohesion. The cohesion parameter and other parameters as follows.

Cohesion: 0.0 kPa, 2.0kPa, 4.0kPa, 6.0kPa, 8.0kPa and 10.0kPa.

Elastic modulus: 5 Mpa

Friction angle: 15°

Poisson's Ratio: 0.3

Dilation angle: 0°

The vertical and horizontal displacement at ground surface for different cohesion are shown in Figures 4.21 and 4.22. The displacement data is listed in Tables 4.14 and 4.15. Both vertical and horizontal displacement increase with increase in the cohesion. The value of cohesion has a smaller effect on the soil displacement than elastic modulus and Poisson's ratio. The reason is that in all the simulation models, the soil around pipe always falls on the pipe, and the structure of soil has been detroyed. So the cohesion of soil does not have much effect on the final ground settlement.

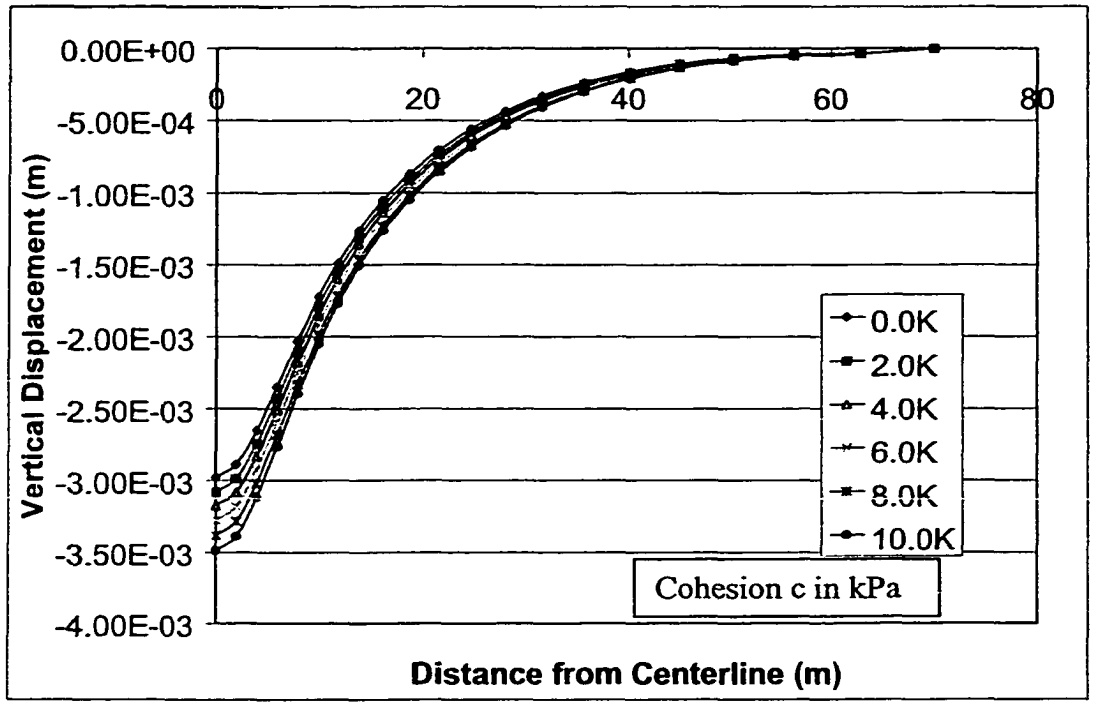

Figure 4.21 Variation of Ground Surface Vertical Displacement with Cohesion

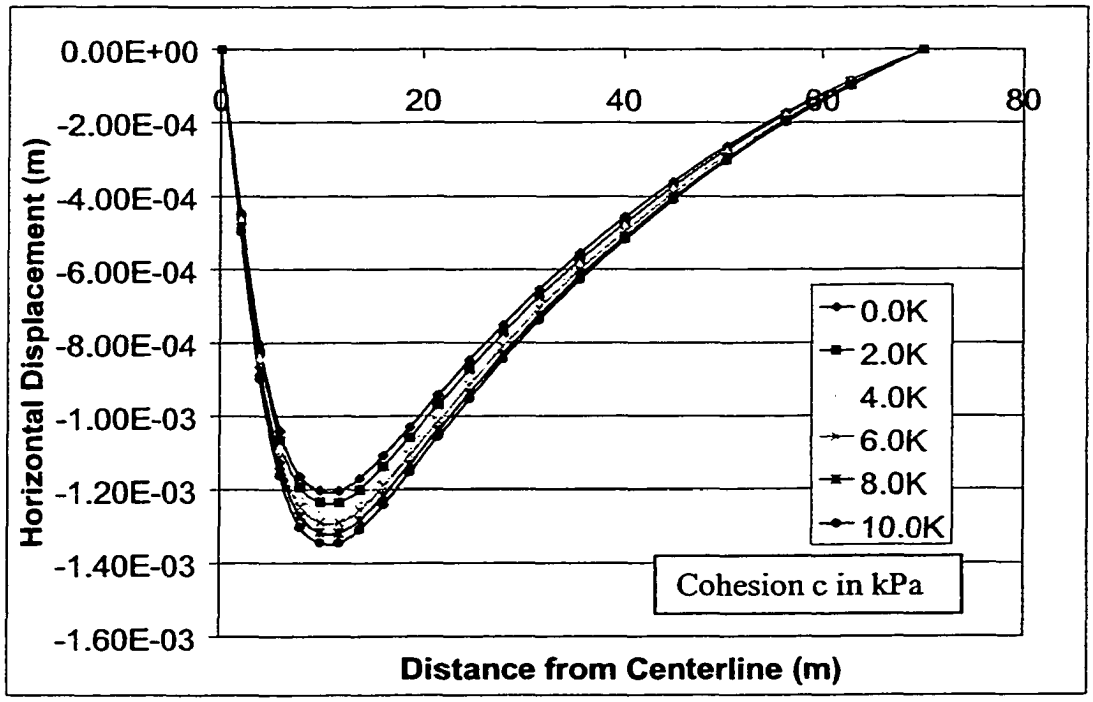

Figure 4.22 Variation of Ground Surface Horizontal Displacement with Cohesion

Table 4.14 Ground Surface Vertical Displacement (meter) for Different Cohesion

Distance from Centerline (m)	Cohesion (kPa)					
	0.0	2.0	4.0	6.0	8.0	10.0
0.0	-2.98E-03	-3.08E-03	-3.18E-03	-3.28E-03	-3.38E-03	-3.49E-03
2.0	-2.89E-03	-2.99E-03	-3.08E-03	-3.18E-03	-3.28E-03	-3.39E-03
4.0	-2.65E-03	-2.75E-03	-2.83E-03	-2.93E-03	-3.02E-03	-3.12E-03
6.0	-2.35E-03	-2.43E-03	-2.51E-03	-2.59E-03	-2.68E-03	-2.76E-03
8.0	-2.03E-03	-2.10E-03	-2.18E-03	-2.25E-03	-2.33E-03	-2.40E-03
10.0	-1.73E-03	-1.79E-03	-1.85E-03	-1.92E-03	-1.99E-03	-2.05E-03
11.9	-1.49E-03	-1.55E-03	-1.60E-03	-1.66E-03	-1.72E-03	-1.77E-03
14.0	-1.26E-03	-1.31E-03	-1.36E-03	-1.41E-03	-1.47E-03	-1.51E-03
16.3	-1.05E-03	-1.10E-03	-1.14E-03	-1.18E-03	-1.23E-03	-1.26E-03
18.8	-8.69E-04	-9.08E-04	-9.41E-04	-9.79E-04	-1.02E-03	-1.05E-03
21.5	-7.06E-04	-7.37E-04	-7.65E-04	-7.97E-04	-8.34E-04	-8.55E-04
24.6	-5.61E-04	-5.87E-04	-6.11E-04	-6.37E-04	-6.67E-04	-6.86E-04
27.9	-4.39E-04	-4.59E-04	-4.77E-04	-4.99E-04	-5.25E-04	-5.38E-04
31.6	-3.30E-04	-3.47E-04	-3.59E-04	-3.79E-04	-3.98E-04	-4.10E-04
35.6	-2.40E-04	-2.52E-04	-2.62E-04	-2.76E-04	-2.94E-04	-3.01E-04
40.1	-1.65E-04	-1.72E-04	-1.80E-04	-1.93E-04	-2.06E-04	-2.11E-04
45.0	-1.08E-04	-1.11E-04	-1.18E-04	-1.25E-04	-1.36E-04	-1.39E-04
50.4	-6.74E-05	-6.87E-05	-7.26E-05	-7.81E-05	-8.51E-05	-8.77E-05
56.3	-4.28E-05	-4.32E-05	-4.57E-05	-4.87E-05	-5.26E-05	-5.45E-05
62.8	-3.28E-05	-3.39E-05	-3.44E-05	-3.67E-05	-3.89E-05	-3.98E-05
70.0	0.00E+00	0.00E+00	0.00E+00	0.00E+00	0.00E+00	0.00E+00

Table 4.15 Ground Surface Vertical Displacement (meter) for Different Cohesion

Distance from Centerline (m)	Cohesion (kPa)					
	0.0	2.0	4.0	6.0	8.0	10.0
0.0	0.00E+00	0.00E+00	0.00E+00	0.00E+00	0.00E+00	0.00E+00
2.0	-4.46E-04	-4.57E-04	-4.65E-04	-4.75E-04	-4.85E-04	-4.97E-04
4.0	-8.04E-04	-8.25E-04	-8.40E-04	-8.59E-04	-8.77E-04	-8.98E-04
6.0	-1.04E-03	-1.07E-03	-1.09E-03	-1.11E-03	-1.14E-03	-1.16E-03
8.0	-1.16E-03	-1.19E-03	-1.22E-03	-1.25E-03	-1.27E-03	-1.30E-03
10.0	-1.20E-03	-1.23E-03	-1.26E-03	-1.29E-03	-1.32E-03	-1.34E-03
11.9	-1.20E-03	-1.24E-03	-1.26E-03	-1.29E-03	-1.32E-03	-1.35E-03
14.0	-1.17E-03	-1.20E-03	-1.23E-03	-1.26E-03	-1.28E-03	-1.31E-03
16.3	-1.11E-03	-1.14E-03	-1.16E-03	-1.19E-03	-1.22E-03	-1.24E-03
18.8	-1.03E-03	-1.06E-03	-1.08E-03	-1.11E-03	-1.13E-03	-1.15E-03
21.5	-9.43E-04	-9.69E-04	-9.92E-04	-1.01E-03	-1.04E-03	-1.06E-03
24.6	-8.48E-04	-8.73E-04	-8.94E-04	-9.14E-04	-9.37E-04	-9.52E-04
27.9	-7.51E-04	-7.74E-04	-7.93E-04	-8.11E-04	-8.32E-04	-8.45E-04
31.6	-6.54E-04	-6.74E-04	-6.90E-04	-7.05E-04	-7.25E-04	-7.37E-04
35.6	-5.56E-04	-5.74E-04	-5.87E-04	-6.01E-04	-6.18E-04	-6.28E-04
40.1	-4.57E-04	-4.73E-04	-4.83E-04	-4.96E-04	-5.11E-04	-5.18E-04
45.0	-3.61E-04	-3.73E-04	-3.81E-04	-3.92E-04	-4.04E-04	-4.10E-04
50.4	-2.65E-04	-2.74E-04	-2.81E-04	-2.89E-04	-2.99E-04	-3.03E-04
56.3	-1.74E-04	-1.79E-04	-1.83E-04	-1.89E-04	-1.96E-04	-1.99E-04
62.8	-8.65E-05	-8.88E-05	-9.13E-05	-9.46E-05	-9.78E-05	-9.97E-05
70.0	0.00E+00	0.00E+00	0.00E+00	0.00E+00	0.00E+00	0.00E+00

4.7.4 Effect of Friction Angle

There are a total of 6 models used in analysis of the effect of the friction angle. The parameters used in the analysis are as follows:

Friction angle 0°, 5°, 10°, 20°, 30°, and 40°

Elastic modulus: 5 MPa.

Poisson's Ratio: 0.3

Dilation angle: 0°

The vertical and horizontal displacement at ground surface are shown in Figures 4.23 and 4.24. The displacement data is listed in Tables 4.16 and 4.17. Both vertical and horizontal displacement increase with the increase of the friction angle. The value of cohesion has a larger effect on the soil displacement than elastic modulus, Poisson's ratio, and cohesion.

4.7.5 Effect of Dilation Angle

There are total 6 models used in analysis of the effect of the friction angle. The parameter used in the analysis are as follow

Dilation angle 0°, 1°, 3°, 5°, 8°, and 10°.

Elastic Modulus: 5MPa

Friction angle: 0°

Cohesion: 5MPa

The vertical and horizontal displacement at ground surface are shown in Figures 4.25 and 4.26. The displacement data is listed in Tables 4.18 and 4.19. Both vertical and horizontal displacement decrease with the increase of the dilation angle.

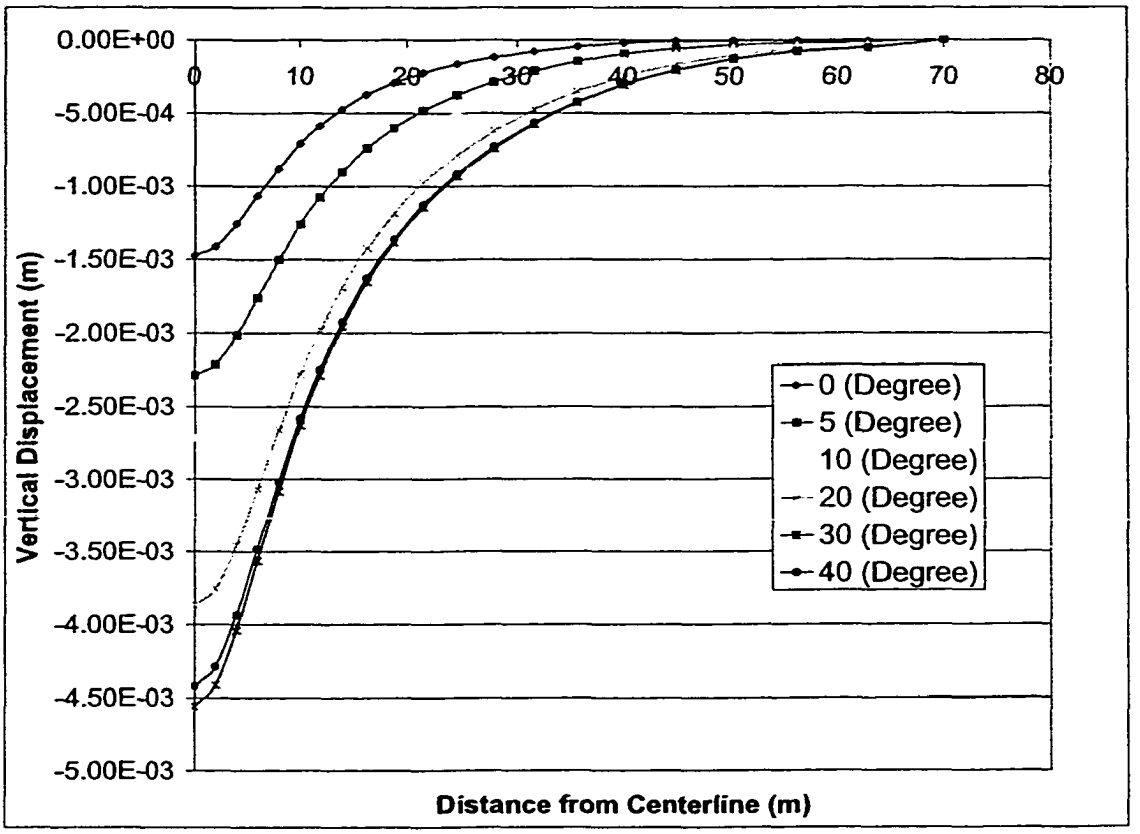

Figure 4.23 Variation of Ground Surface Vertical Displacement with Friction Angle

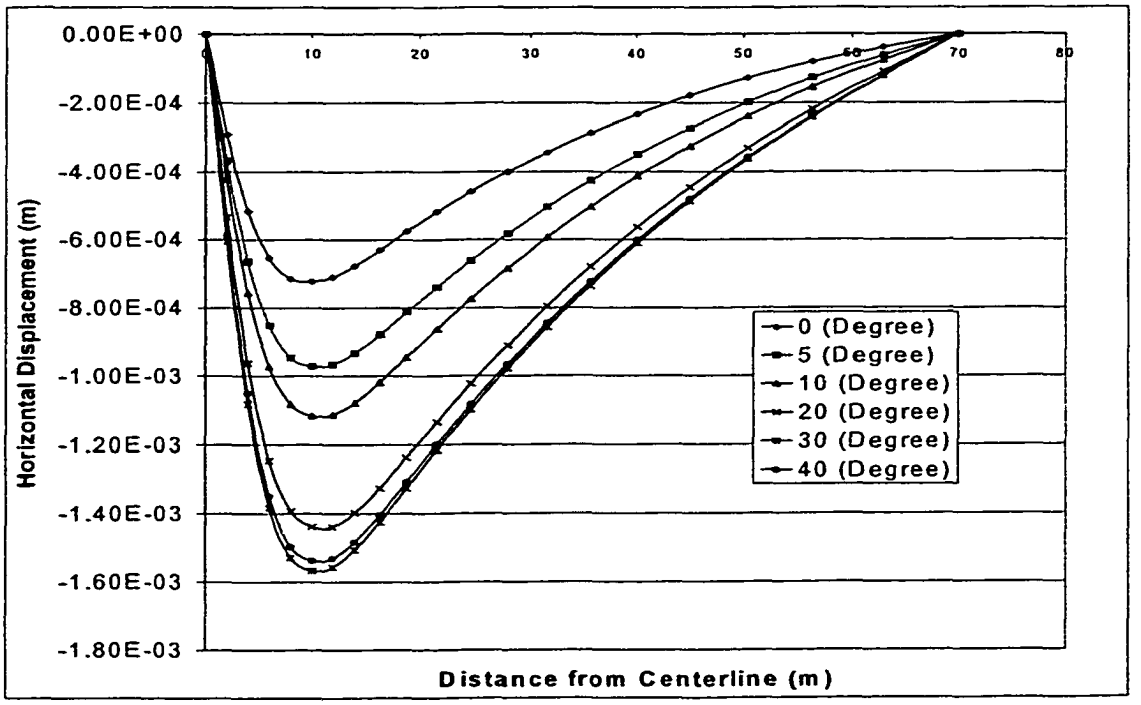

Figure 4.24 Variation of Ground Surface Horizontal Displacement with Friction Angle

Table 4.16 Ground Surface Vertical Displacement (meter) for Different Friction Angle

Distance from Centerline (m)	Friction Angle (degree)					
	0	5	10	20	30	40
0.0	-1.48E-03	-2.29E-03	-2.72E-03	-3.87E-03	-4.56E-03	-4.42E-03
2.0	-1.41E-03	-2.21E-03	-2.63E-03	-3.75E-03	-4.41E-03	-4.29E-03
4.0	-1.26E-03	-2.02E-03	-2.41E-03	-3.46E-03	-4.04E-03	-3.93E-03
6.0	-1.07E-03	-1.76E-03	-2.12E-03	-3.07E-03	-3.56E-03	-3.48E-03
8.0	-8.81E-04	-1.51E-03	-1.82E-03	-2.66E-03	-3.08E-03	-3.02E-03
10.0	-7.11E-04	-1.26E-03	-1.54E-03	-2.28E-03	-2.63E-03	-2.58E-03
11.9	-5.89E-04	-1.08E-03	-1.32E-03	-1.98E-03	-2.29E-03	-2.25E-03
14.0	-4.76E-04	-9.02E-04	-1.11E-03	-1.69E-03	-1.96E-03	-1.93E-03
16.3	-3.76E-04	-7.42E-04	-9.23E-04	-1.42E-03	-1.66E-03	-1.63E-03
18.8	-2.95E-04	-6.04E-04	-7.59E-04	-1.19E-03	-1.39E-03	-1.37E-03
21.5	-2.24E-04	-4.83E-04	-6.11E-04	-9.74E-04	-1.14E-03	-1.13E-03
24.6	-1.65E-04	-3.77E-04	-4.83E-04	-7.86E-04	-9.31E-04	-9.16E-04
27.9	-1.20E-04	-2.89E-04	-3.76E-04	-6.21E-04	-7.43E-04	-7.30E-04
31.6	-7.90E-05	-2.12E-04	-2.80E-04	-4.76E-04	-5.74E-04	-5.65E-04
35.6	-4.60E-05	-1.48E-04	-2.01E-04	-3.52E-04	-4.30E-04	-4.24E-04
40.1	-2.19E-05	-9.47E-05	-1.36E-04	-2.48E-04	-3.08E-04	-3.02E-04
45.0	-9.35E-06	-5.80E-05	-8.72E-05	-1.66E-04	-2.09E-04	-2.04E-04
50.4	-3.58E-06	-3.32E-05	-5.23E-05	-1.04E-04	-1.34E-04	-1.30E-04
56.3	-5.19E-06	-2.17E-05	-3.21E-05	-6.38E-05	-8.07E-05	-7.87E-05
62.8	-1.03E-05	-1.98E-05	-2.64E-05	-4.51E-05	-5.34E-05	-5.24E-05
70.0	0.00E+00	0.00E+00	0.00E+00	0.00E+00	0.00E+00	0.00E+00

Table 4.17 Ground Surface Horizontal Displacement (meter) for Different Friction Angle

Distance from Centerline (m)	Friction Angle (Degree)					
	0	5	10	20	30	40
0.0	0.00E+00	0.00E+00	0.00E+00	0.00E+00	0.00E+00	0.00E+00
2.0	-2.92E-04	-3.70E-04	-4.20E-04	-5.35E-04	-6.06E-04	-5.87E-04
4.0	-5.17E-04	-6.64E-04	-7.56E-04	-9.64E-04	-1.08E-03	-1.05E-03
6.0	-6.54E-04	-8.53E-04	-9.73E-04	-1.25E-03	-1.38E-03	-1.35E-03
8.0	-7.14E-04	-9.47E-04	-1.08E-03	-1.39E-03	-1.53E-03	-1.50E-03
10.0	-7.22E-04	-9.72E-04	-1.12E-03	-1.44E-03	-1.57E-03	-1.54E-03
11.9	-7.09E-04	-9.67E-04	-1.11E-03	-1.44E-03	-1.56E-03	-1.53E-03
14.0	-6.77E-04	-9.34E-04	-1.08E-03	-1.40E-03	-1.51E-03	-1.48E-03
16.3	-6.30E-04	-8.79E-04	-1.02E-03	-1.33E-03	-1.43E-03	-1.40E-03
18.8	-5.76E-04	-8.13E-04	-9.46E-04	-1.24E-03	-1.33E-03	-1.31E-03
21.5	-5.19E-04	-7.39E-04	-8.63E-04	-1.13E-03	-1.22E-03	-1.20E-03
24.6	-4.59E-04	-6.62E-04	-7.74E-04	-1.02E-03	-1.10E-03	-1.08E-03
27.9	-4.01E-04	-5.83E-04	-6.85E-04	-9.11E-04	-9.79E-04	-9.66E-04
31.6	-3.44E-04	-5.05E-04	-5.94E-04	-7.96E-04	-8.58E-04	-8.46E-04
35.6	-2.88E-04	-4.27E-04	-5.04E-04	-6.80E-04	-7.35E-04	-7.25E-04
40.1	-2.32E-04	-3.49E-04	-4.13E-04	-5.63E-04	-6.11E-04	-6.02E-04
45.0	-1.78E-04	-2.73E-04	-3.25E-04	-4.47E-04	-4.87E-04	-4.80E-04
50.4	-1.28E-04	-1.99E-04	-2.39E-04	-3.31E-04	-3.63E-04	-3.58E-04
56.3	-8.07E-05	-1.28E-04	-1.55E-04	-2.18E-04	-2.41E-04	-2.38E-04
62.8	-3.91E-05	-6.20E-05	-7.63E-05	-1.10E-04	-1.22E-04	-1.20E-04
70.0	0.00E+00	0.00E+00	0.00E+00	0.00E+00	0.00E+00	0.00E+00

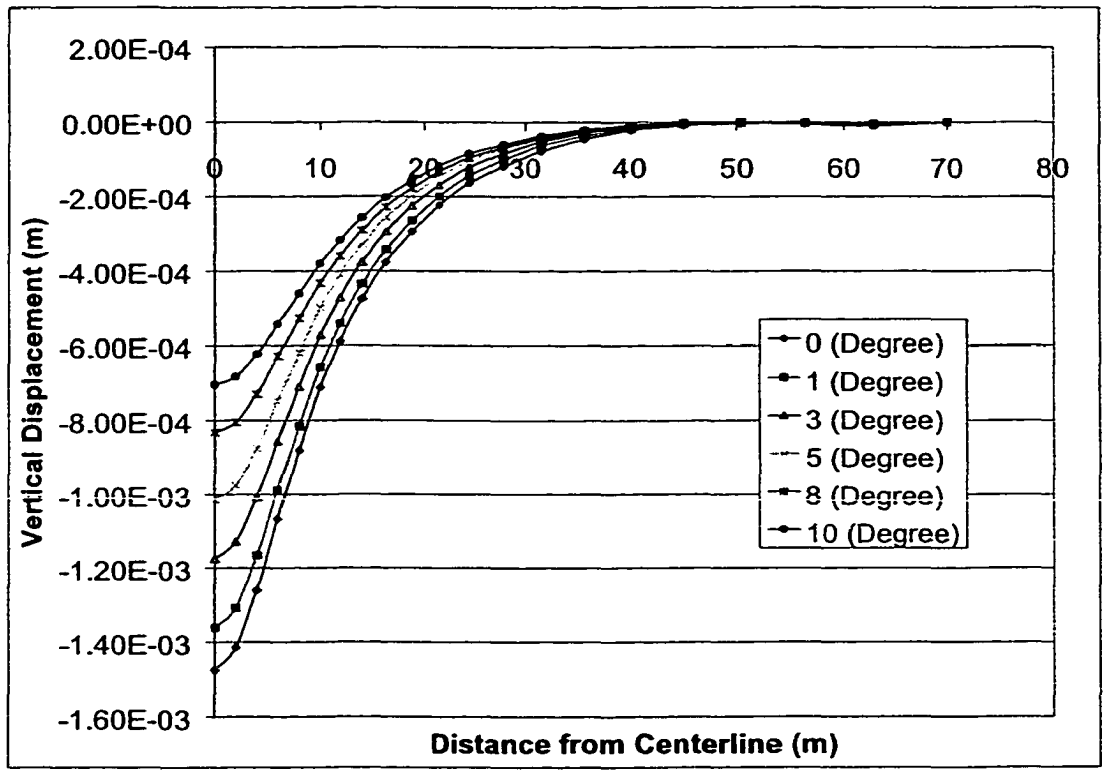

Figure 4.25 Variation of Ground Surface Vertical Displacement with Dilation Angle

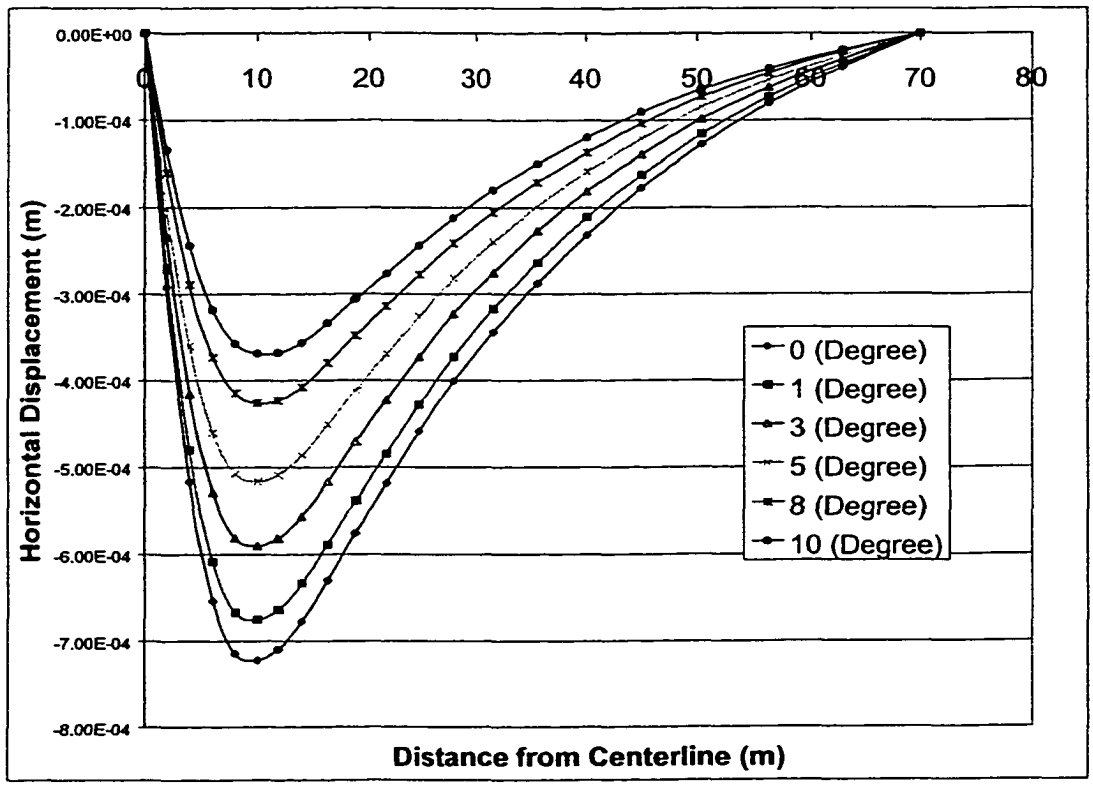

Figure 4.26 Variation of Ground Surface Horizontal Displacement with Dilation Angle

Table 4.18 Ground Surface Vertical Displacement (meter) for Different Dilation Angle

Distance from Centerline (m)	Dilation Angle (Degree)					
	0	1	3	5	8	10
0.00E+00	-1.48E-03	-1.36E-03	-1.18E-03	-1.01E-03	-8.33E-04	-7.04E-04
2.00E+00	-1.41E-03	-1.31E-03	-1.13E-03	-9.76E-04	-8.05E-04	-6.82E-04
4.00E+00	-1.26E-03	-1.17E-03	-1.01E-03	-8.75E-04	-7.30E-04	-6.23E-04
6.00E+00	-1.07E-03	-9.89E-04	-8.57E-04	-7.47E-04	-6.29E-04	-5.44E-04
8.00E+00	-8.81E-04	-8.16E-04	-7.09E-04	-6.19E-04	-5.28E-04	-4.61E-04
1.00E+01	-7.11E-04	-6.58E-04	-5.73E-04	-4.99E-04	-4.33E-04	-3.80E-04
1.19E+01	-5.89E-04	-5.43E-04	-4.73E-04	-4.10E-04	-3.61E-04	-3.18E-04
1.40E+01	-4.76E-04	-4.36E-04	-3.77E-04	-3.28E-04	-2.92E-04	-2.58E-04
1.63E+01	-3.76E-04	-3.43E-04	-2.94E-04	-2.56E-04	-2.28E-04	-2.03E-04
1.88E+01	-2.95E-04	-2.66E-04	-2.26E-04	-1.98E-04	-1.79E-04	-1.59E-04
2.15E+01	-2.24E-04	-2.01E-04	-1.70E-04	-1.46E-04	-1.34E-04	-1.19E-04
2.46E+01	-1.65E-04	-1.46E-04	-1.22E-04	-1.05E-04	-9.69E-05	-8.58E-05
2.79E+01	-1.20E-04	-1.02E-04	-8.51E-05	-7.24E-05	-6.82E-05	-6.09E-05
3.16E+01	-7.90E-05	-6.32E-05	-5.31E-05	-4.60E-05	-4.36E-05	-3.78E-05
3.56E+01	-4.60E-05	-3.75E-05	-2.92E-05	-2.56E-05	-2.42E-05	-2.16E-05
4.01E+01	-2.19E-05	-1.76E-05	-1.27E-05	-1.01E-05	-9.27E-06	-9.46E-06
4.50E+01	-9.35E-06	-5.83E-06	-3.22E-06	-1.98E-06	-1.60E-06	-2.16E-06
5.04E+01	-3.58E-06	-2.29E-06	-7.19E-07	-3.98E-07	3.58E-07	1.04E-08
5.63E+01	-5.19E-06	-4.03E-06	-2.77E-06	-2.23E-06	-9.08E-07	-9.69E-07
6.28E+01	-1.03E-05	-8.92E-06	-7.12E-06	-5.84E-06	-4.07E-06	-3.55E-06
7.00E+01	0.00E+00	0.00E+00	0.00E+00	0.00E+00	0.00E+00	0.00E+00

Table 4.19 Ground Surface Horizontal Displacement (meter) for Different Dilation Angle

Distance from Centerline (m)	Dilation Angle (Degree)					
	0	1	3	5	8	10
0.00E+00	0.00E+00	0.00E+00	0.00E+00	0.00E+00	0.00E+00	0.00E+00
2.00E+00	-2.92E-04	-2.71E-04	-2.34E-04	-2.02E-04	-1.60E-04	-1.34E-04
4.00E+00	-5.17E-04	-4.81E-04	-4.16E-04	-3.60E-04	-2.89E-04	-2.44E-04
6.00E+00	-6.54E-04	-6.09E-04	-5.29E-04	-4.61E-04	-3.74E-04	-3.18E-04
8.00E+00	-7.14E-04	-6.67E-04	-5.81E-04	-5.08E-04	-4.15E-04	-3.58E-04
1.00E+01	-7.22E-04	-6.75E-04	-5.90E-04	-5.16E-04	-4.26E-04	-3.69E-04
1.19E+01	-7.09E-04	-6.64E-04	-5.82E-04	-5.09E-04	-4.23E-04	-3.68E-04
1.40E+01	-6.77E-04	-6.34E-04	-5.57E-04	-4.86E-04	-4.08E-04	-3.56E-04
1.63E+01	-6.30E-04	-5.89E-04	-5.17E-04	-4.51E-04	-3.80E-04	-3.34E-04
1.88E+01	-5.76E-04	-5.38E-04	-4.71E-04	-4.12E-04	-3.48E-04	-3.06E-04
2.15E+01	-5.19E-04	-4.85E-04	-4.23E-04	-3.70E-04	-3.14E-04	-2.77E-04
2.46E+01	-4.59E-04	-4.28E-04	-3.73E-04	-3.26E-04	-2.78E-04	-2.44E-04
2.79E+01	-4.01E-04	-3.73E-04	-3.23E-04	-2.82E-04	-2.41E-04	-2.13E-04
3.16E+01	-3.44E-04	-3.17E-04	-2.75E-04	-2.40E-04	-2.06E-04	-1.80E-04
3.56E+01	-2.88E-04	-2.64E-04	-2.27E-04	-1.99E-04	-1.71E-04	-1.50E-04
4.01E+01	-2.32E-04	-2.11E-04	-1.81E-04	-1.59E-04	-1.37E-04	-1.20E-04
4.50E+01	-1.78E-04	-1.63E-04	-1.39E-04	-1.21E-04	-1.04E-04	-9.09E-05
5.04E+01	-1.28E-04	-1.16E-04	-9.88E-05	-8.51E-05	-7.32E-05	-6.47E-05
5.63E+01	-8.07E-05	-7.34E-05	-6.25E-05	-5.34E-05	-4.57E-05	-4.09E-05
6.28E+01	-3.91E-05	-3.52E-05	-2.97E-05	-2.57E-05	-2.11E-05	-1.94E-05
7.00E+01	0.00E+00	0.00E+00	0.00E+00	0.00E+00	0.00E+00	0.00E+00

4.7.6 Effect of Microtunneling Depth

There are 4 models used in analysis of the effect of microtunneling depth. Figure 4.27 shows the maximum surface vertical displacement. The parameters used in the analysis are as follows: Elastic Modulus: 20.0 MPa, Poisson's Ratio: 0.3, Friction angle: 15°, Dilation angle: 0°. The result shows that the maximum surface vertical displacement decreases with an increase of the microtunneling depth. Beyond an H/D ratio = 10, the maximum vertical settlement changes very slowly with depth.

4.7.7 Effect of Product Pipe Radius

The vertical and horizontal displacement at ground surface for different radius of product pipe are shown in Figures 4.28 and 4.29. Both the vertical and horizontal displacement increase with the increase of the radius of product pipe.

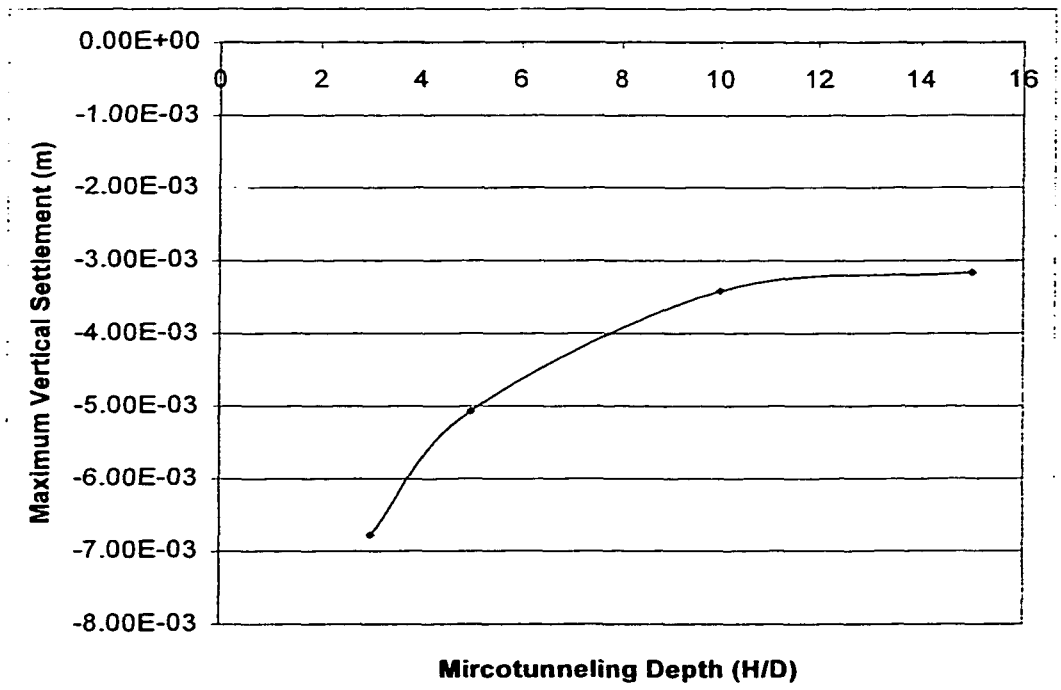

Figure 4.27 Maximum Vertical Displacement at Ground Surface with Different Microtunneling Depth

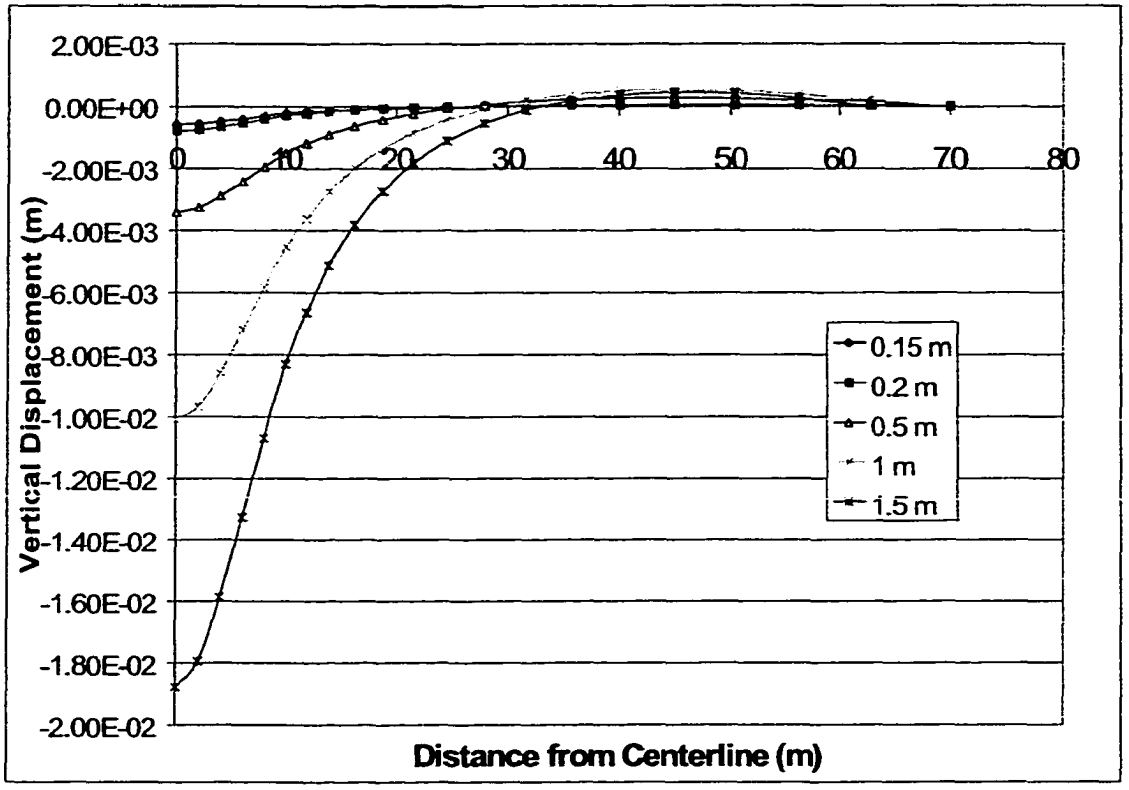

Figure 4.28 Variation of Vertical Displacement with Product Pipe Radius

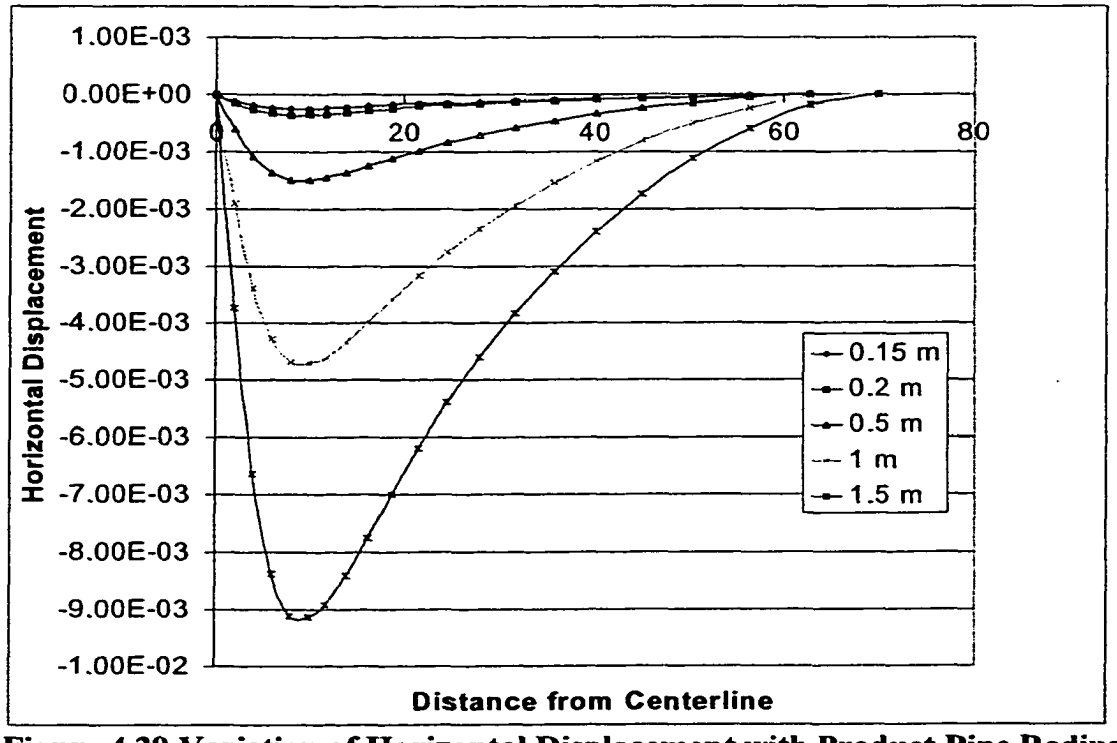

Figure 4.29 Variation of Horizontal Displacement with Product Pipe Radius

4.8 Comparisons Between Case History Data and Simulation Results

Case 1: Barcelona Subway Network Extension, Barcelona

An 8 meter diameter subway network tunnel was built in 1993 in Barcelona. The tunneling details, soil parameter, and field measurements were reported by Ledesma and Romero [1997]. The soil type is predominantly red clay with sand and gravel.

A simplified soil profile is listed in Figure 4.30, along with typical published soil data. Soil parameters used are shown in Figure 4.30. The equivalent ground loss parameter estimated using the proposed method by Lee (0.8%) is of the same order as the reported empirical ground loss (1.2%). Figure 4.30 shows that the predicted and observed surface settlements are in good agreement, especially in terms of the maximum value of the maximum value of vertical settlement. The settlement trough as measured is narrower than the simulated data.

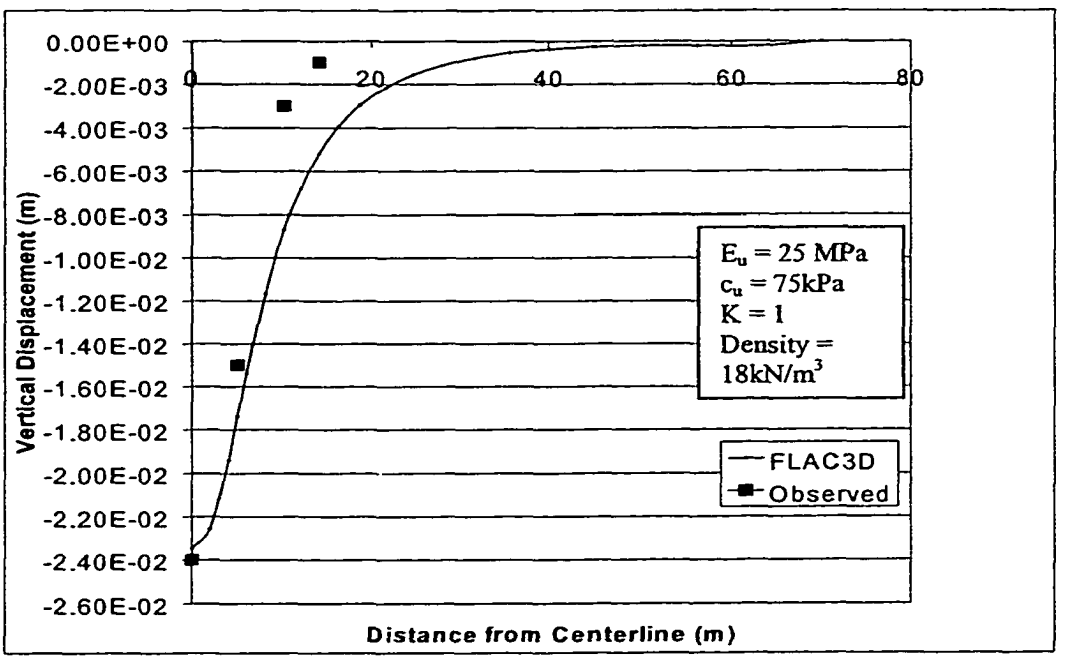

Figure 4.30 Observed and Predicted Surface Settlement – Barcelona Subway Network

Case 2: Green Park Tunnel, U.K.

This case involved a 4.14 meter diameter shield driven tunnel running 29.4 meters below ground in stiff, fissured, heavily overconsolidated London clay. The tunnel details, soil parameters, and field measurements are based on Attewell and Farmer [1974].

Soil parameters used are shown in Figure 4.31. The equivalent ground loss estimated using the modified method is 1.6%. The predicted and observed maximum surface settlements are in good agreement as shown in Figure 4.31

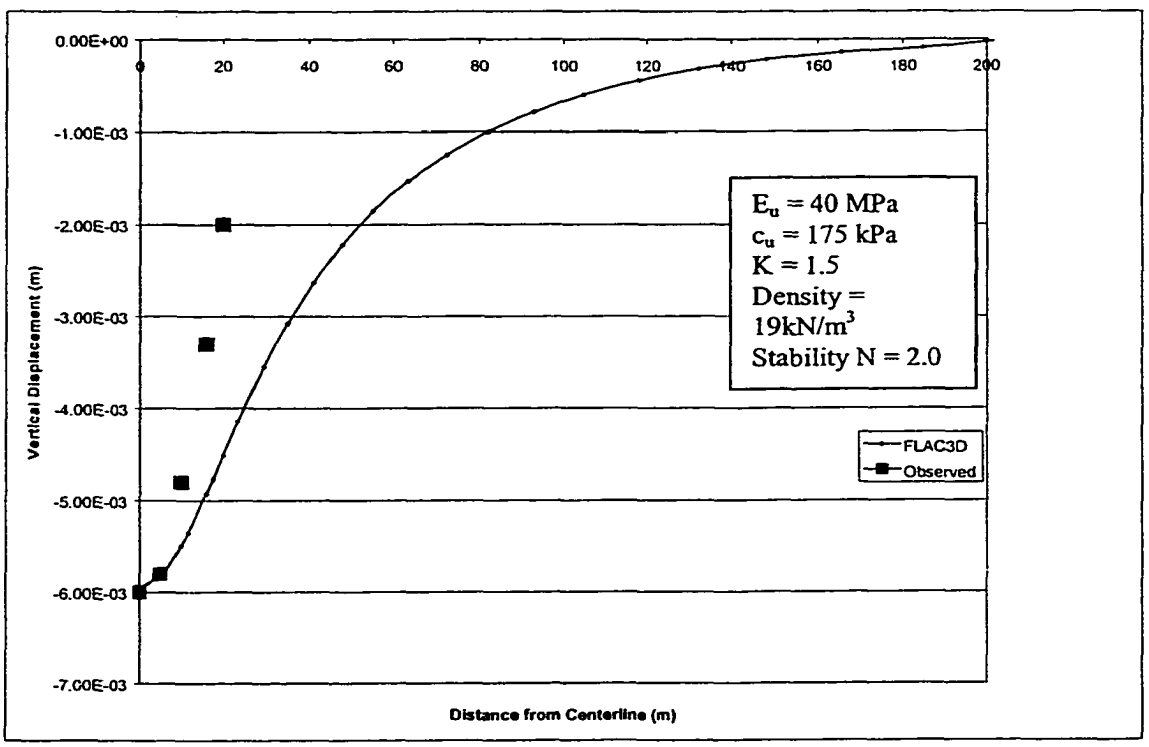

Figure 4.31 Observed and Predicted Surface Settlement – Green Park Tunnel, U.K.

As in case 1 and case 2, the predicted surface settlement is very close to the observed surface settlement near the centerline of microtunneling, but FLAC3D predicts a wider trough and a higher ground settlement at the ground surface far from the centerline.

CHAPTER 5

ARTIFICIAL INTELLIGENCE APPROACH

An artificial neural network is an information-processing system that has certain performance characteristics in common with biological neural networks. Artificial neural networks have been developed as generalizations of mathematical models of assumption cognition or neural biology based on the following assumptions:

1. Information processing occurs at many simple elements called neurons;
2. Signals are passed between neurons over connection links;
3. Each connection link has an associated weight, which, in a typical neural net, multiplies the signal transmitted; and
4. Each neuron applies an activation function (usually nonlinear) to its net input (sum of weighted input signals) to determine its output signal.

A neural network is characterized by (1) its pattern of connections between the neurons (called its architecture), (2) its method of determining the weights on the connections (called its training, or learning, algorithm), and (3) its activation function.

5.1 Introduction to Neural Network

A neural net consists of a large number of simple processing elements called neurons, units, cells, or nodes. Each neuron is connected to other neurons by means of directed communication links, each with an associated weight. The weights represent

information being used by the net to solve a problem. Neural nets can be applied to a wide variety of problems such as storing and recalling data or patterns, classifying patterns, performing general mappings from input patterns to output patterns, grouping similar patterns, or finding solutions to constrained optimization problems.

Each neuron has an internal state called its activation or activity level, which is a function of the inputs it has received. Typically, a neuron sends its activation as a signal to several other neurons. It is important to note that a neuron can send only one signal at a time, although that signal is broadcast to several other neurons.

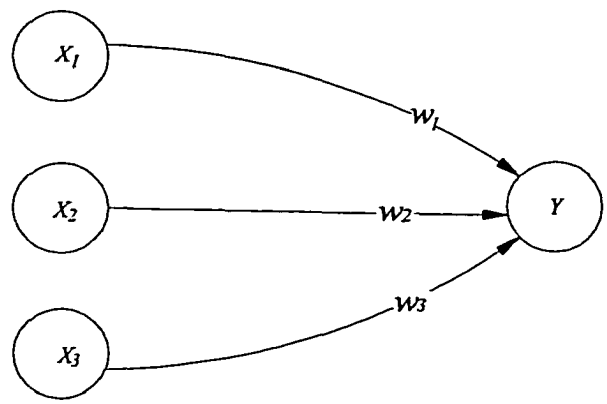

Figure 5.1 A Simple Artificial Neuron

For example, consider a neuron Y, illustrated in Figure 5.1, that receives input from neurons X_1, X_2, and X_3. The activation (output signals) of these neurons are x_1, x_2, and x_3, respectively. The net input, y_{in}, to neuron Y is the sum of the weighted signals from neurons X_1, X_2, and X_3:

$$y_{in} = w_1 x_1 + w_2 x_2 + w_3 x_3 \tag{5.1}$$

The activation y of neuron Y is given by some function of its net input, $y = f(y_{in})$. The logistic sigmoid function:

$$f(x) = \frac{1}{1 + e^{-x}} \tag{5.2}$$

or any of a number of other activation functions can be used.

Now suppose further that neuron Y is connected to neurons Z_1 and Z_2, with weights v_1 and v_2, respectively, as shown in Figure 5.2. Neuron Y sends its signal y to each of these unites. However, in general, the values received by neurons Z_1 and Z_2 will be different because each signal is scaled by the appropriated weight, v_1 or v_2. In a typical net, the activation z_1 and z_2 of neurons Z_1 and Z_2 would depend on inputs from several or even many neurons, not just one.

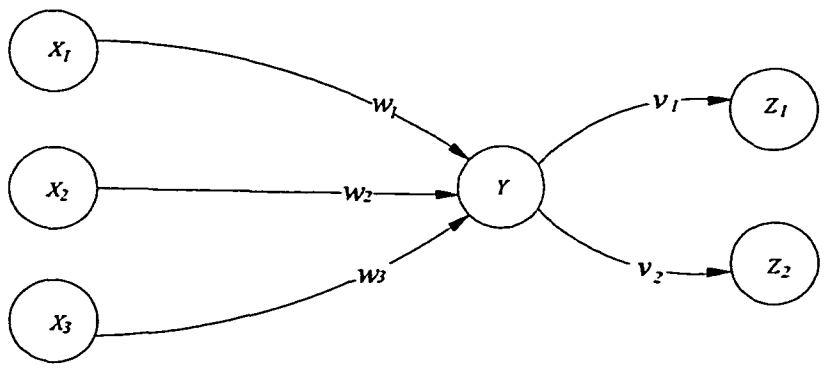

Figure 5.2 A Very Simple Neural Network

Although the neural network in Figure 5.2 is very simple, the presence of a hidden unit, together with a nonlinear activation function, gives it the ability to solve many more problems than can be solved by a net with only input and output units. On the other hand it is more difficult to train (i.e., find optimal values for the weights) for a net with hidden units.

The following desciption of neural networks largely follows the dicussion of Lin, [1995].

5.2 Biological Neural Networks (Discussion after Lin, 1995)

There is a close analogy between the structure of a biological neuron. The structure of an individual neuron varies much less from species to species than does the organization of the system of which the neuron is an element.

A biological neuron has three types of components that are of particular interest in understanding an artificial neuron: its dendrites, soma, and axon. The many dendrites receive signals from other neurons. The signals are electric impulses that are transmitted across a synaptic gap by means of a chemical process. The action of the chemical transmitter modifies the incoming signal (typically by scaling the frequency of the signals that are received) in a manner similar to the action of the weights in a artificial neural networks.

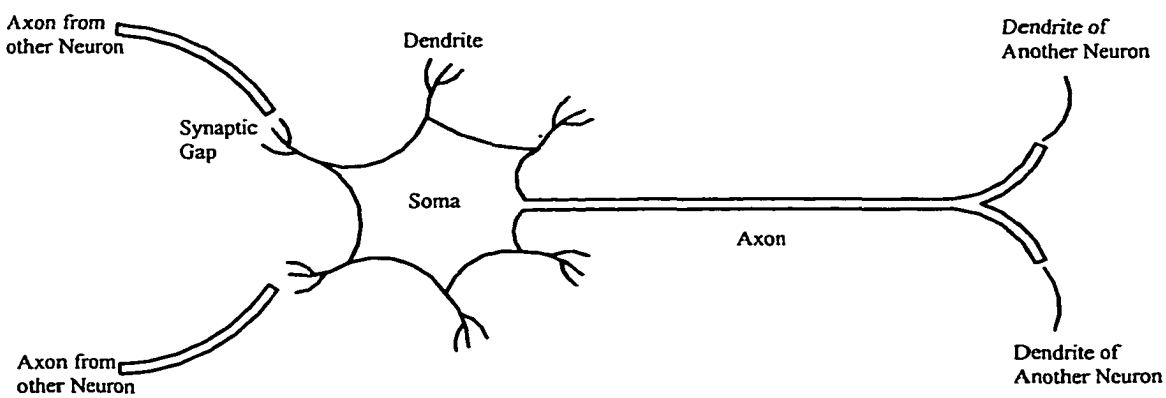

Figure 5.3 Biological Neuron

The soma, or cell body, sums the incoming signals. When sufficient input is received, the cell fires; that is, it transmits a signal over its axon to other cells. It is often supposed that a cell either fires or does not at any instant of time so that transmitted signals can be treated as binary. However, the frequency of firing varies and can be viewed as a signal of either greater or lesser magnitude. This corresponds to looking at

discrete time steps and summing all activity (signals received or signals sent) at a particular point in time.

The transmission of the signal from a particular neuron is accomplished by an action potential resulting from differential concentrations of ions on either side of a neuron's axon sheath (the brain's "white matter"). The ions most directly involved are potassium, sodium, and chloride.

A generic biological neuron is illustrated in Figure 5.3, together with axons from two other neurons and dendrites for two other neurons. Several key features of the processing elements of artificial neural networks are suggested by the properties of biological neurons:

1. The processing element receives many signals;
2. Signals may be modified by a weight at the receiving synapse;
3. The processing element sums the weighted inputs;
4. Under appropriate circumstances (sufficient input), the neuron transmits a single output;
5. The output from a particular neuron may go to many other neurons (the axon branches).

Other features of artificial neural networks that are suggested by biological neurons are:

6. Information processing is local (although other means of transmission, such as the action of hormones, may suggest means of overall process control);
7. Memory is distributed:
   a. Long-term memory resides in the neurons' synapses or weights;
   b. Short-term memory corresponds to the signals sent by the neurons;

8. A synapse's strength may be modified by experience;

9. Neurontransmitters for synapses may be excitatory or inhibitor.

Yet another important characteristic that artificial neural networks share with biological neural systems is fault tolerance. A biological neural system is fault tolerant in two respects. First, we are able to recognize many input signals that are somewhat different from any signal we have seen before. Second, we are able to tolerate damage to the neural system itself. Humans are born with as many as 100 billion neurons. Most of these are in the brain, and most are not replaced when they die. In spite of our continuous loss of neurons, we continue to learn. Even in cases of traumatic neural loss, other neurons can sometimes be trained to take over the function of the damaged cells. In a similar manner, artificial neural networks can be designed to be insensitive to small damage to the network, and the network can be retrained in cases of significant damage (e.g., loss of data and some connections).

Even for uses of artificial neural networks that are not intended primarily to model biological neural systems, attempts to achieve biological plausibility may lead to improved computational features.

5.3 Fundamental feature of Neural Networks

Often, it is convenient to visualize neurons as arranged in layers. Typically, neurons in the same layer behave in the same manner. Key factors in determining the behavior of a neuron are its activation function and the pattern of weighed connections over which it sends and receives signals. Within each layer, neurons usually have the same activation function and the same pattern of connection to other neurons. To be more

specific, in many neural networks, the neurons within a layer are fully interconnected or not interconnected at all. If any neuron in a layer (for instance, the layer of hidden units) is connected to a neuron in another layer, then each hidden unit is connected to every output neuron.

The arrangement of neurons into layers and the connection patterns within and between layers is called the net architecture. Many neural nets have an input layer in which the activation of each unit is equal to an external input signal. The net illustrated in Figure 5.2 has two layers of weights.

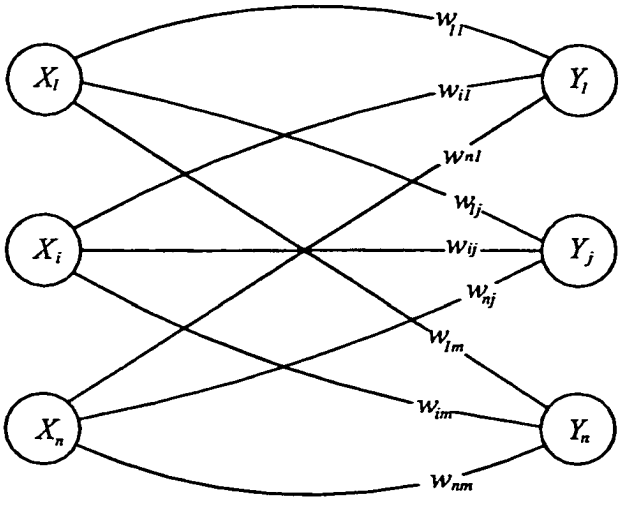

Figure 5.4 Single-Layer Feed Forward Neuron Network

The single-layer and multilayer nets illustrated in Figures 5.4 and 5.5 are example of feed forward nets – nets in which the signals flow from the input units to the output units in a forward direction. The fully interconnected competitive net in Figure 5.6 is an example of a recurrent net, in which there are closed-loop signal paths from a unit back to itself

5.4 Feed Forward Multilayer Neural Networks

A feed forward multilayer network is a net with one or more layers of nodes (the so-called hidden layers) between the input units and the output layer. Multilayer nets can solve more complicated problems than can single layer nets, but training may be more difficult. However, in some cases, training may be more successful because it is possible to solve a problem that a single layer net cannot be trained to perform correctly at all.

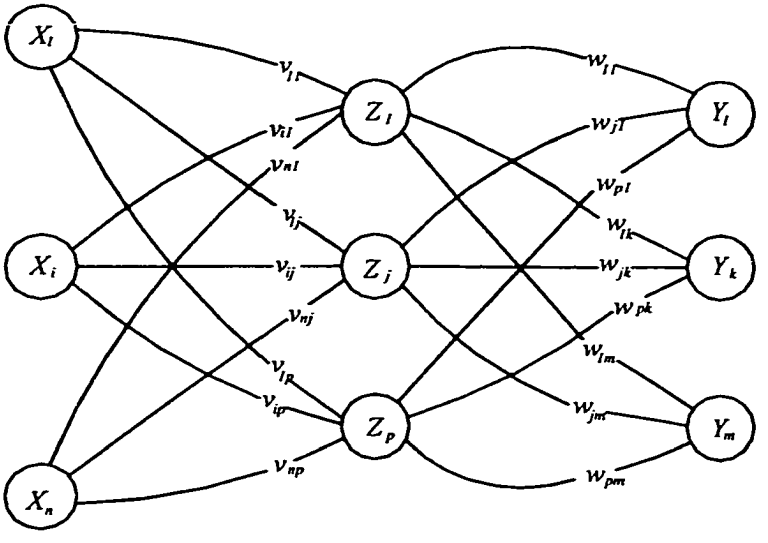

Figure 5.5 A Multilayer Neural Network

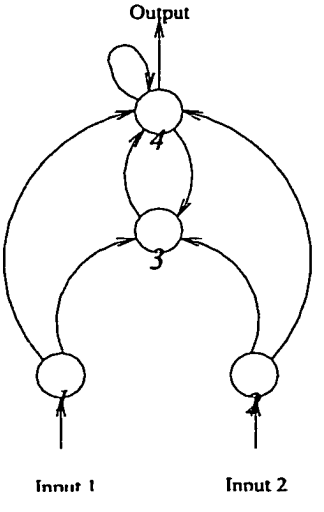

Figure 5.6 Recurrent Neural Network

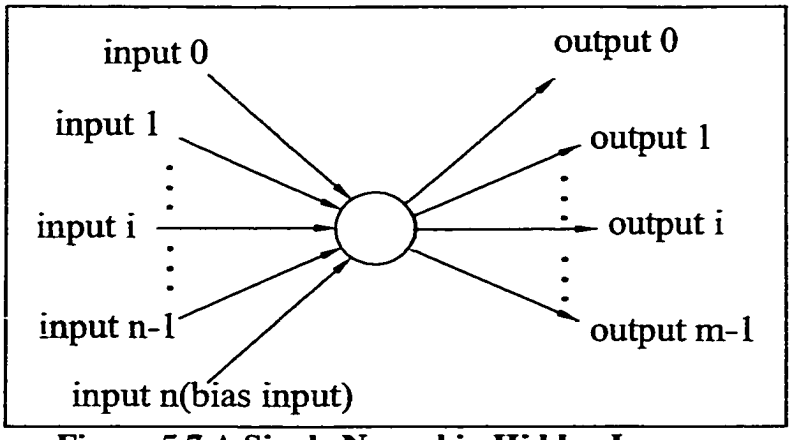

Figure 5.7 A Single Neural in Hidden Layer

A single neuron of a hidden layer is shown schematically in Figure 5.7. It has n inputs, labeled from 0 through n-1. It also has the n^{th} assumed input, called bias, which is always equal to 1.0 or some other fixed number. The neuron is characterized by $n+1$ weights which multiply each input, and an activation function which is applied to the weighted sum of inputs in order to produce the neuron's output. The weighted sum of inputs, including the bias, is frequently called the net input. Thus, the neuron's output is calculated as:

$$out = f(net) = f(\sum_{i=0}^{n-1} x_i w_i + w_n) \tag{5.3}$$

The operation characteristics of this neuron are primarily controlled by the weights, w_i. Although the activation function f(net) is also obviously important, it can be seen that in practice that the neuron's operation is generally little affected by the exact nature of the activation function as long as some basic requirements are met. Training speed, on the other hand, may be strongly impacted by the activation function.

Normally, a feed forward network usually has one single layer of hidden neurons between the input and output layers. Such a network is called a three-layer network.

Rarely, two hidden layers will be needed. A four-layer network is shown schematically in Figure 5.8.

5.4.1 Activation function

The activation function is a nonlinear function that, when applied to the net input of a neuron, determines the output of that neuron. Its domain must generally be all real number, as there is no theoretical limit to what the net input can be. The range of the activation function is usually limited. The most common limits are 0 – 1, while some range from –1 – 1.

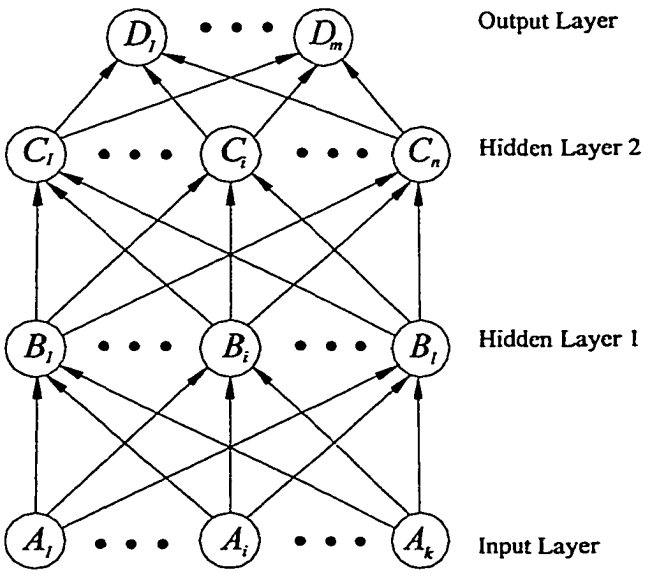

Figure 5.8 Four-Layer Feed Forward Neural Network

The majority of current models use a sigmoid (S-shaped) activation function. A sigmoid function may be loosely defined as a continuous, real-valued function whose domain is real, whose derivative is always positive, and whose range is bounded. The most commonly employed sigmoid function is the logistic function:

$$f(x) = \frac{1}{1+e^{-x}} \tag{5.4}$$

One advantage of this function is that its derivative is easily found:

$$f'(x) = f(x)(1 - f(x)) \tag{5.5}$$

It must be kept in mind that sigmoid functions never reach their theoretical minimum or maximum. For example, neurons that use the logistic function should be considered fully activated at around 0.9, and turn off at about 0.1 or so. It is futile to attempt to train a network to achieve extreme values as its output.

5.4.2 Back Propagation

The back propagation learning algorithm is a key feature of most neural networks. It has reawakened the scientific and engineering community to the modeling and processing of many quantitative phenomena using neural networks. This learning algorithm is applied to multilayer feed forward networks consisting of processing elements with continuous differentiable activation functions. Such networks associated with the back-propagation learning algorithm are also called back-propagation networks. Given a training set of input-output pairs, the algorithm provides a procedure for changing the weights in a back-propagation network to classify the given input pattern correctly. The basis for this weight update algorithm is simply the gradient-descent method as used for simple perceptions with differentiable units.

For a given input-output pair ($x^{(k)}$, $d^{(k)}$), the back-propagation algorithm performs two phases of data flow. As a result of this forward flow of data, it produces an actual output $y.^{(k)}$ Then the error signals resulting from the difference between $d,^{(k)}$ and $y^{(k)}$ are back propagated from the output layer to the previous layers update their weights. A three layer network is shown in Figure 5.8. In Figure 5.8, the network has m nodes in the input layer, l nodes in the hidden layer, and n nodes in the output layer; the solid lines show the

forward propagation of signals, and the dashed lines show the backward propagation of errors.

First consider an input-output training pair $(x^{(k)},d^{(k)})$. Given an input pattern x, a node q in the hidden layer receives a net input of:

$$net_p = \sum_{j=1}^{m} v_{qj} x_j \tag{5.6}$$

and produces an output of:

$$z_q = f(net_q) \tag{5.7}$$

The net input for a node in the output layer is then:

$$net_i = \sum_{q=1}^{l} w_{iq} z_q = \sum_{q=1}^{l} w_{iq} f(\sum_{j=1}^{m} v_{qj} x_j) \tag{5.8}$$

and it produces an output of :

$$y_i = f(net_j) = f(\sum_{q=1}^{l} w_{iq} z_q) = f(\sum_{q=1}^{l} w_{iq} f(\sum_{j=1}^{m} v_{qj} x_j)) \tag{5.9}$$

The above equations indicate the forward propagation of input signals through the layers of neurons. Next, the error signals and their back propagation should be considered. First define a error function:

$$E(w) = \frac{1}{2}\sum_{i=1}^{n}(d_i - y_i)^2 = \frac{1}{2}\sum_{i=1}^{n}[d_i - f(neti)]^2 = \frac{1}{2}\sum_{i=1}^{n}[d_i - f(\sum_{q=1}^{l} w_{iq} z_q)]^2 \tag{5.10}$$

Then according to the gradient-descent method, the weights in the hidden-to-output connections are updated by:

$$\Delta w_{iq} = -\eta \frac{\partial E}{\partial w_{iq}} \tag{5.11}$$

Using Equations 5.8 – 5.10 and the chain rule, we have:

$$\Delta w_{iq} = -\eta\left[\frac{\partial E}{\partial y_i}\right]\left[\frac{\partial y_i}{\partial (net_i)}\right]\left[\frac{\partial (net_i)}{\partial w_{iq}}\right] = \eta[d_i - y_i][f'(net_i)[z_q] = \eta\delta_{oi} z_q \qquad (5.12)$$

where δ_{oi} is the error signal, and its double subscript indicates the ith node in the output layer. The error signal is defined by:

$$\delta_{oi} = \frac{\partial E}{\partial (net_i)} = \left[\frac{\partial E}{\partial y_i}\right]\left[\frac{\partial y_i}{\partial (net_i)}\right] = [d_i - y_i][f'(net_i)] \qquad (5.13)$$

where net_i is the net input to node i of the output layer, and $f'(net_i)=\partial f(net_i)/\partial(net_i)$. The result thus far is identical to the delta learning rule obtained for a single-layer.

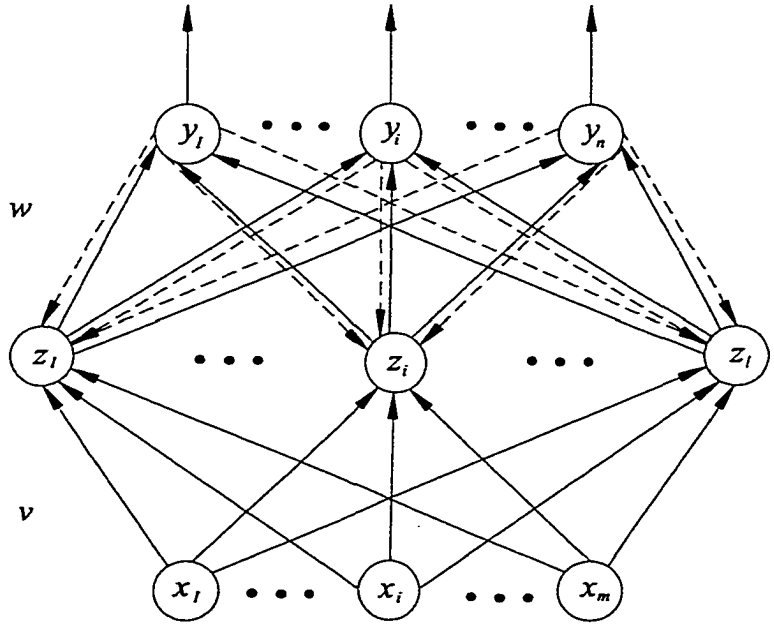

Figure 5.9 Three-Layer Back Propagation Network

For the weight update on the input-to-hidden connection, we can use the chain rule with the gradient-descent method and obtain the weight update on the link weight connecting node j in the input layer to node q in the hidden layer:

$$\Delta v_{qj} = -\eta\left[\frac{\partial E}{\partial v_{qj}}\right] = -\eta\left[\frac{\partial E}{\partial (net_q)}\right] = -\eta\left[\frac{\partial E}{\partial z_q}\right]\left[\frac{\partial z_q}{\partial (net_q)}\right]\left[\frac{\partial (net_q)}{\partial w_{qj}}\right] \qquad (5.14)$$

From Equation 5.10, it is clear that each error tern $[d_i-y_i]$, $i = 1,2,...n$, is a function of z_q. Evaluating the chain rule, we have:

$$\Delta v_{qj} = \eta \sum_{i=1}^{n} [(d_i - y_i) f'(net_i) w_{iq}] f'(net_q) x_j \tag{5.15}$$

Using Equation 5.13, we can rewrite Equation 5.15 as:

$$\Delta v_{qj} = \eta \sum_{i=1}^{n} [d_{oi} w_{iq}] f'(net_q) x_j = \eta \delta_{hq} x_j \tag{5.16}$$

where δ_{hq} is the error signal of node q in the hidden layer and is defined as:

$$\delta_{hq} = -\frac{\partial E}{\partial (net_q)} = -\left[\frac{\partial E}{\partial z_q}\right]\left[\frac{\partial z_q}{\partial (net_q)}\right] = f'(net_q) \sum_{i=1}^{n} \delta_{oi} w_{iq} \tag{5.16}$$

where net_q is the net input to the hidden node q. The error signal of a node in a hidden layer is different from the error signal of a node in the output layer, as seen in Equations 5.13 and 5.17. Because of this difference, the above weight update procedure is called the generalized delta learning rule. We observe from Equation 5.17 that the error signal δ_{hq} of a hidden node q can be determined in terms of the error signal δ_{oi} of the nodes, y_i, that it feeds. The coefficients are just the weights used for the forward propagation, but here they are propagating error signals (δ_{oi}) backward instead of propagating signals froward. This is shown by a dashed line in Figure 5.9. This also demonstrates one important feature of the back-propagation algorithm – the update rule is local; that is, to compute the weight change for a given connection, we need only quantities available at both ends of that connection.

Note that both Equations 5.12 and 5.16 are in the same form of the general weight learning rule in Equation 5.10, except that the learning signals, $r = \delta$, are different. The above derivation can be easily extended to the network with more than one hidden layer

by using the chain rule continuously. In general, with an arbitrary number of layers, the back propagation update rule in the form:

$$\Delta w_{ij} = \eta \delta_i x_j = \eta \delta_{output-i} \times x_{input-j} \tag{5.18}$$

where *output-i* and *input-j* refer to the two ends of the connection from node j to node *i*, x_j is the proper input-end activation from a hidden node or an external input, and δ_i is the learning signal which is defined by Equation 5.13 for the last (or output) layer of connection weights and defined by Equation 5.17 for all the other layers, When the bipolar sigmoid function is used as the activation function, then Equations 5.13 and 5.17, respectively, become:

$$\delta_{oi} = \frac{1}{2}(1 - y_i^2)[d_i - y_i] \tag{5.19}$$

and

$$\delta_{hq} = \frac{1}{2}(1 - z_q^2)\sum_{i=1}^{n} \delta_{oi} w_{iq} \tag{5.20}$$

In summary, the error back-propagation learning algorithm Back Propagation is shown below.

Algorithm BP: Back-propagation Learning Rule

Consider a network with Q feedforward layers, $q=1,2....Q$, and let ${}^{q}net_i$ and ${}^{q}y_i$ denote the net input and output of the *i*th unit in the *q*th layer, respectively. The network has m input nodes and n output nodes. Let ${}^{q}w_{ij}$ denote the connection weight from ${}^{q-1}y_j$ to ${}^{q}y_i$.

Input: A set of training pairs $\{(x^{(k)},d^{(k)})|\ k = 1,2,...p\}$ where the input vectors are augmented with the last elements as 1, that is, $x^{(k)}_{m+1}=1$.

Step 0 (Initialization): choose $\eta>0$ and E_{max} (maximum tolerable error). Initialize the weights to small random values. Set $E=0$ and $k=1$.

Step 1 (Training loop): Apply the kth input pattern to the input layer ($q=1$):

$$^{q}y_i = {}^{1}y_i = x_i^{(k)} \text{ for all i.} \tag{5.21}$$

Step 2 (Forward propagation): Propagate the signal forward through the network using:

$$a_{yi} = a(^{q}net_j) = a(\sum_j {}^{q}w_{ij}{}^{q-1}y_j) \tag{5.22}$$

for each i and q until the outputs of the output layer ${}^{Q}y_i$ have all been obtained.

Step 3 (Output error measure): Compute the error value and error signals ${}^{Q}\delta_i$ for the output layer:

$$E = \frac{1}{2}\sum_{i=1}^{n}(d_i^{(k)} - {}^{Q}y_i)^2 + E \tag{5.23}$$

$${}^{Q}\delta_i = (d_i^{(k)} - {}^{Q}y_i)f'({}^{Q}net_i) \tag{5.24}$$

Step 4 (Error back-propagation): Propagate the errors backward to update the weights and compute the error signals ${}^{q-1}\delta_i$ for the preceding layers:

$$\Delta^{q}w_{ij} = \eta^{q}\delta_i^{q-1}y_j \quad \text{and} \quad {}^{q}w_{ij}^{new} = {}^{q}w_{ij}^{old} + \Delta^{q}w_{ij} \tag{5.25}$$

$$^{q-1}\delta_i = f'(^{q-1}net_i)\sum {}^{q}w_{ji}{}^{q}\delta_j \quad \text{for q = Q, Q-1,....2.} \tag{5.26}$$

Step 5 (One epoch looping): Check whether the whole set of training data has been cycled once, If $k<p$, then $k = k+1$ and go to step 1; otherwise go to step 6.

Step 6 (Total error checking): Check whether the current total error is acceptable, If $E < E_{max}$, then terminate the training process and output the final weights; otherwise $E = 0$, and $k = 1$, and initiate the new training epoch by going to step 1.

End BP

The above algorithm adopts the incremental approach in updating the weights; that is the weights are changed immediately after a training pattern in presented. The alternative is batch-mode training – where the weights are changed only after all the training patterns have been presented. The relative effectiveness of the two approaches depends on the problem, but batch-mode training requires additional local storage for each connection to maintain the immediate weight change. Furthermore, for best results, patterns should be chosen at random from the training set instead of following a fixed order as in step 1 of the algorithm BP.

Before discussing the convergence property of the back-propagation learning algorithm, we first take a look at the function approximation capability of multilayer feed forward networks. The following theorem addresses this issue which is presented and proved in [Homik et al., 1989]

Theorem 5.1

Multilayer feed forward network architectures, with as few as one hidden layer using arbitrary squashing activation functions and linear or polynomial integration functions, can approximate virtually any (Borel-measurable) function of interest to any desired degree of accuracy provided sufficiently many hidden units are available. A function a: $\Re \rightarrow [0,1]$ (or [-1.1]) is a squashing function if it is non-

decreasing, $\lim_{\lambda \to \infty} f(\lambda) = 1$, and $\lim_{\lambda \to -\infty} f(\lambda) = 0$ or (-1), where λ is a parameter in the squashing function.

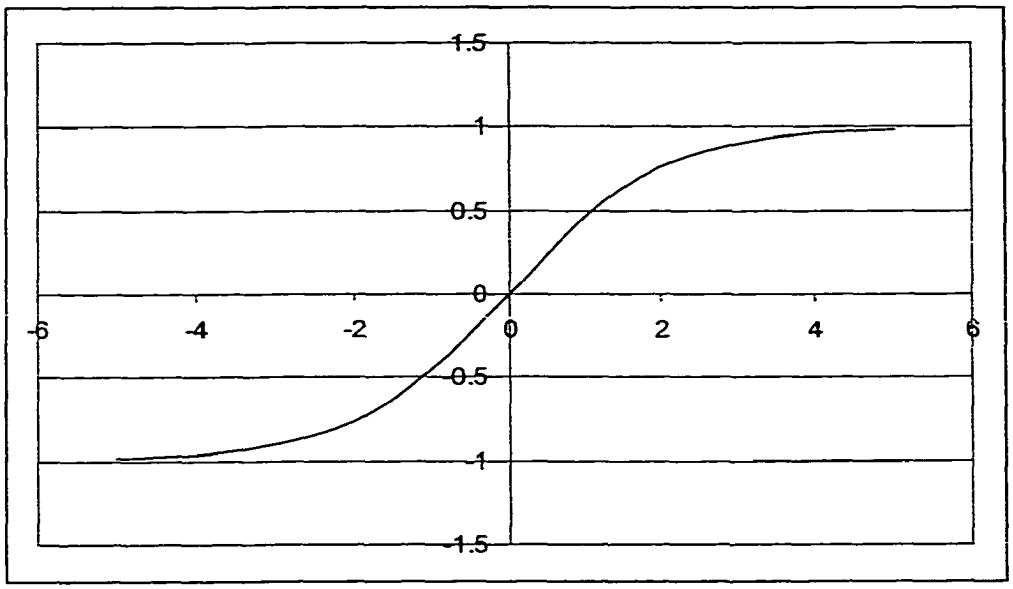

Figure 5.10 Bipolar Sigmoid Function $f(x) = \frac{2}{1+e^{-x}} - 1$

It is clear that the activation function defined in Equation 5.4 is a squashing function. Theorem 5.1 establishes multilayer feed forward networks as a class of universal approximators. This implies that any lack of success in application must arise from inadequate learning, insufficient numbers of hidden units, or lack of a deterministic relationship between input and desired output. Although this theorem indicates that three layers are always enough, some times it is essential to have four, five, or even more layers in solving real world problems. This is because an approximation with three layers would require an impracticably large number of hidden nodes for some problem, whereas an adequate solution can be obtained with a tractable network size by using more than three layers.

5.4.3 Learning Factors of Back Propagation

We shall address the issue of convergence of the back-propagation algorithm based on some important learning factors such as the initial weights, the learning constant, the cost function, the update rule, the size and nature of the training set, and the architecture (number of layer and number of nodes per layer). Our concern will focus on the problems of learning speed, local minima, and the generalization capability of back-propagation networks. Some variations on back propagation will also be introduced.

5.4.3.1 Initial Weights. The initial weights of a multilayer feed forward network strongly affects the ultimate solution. They are typically initialized at small random value. Equal initial weight values cannot train the network properly if the solution requires unequal weights to be developed. The initial weights cannot be large, otherwise the sigmoid will saturate from the beginning, and the system will become stuck at a local minimum or in a very flat area new the starting point. One proper way is to choose the weight w_{ij} in the range of $\left[-3/\sqrt{k_i}, 3/\sqrt{k_i}\right]$, where k_i is the numbers of node that feed forward to node i (the number of input links of node i).

5.4.3.2 Learning Constant (Learning Rate). Another important factor that effects the convergence of the back propagation learning algorithm significantly is the learning constant η. There is no single learning constant value suitable for different training cases, and η is usually chosen experimentally for each problem. A larger value of η could speed up the convergence but might result in overshooting, while a smaller value of η has a complementary effect. Values of η ranging from 10^{-3} to 10 have been used successfully for many computational back-propagation experiments.

Another problem is that the best values of the learning constant at the beginning of training may not be as good in later learning. Thus a more efficient approach is to use an adaptive learning constant [Vogl et al., 1988; Jacobs, 1988]. The intuitive method is to check whether a particular weight update has decreased the cost function. If it has not, then the process has overshot, and η should be reduced. On the other hand, if several steps in a row have decreased the cost function, then we may be too conservative and should try increasing η. More precisely, the learning constant should be updated according to the following rule [Hertz.et al., 1991]:

$$\Delta\eta = \begin{cases} +a & \text{if } \Delta E < 0 \text{ consistently} \\ -b\eta & \text{if } \Delta E > 0 \\ 0 & \text{otherwise} \end{cases} \tag{5.27}$$

where ΔE is the change in the cost function, and a and b are positive constants. The meaning of "consistently" in Equation 5.27 can be judged based on the last k learning steps or on a weighted moving average of the observed ΔE.

5.4.3.3 Cost Functions. The quadratic cost function in Equation 5.10 is not the only possible choice. The squared error term $(d_i-y_i)^2$ can be replaced by any other differentiable function $f(d,y)$ which is minimized when its arguments are equal. Based on this new cost function, we can derive a corresponding update rule. It can be easily seen that only the error signal δ_{oi} in Equation 5.13 for the output layer changes for different cost functions, while all the other equations of the back-propagation algorithm remain unchanged.

The cost functions usually used are those based on L_p norm ($1 \leq p \leq \infty$) because of the advantage of easier mathematical formulation. Such cost functions are in the form of:

$$E = \frac{1}{p}\sum_i (d_i - y_i)^p \tag{5.28}$$

In particular, the least squares criteria used in the quadratic cost function is widely employed because of its simplicity.

5.4.3.4 Momentum. The gradient descent can be very slow if the learning constant η is small and can oscillate widely if η is too large. This problem essentially results from error surface valleys with steep sides but a shallow slope along the valley floor. One efficient and commonly used method that allows a larger learning constant without divergent oscillations occurring is the addition of a momentum term to the normal gradient-descent method (Palut et al., 1986). This idea is to give each weight some inertia or momentum so that it tends to change in the direction of the average downhill force that it feels. This scheme is implemented by giving a contribution from the previous time step weight change:

$$\Delta w(t) = -\eta \nabla E(t) + \alpha \Delta w(t-1) \tag{5.30}$$

where $0 \leq \alpha \leq 1$ is a momentum parameter, and a value of 0.9 is often used. Figure 5.10 shows the trajectories of gradient descent with and without momentum on a simple quadratic surface. Note that the trajectory without momentum (the left curve) has larger oscillations than the one with momentum (the right curves). We further observe from the right curves in Figure 5.9 that the momentum can enhance progress toward the target point if the weight update is in the right direction (point A to A'). On the other hand, it can redirect movement in a better direction toward the target point in the case of overshooting (Point B to B'). This observation indicates that the momentum term

typically helps to speed up the convergence and to achieve an efficient and more reliable learning profile.

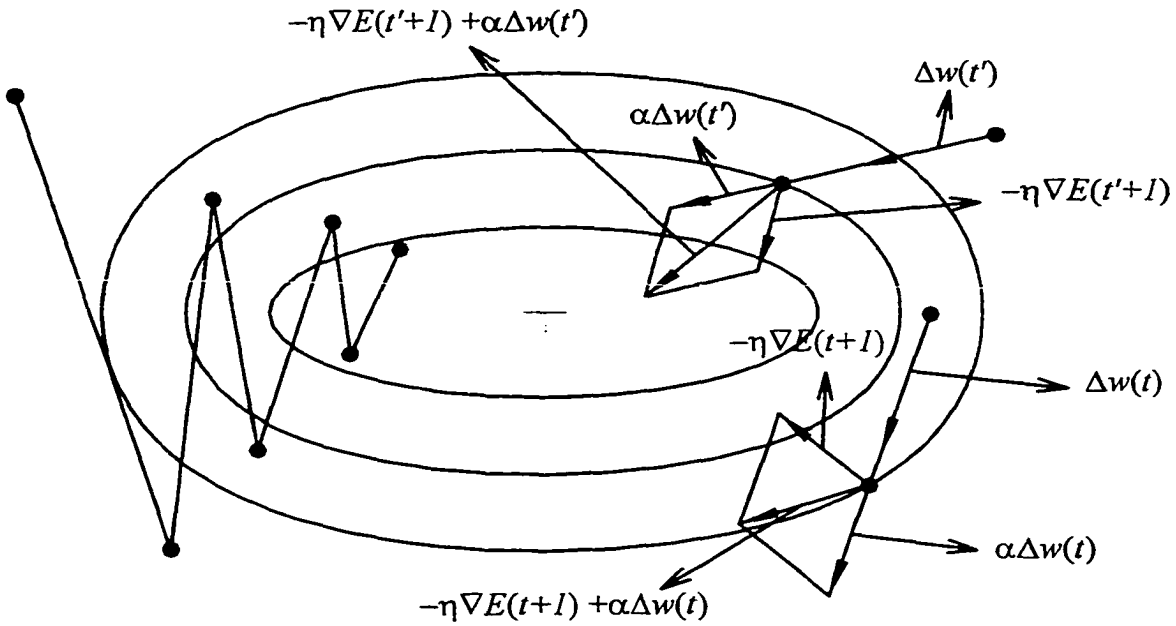

Figure 5.11 Gradient Descent on a Simple Quadratic Surface

5.4.3.5 Number of Hidden Nodes. The size of a hidden layer is a fundamental question often raised in the application of multilayer feedforward networks to real-world problems. The exact analysis of this issue is rather difficult because of the complexity of the network mapping and the non-deterministic nature of many successfully completed training procedures. Hence, the size of a hidden layer is usually determined experimentally. One empirical guideline is as follows. For a network of reasonable size (e.g., hundreds or thousands of inputs), the size of hidden nodes needs to be only a relative small fraction of the input layer. If the network fails to converge to a solution, it may be that more hidden nodes are required. If it does converge, fewer hidden nodes can

be tried and then settle on a size based on overall system performance (Freeman and Skapura, 1991).

5.4.3.6 Local Minimum. Every person charged with minimizing a function hopes that it resembles a trampoline with a cannon ball resting in its center. Unfortunately, real-life problems often have cross sections that look more like Figure 5.11. Obviously, any algorithm that relentlessly crawls downward must have a very lucky starting position if it is to settle into the lowest local minimum.

Avoiding false minima requires two separate procedures. First, we must avoid starting in local minimum vicinity. Referring to the figure above, it behooves us to start somewhere in the left half. If we settle into the broad minimum in the right half, it will be very difficult to escape later. Second, we require a procedure for determining whether or not we are in a local minimum and escaping if we are. This procedure will be constructive in that we simply attempt to escape. If we succeed, we conclude that we were in a local minimum. Otherwise, we assume that we have found the global minimum.

5.4.3.7 Local Minima Happen Easily. It is surprisingly easy for gradient algorithms to get stuck in local minima when learning feed forward network weights. Their error surfaces lend a whole new meaning to the term ill-conditioned. Even tiny problems can sport local minima, and these minima can be very broad, attracting us in from distant locations. This means that we should always repeat the learning process from several different starting positions. It is reckless to use just one starting-weight configuration, assuming that the minimum to which it leads is the best that we can do.

Neural networks always have many equally good global minima. This is because of the numerous symmetric inherent in the architecture. Swapping weight vectors among hidden neurons obviously yields identical networks in terms of input/output mapping. Other symmetries are possible. These multiple global minima are no problem and must not be confused with the serious problem of inferior local minima.

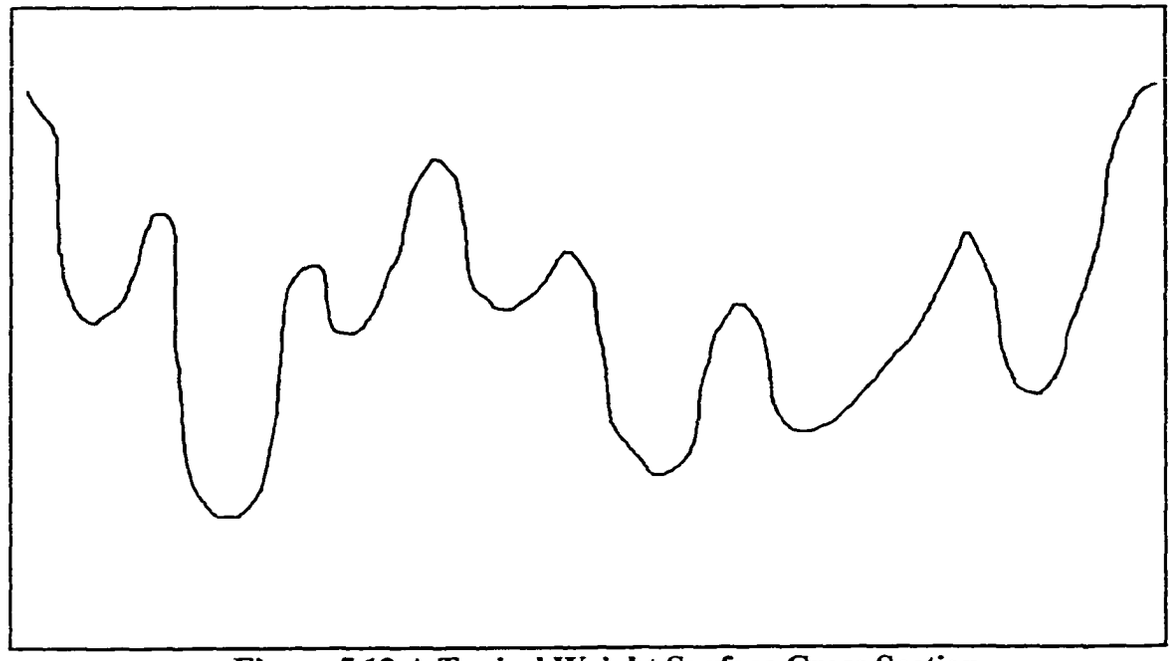

Figure 5.12 A Typical Weight Surface Cross Section

Gori and Tesi, [1990] give a demonstration of just how easily local minima can arise. The details in their proof are tedious and so will not be reproduced here. But one of their main results is definitely worth presenting.

Consider the XOR problem. We have two inputs and one output, the training set consist of four cases, being each of the four possible combinations of 1 and 0 which the two inputs can take on. The output is on if and only if exactly one of the two inputs is 1. This is shown graphically in Figure 5.13. The four corner circles in that figure represent the classical XOR problem

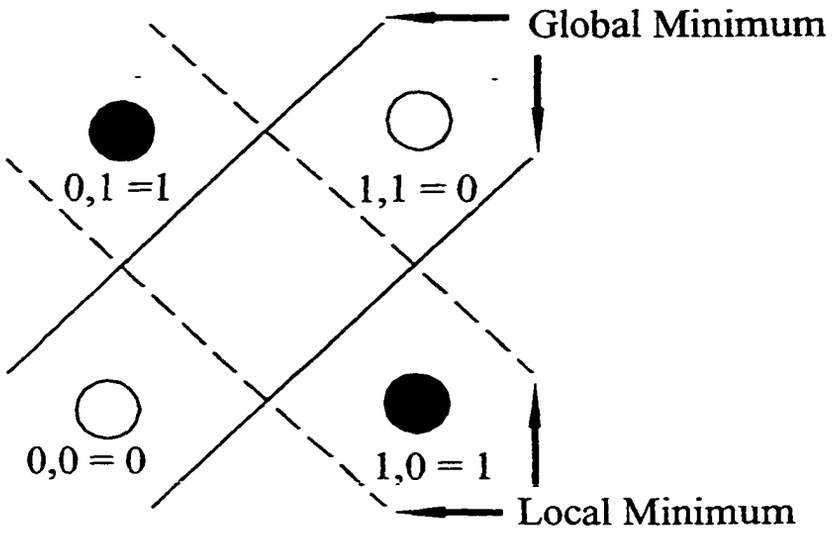

Figure 5.13 A Local Minimum in Gradient Learning

The minimal feedforward network capable of solving this problem has two hidden neurons. Such a network operates by partitioning its bivariate input domain into three regions. The two outer regions correspond to one output state, while the inner region is the other output state. Two such partitionings are shown in that figure, one with dark lines and the other with dotted lines. Observe that either will solve the XOR problem so that both correspond to global minimum-weight configurations.

Two very different techniques can be used. The first, simulated annealing, is easy to understand and implement and has low memory requirements. It may be used for both initially avoiding and later escaping local minimum. The second, a genetic algorithm, is more complex and has quite large memory needs.

In broad outline, the idea of a genetic algorithm is to encode the problem in a string. For example, if the problem is to find the maximum of a scalar function f(x), the string can be obtained by representing x in binary. A population represents a diverse set of strings that are different possible solutions to the problem. The fitness function scores

each of these as to its optimality. In the example, the associated value of f for each binary string is its optimality. In the example, the associated value of f for each binary string is its fitness. At each generation, operators produce new individuals (strings) that are on average fitter. After a given set of generations, the fittest member in the population is chosen as the answer.

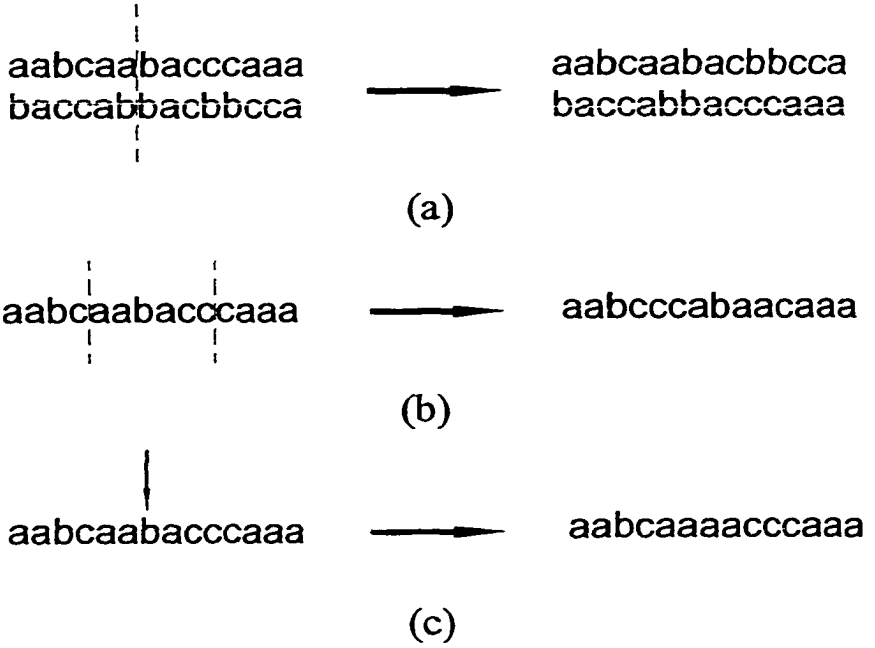

Figure 5.14 Genetic Operations on a Three-Letter Alphabet of {a,b,c}; (a) Crossover Swaps Strings at a Crossover Point; (b) Inversion Reverses the Order of Letters in Substring; (c) Mutation Changes a Single Element

Genetic Algorithm can be decrbed as follow:

Choose a population size

Choose the number of generations N

Initialize the population

Repeat the following for N generations

1. Select a given number of pairs of individuals from the population probabilistically after assigning each structure a probability proportional to observed performance
2. Copy the selected individuals, then apply operators to them to produce new individuals
3. Select other individuals at random and replace them with the new individuals
4. Observe and record the fitness of the new individuals

Output the fittest individual as the answer

Genetic Operators are Crossover, Inversion Reverse and Mutation.

5.4.5.8 Simulated Annealing. Annealing is a term from metallurgy. When the atoms in a piece of metal are aligned randomly, the metal is brittle and fractures easily. In the process of annealing, the metal is heated to a high temperature causing the atoms to shake violently. If it were cooled suddenly, the microstructure would be locked into a random unstable state. Instead, it is cooled very slowly. As the temperature drops, the atoms tend to fall into patterns that are relatively stable for that temperature. Providing that the temperature drop is slow enough, the metal will eventually stabilize into an orderly structure.

The analogue of this process in optimization may be seen by examining Figure 5.12. Suppose one were to toss a ball onto that function and shake it strongly. After each shake, the ball might land anywhere. If the strength of the shaking is reduced, eventually the ball will land somewhere in the right half and henceforth be unable to jump high enough to move to the left half. If it lands in one of the small pockets in the right side, relatively little shaking will be needed to toss it over the edge into a deeper pocket. Once

down low, the relatively weak shaking will be unable to toss it into a higher pocket. This process continues until it eventually settles into the lowest pocket.

Simulated annealing can be performed in optimization by randomly perturbing the independent variables (weights in the case of a neural network) and keeping track of the best (lowest error) function value for each randomized set of variable. A relatively high standard deviation for the random number generator is used at first. After many tries, the set that produced the best function value is designated to be the center about which perturbation will take place for the next temperature. The temperature (standard deviation of the random number generator) is then reduced and new tries done.

5.4.3.9 Choosing the Annealing Parameters. Each trial of a random weight set can be very time consuming. Thus, we wish to use as few trials as possible. The total number of trails in our method is equal to the product of the number of temperatures times the number of iterations at each temperature. The obvious question is how we choose each of these quantities. Recall that after iterations at a particular temperature are complete. The best weights at that temperature become the center of iteration for the next temperature. So we must consider how quickly we want to become locked into an area. We also need to choose a starting and ending temperature.

The proper choice of these quantities depends on our purpose. If we are initially selecting weights for a starting point, we want to search a broad area. Also, we are not interested in optimizing by slowly dropping the temperature. That task is best left to the conjugate gradient algorithm. Thus we would choose very few temperatures. Two, or at most three, are best. Also, a high starting and stopping temperature would be most appropriate. On the other hand, if we have already progressed to a local minimum and are

trying to escape, it is better to use a few more temperatures, four or so. This is more because of the variety needed, rather than because we want to avail ourselves of the optimization gained by many temperatures. We simply do not know how far we must jump in order to escape the local minimum. It may be very broad, requiring a high temperature. Or it may be a small pocket in a narrow channel. In this case, a high temperature would nearly always toss us too far. By using a moderately high starting temperature and a low stopping temperature, we are most likely to hit the lucky spot.

If the optimization problem does not have a good direction solution, making simulated annealing our only choice, then we must use many temperatures and cover a wide range. The tradeoff now becomes one of "How sure do we want to be that we have the global minimum?" versus "How accurately do we need to estimate the minimum?" If we prefer a rough approximation in exchange for high probability of having the global minimum, the 5 to 10 temperature with a fairly high stopping temperature may be best. On the other hand, if we need high accuracy, we are forced to use many temperatures and drop low. The price we pay is less iteration at each temperature, making it more likely that we will become trapped in a local minimum.

5.5 Neural Network Used in This Research

The neural network used in this research has three layers. Between the input layer and the output layer there is one hidden layer. The input nodes are the microtunneling project properties. They include microtunneling depth, microtunneling product pipe diameter, ground water conditions, and soil properties. The output will be the ground settlement at different points. The input layer has 10 nodes, the hidden layer has 100

nodes, and the output layer has 10 nodes. Each node in the output layer represents the ground settlement at a certain point.

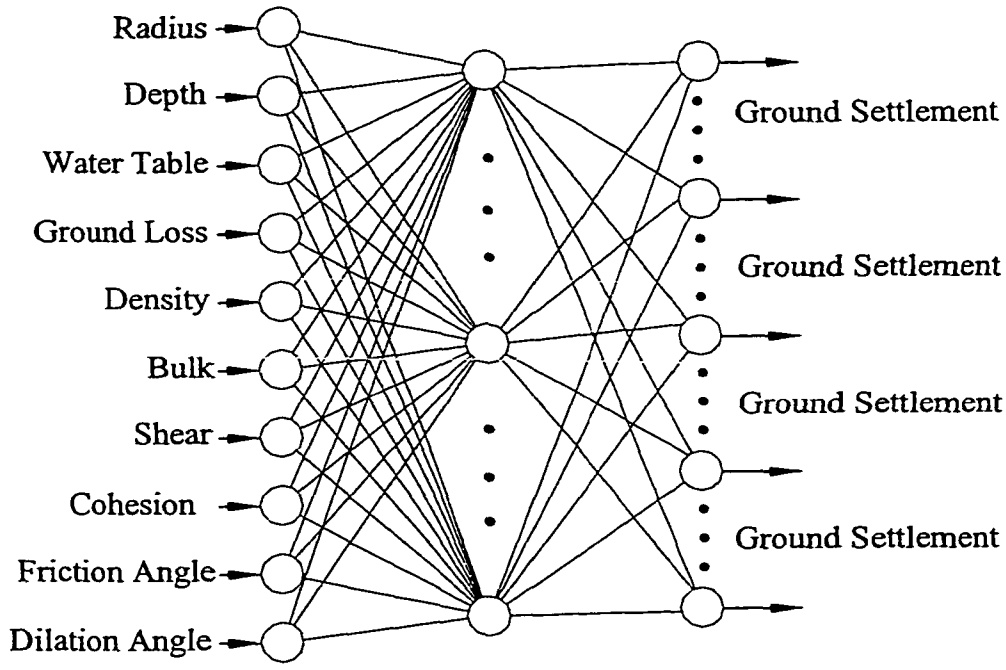

Figure 5.15 Structure of Neural Network Used to Predict the Ground Settlement

5.5.1 Training Set Used to Train Neural Network

The training sets used to train the neural network are the results of the FLAC^{3d} program. Before training, 300 models have been set up with FLAC,^{3d} and the results of these 300 models are used as training set of the neural network.

Several programs were written to speed up the research. First, a program was written to generate the random input value for the neural network and FLAC.^{3D} Because no matter how humans choose, the random test value still contains bias. Using a program can totally eliminate the bias. This program is written in Java (DataGen.java. Appendix A).

In order to allow these random selected data to be shared by the neural network, FLAC^{3D} and other programs, these data are saved in a database. This allows every client program to use the same data and makes the data more organized.

DataFileGen.java (Appendix B) is the program which reads input data from the database and generates a data file suitable for input into FLAC.^{3D} DataFileGen.java is listed in Appendix B, and a typical data file generated by DataFileGen.java is listed in Appendix C.

FLAC^{3D} runs each of these data files that are generated by DataFileGen.java. FLAC^{3D} saves the ground settlement data into a data file. Another program ReadLog.java (Appendix C) reads the ground settlement data from these data files and transfers the settlement data into another format that is suitable to save in the database.

Although ground settlement data from FLAC^{3D} is sufficient to describe the ground profile, it does not always give the ground settlement value at the same fixed distances from the centerline of the pipe. Another program, LeastSquare.java (Appendix D), uses a 10^{th} degree polynomial to fit these data and generate ground settlement at the fixed distances of 0,1,2,3,...,9 meters from center line. These ground settlement data are used to train the neural network.

Specifically 300 sets of random site and project data was saved in the database. The program used these 300 sets of data to generate 300 data input files for FLAC.^{3D} Then FLAC^{3d} ran these 300 data input files to get 300 sets of settlement data, saved in 300 FLAC^{3D} ground settlement output files. These 300 ground settlement data sets, at variable distance from the centerline of the pipe, are then converted to 300 data sets settlement at fixed distances of 0,1,3,...9 meters from the centerline. These 300 sets of

settlement data are combined with their associated site, and project information is used as the training sets for the neural network.

The inputs for the neural network are radius, depth, water table, ground loss, unit weight of soil bulk modulus of soil, shear modulus of soil, cohesion of soil, friction angle of soil, and dilation angle of soil. These inputs and their range are listed in Table 5.1.

Table 5.1 Range of Microtunneling Properties

	Pipe Radius (m)	Depth (m)	Ground Loss (%)
Min Value	0.15	2.0	1.0
Max Value	1.5	24.0	10.0

Table 5.2 Range of Soil Properties

		Unit Weight (kg/m^3)	Young's Modulus (Mpa)	Poisson's Ratio	Cohesion (kPa)	Friction Angle	Dilation Angle
Dense Sand	Min	1800	10.0	0.30	0	32°	0°
	Max	2100	21.0	0.45	0	26°	10°
Medium Sand	Min	1650	5.0	0.25	0	30°	0°
	Max	1850	10.5	0.4	0	33°	10°
Loose Sand	Min	1500	2.4	0.2	0	27°	0°
	Max	1700	5.2	0.4	0	30°	10°
Hard Clay	Min	1800	48	0.2	48.0	0°	0°
	Max	2100	191	0.5	100.0	0°	0°
Medium Clay	Min	1650	24	0.2	24.0	0°	0°
	Max	1850	48	0.5	48.0	0°	0°
Soft Clay	Min	1500	12	0.2	12.0	0°	0°
	Max	1700	24	0.5	24.0	0°	0°

The range of radius is between 0.15 meter and 1.5 meter. The range of depth of microtunneling is between 3.0 meters and 24 meter because typically few microtunneling projects are carried out at the depth of less than 3.0 meters or more than 24 meters. Microtunneling projects at depth of less than 3.0 meters are seldom cost efficient compared to open cut methods, and few sewer pipes are installed below 24 meters. The

range of ground loss is between 1% to 10%. The ground loss parameter is calculated with the method mentioned in chapter 2.

The soil properties range is listed in Table 5.2. A program was written to select soil properties randomly from Table 5.2. All these soil properties conform to values provided in FLAC^{3D} User Manual Volume I.

The back propagation learning algorithm used the gradient descent method to find a local minimum. The back propagation algorithm trains the neural network by adjusting the connection weight between each node. The magnitude of each adjustment can not be too small or too large, and the magnitude heavily depends on the differential value of each node, $f'(net_{input})$. This requires that the value of the differential function can not be too small or too large. A small differential value will make the back propagation very slow to converge, and a large differential value will cause overshooting. The activation function used in this neural network is logistic activation function.

If the input of the derivative function is large (>5), the derivative function output value will be very small. If this happens during training of the neural network, it will cause the function not to converge or to converge very slowly.

There are two causes of large input value of derivative function in the neural network used in this research. First, the absolute value of the input of the neural network is very large. For example, the soil density ranges from 1550 to 2100. This could cause the hidden node input value to be very big. The input to the output layer node will also be very large. Secondly, the hidden layer consists of 100 nodes. This also will cause the input to the output layer node to be very large. As mentioned before, a large input value will cause the back propagation algorithm to converge very slowly.

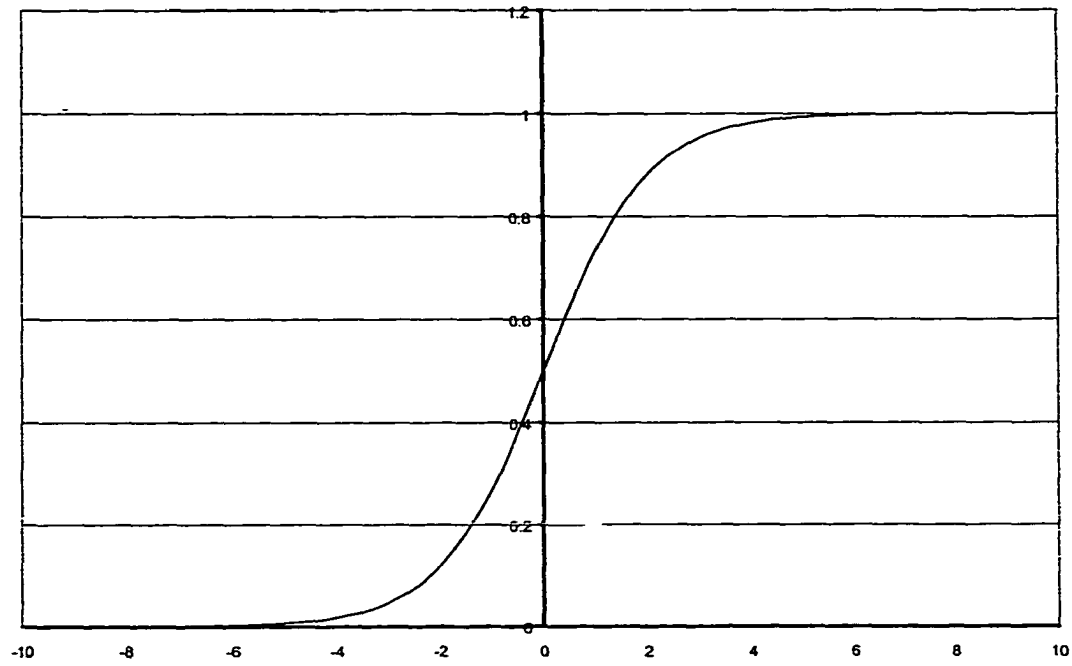

Figure 5.16 Logistic Function

There are two methods to reduce a large input value problem. First, before we input the input value of neural network, we pre-process the input data to make it smaller. For example, we divide the soil density value by 100 and divide the other input values by proper factors. Second, we change the logistic function slope and use an adjusted logistic function:

$$f(x) = \frac{1}{1+e^{-\lambda x}} \tag{5.31}$$

where λ is the coefficient to adjust the slope of logistic function to make the slope smaller around $x = 0$ and make the slope larger around $x = \pm\infty$. This makes the drive value larger even when the x is very large. But the trade off is that it makes the differential function value smaller at x near 0.

In this research, the pre-process input data method is used. The soil density value is divided by 1000 to make the value between 1.55 to 2.1. Other input values are also pre-processed in a similar manner.

Then the back propagation method is used to train neural network using an adaptive learning rate.

5.5.1.1 Initial Weight. The choice of initial weights will influence whether the net reaches a global (or only a local) minimum of the error and, if so, how quickly it converges. The update of the weight between two units depends on both the derivative of the upper unit's activation function and the activation of the lower unit. For this reason, it is important to avoid choices of initial weights that would make it likely that either activation or derivatives of activation are zero. The values for the initial weights must not be too large, or the initial input signals to each hidden or output unit will be likely to fall in the region where the derivative of the sigmoid function has a very high value (the so-called saturation region). On the other hand, if the initial weights are too small, the net input to a hidden or output unit will be close to zero, which causes extremely slow learning. A common procedure is to initialize the weights (and bias) to random values between –0.5 and 0.5 (or between —1 and 1 or some other suitable interval). The values may be positive or negative because the final weights after training may be of either sign also.

A simple modification of random initialization, developed by Nguyen and Widrow, gives much faster learning. The approach is based on a geometrical analysis of the response of the hidden neurons to a single input; the analysis is extended to the case of several inputs by using Fourier transforms. Weights from the hidden units to the output units (and bias on the output units) are initialized to random values between –0.5 and 0.5, as is commonly used

The initialization of the weights from the input units to the hidden units is designed to improve the ability of the hidden units to learn. This is accomplished by distributing initial weights and biases so that, for each input pattern, it is likely that the net input to one of the hidden units will be in the range in which that hidden neuron will learn most readily. The definitions we use are as follows:

n number of input units

p number of hidden units

β scale factor: $\beta = 0.7(p)^{1/n} = 0.7\sqrt[n]{p}$

The procedure consists of the following simple steps:

for each hidden unit j :

initialize its weight vector (from the input units);

$weight_{ij}$ = random number between – 0.5 and 0.5 (or between -γ and γ).

Compute $\|v_j(old)\| = \sqrt{v_{1j}(old)^2 + v_{2j}(old)^2 + \ldots + v_{nj}(old)^2}$

Reinitialize weights:

$$v_{ij} = \frac{\beta v_{ij}(old)}{\|v_j(old)\|} \tag{5.32}$$

Set bias:

v_{oj} = random number between -β and β

The use of Nguyen-Widrow initialization not only improved the training speed but also greatly reduced the chances of generating initial weights for which the neural network fails to converge.

In Chapter 4, Numerical Approach, the effect of all the ten factors is examined. It shows that the microtunneling depth, product pipe diameter, and ground loss have larger

impact on the final ground settlement than any other factor. If the weights, which connect these three inputs of the neural network, have a higher value than the other weights, the network will converge faster. So in this research, the weights connecting these three inputs have a slightly higher initial weight value than the other weights.

5.5.1.2 Number of Hidden Layers. The size of a hidden layer is a fundamental question often raised in the application of multilayer feed forward networks to real-world problems. The exact analysis of this issue is rather difficult because of the complexity of the network mapping and nodeterministic nature of many successfully completed training procedures. Hence the size of a hidden layer is usually determined experimentally. One empirical guideline is as follows: For a network of reasonable size (e.g., hundreds or thousands of inputs), the size of hidden nodes needs to be only a relatively small fraction of the input layer. If the network fails to converge, fewer hidden nodes are tried, and then a size is chosen based on overall system performance.

In this research, the hidden layer contain 100 nodes. This number was selected based on hundreds of tests. Almost every number of hidden node between 50 to 150 was tested. A hidden layer with 100 nodes was selected based on overall system performance.

5.5.1.3 Desired Output Data. The neural network outputs are ground surface settlements at 10 points. These points are the points 0, 1, 2, 3, 4, 5, ...9 meters from the centerline of the pipe. Since the theoretical ground settlement profile of microtunneling project is symmetric, based on these 10 ground settlement values, we can get the ground settlement profile on both side of the pipe with a total width of 18 meters. This profile of settlement profile is typically networks give is typically enough for engineering use.

Some values of the desired outputs are too small to allow effective training of the neural network. As stated before, if the output of an activation function is too small or too large, it will cause the derivative to be value too small to be used to update the weights. So before the raw ground settlement data were used, they were normalized to the interval between 0 to 1 by the equation 5.33:

$$desired\_output = \frac{old\_initial\_output - min\_output}{max\_output - min\_output} \tag{5.33}$$

After processed by equation 5.33, there would be still be some values that are too small. These values are treated by equation 5.34 again to make sure no value is too small. After processing the output value using equation 5.34, the ground settlement value (desired neural network output value) would be at least 0.3. These values allow the derivative value of the activation function to have a suitably large value to training the neural network:

$$new\_desire\_output = \frac{desire\_output + 0.5}{1.5} \tag{5.34}$$

5.5.1.4 Local Minimum. To avoid a local minimum, this neural network used simulated annealing. There is rarely any need for extremely large weights. In fact, large weights can lead to extreme activation levels (near the theoretical limits of the activation function). This is turn gives rise to very small derivatives of the activation function, which in turn tends to paralyze that weight. At each stage, a new random perturbation should not exceed 1. Each new value should be tested against the absolute upper limit. The absolute value of the new weight should not be allowed to exceed this limit. A limit of 1 in this network is sufficiently large to permit wide variation, yet small enough to let gradient techniques pull it in later if necessary.

The first step in the annealing is to copy the input guess v and w matrix to the work matrix-center_v and center_w. The objective function is evaluated at this guess, and the function value preserved as the best so far. The standard deviation of the random perturbation initialized to the user's starting temperature, and the reduction factor is computed.

At the start of each pass through the temperature loop, the improved flag is set to zero. When all iterations at that temperature are complete, the perturbation center for the next temperature will be updated only if that flag was set to 1 due to improvement. Otherwise, the same center will be used again.

The function shake is used to perturb around the center point. It sums uniform deviates to realize a more bell shaped curve than would be attained with one deviate alone. By adding two and subtracting two, the random variable has mean zero.

If the new trial point has a superior function value, update the best function value and save the weight matrix. Set improved flag to indicate that we has a success at this temperature. If the function has been minimized enough to suit the user, break out of the loop. Finally, set back the iteration counter to give us more tries at this temperature, Regardless of whether of not we improved, verify that we have not called the objective function the limiting number of times.

When all iterations at a temperature are complete, test the improved flag. If we improved, set the work weight matrix to the best weight matrix.

5.6 Results

The training of neural network was carried out on a personal computer with a Pentium III processor operating at 500 MHz, 128 MB memory, and the operating system Windows NT 4.0. The total training time was about 26 hours. The average error is about 0.02mm. The absolute error ranges from 0 mm to 0.5 mm, and the relative error ranges from 0% to 55%. The high relative error only occurs at small ground settlement, in test data 4, in which the desired output of the neural network is 0.052 cm, the real output is 0.0807 cm, the absolute error is 0.029 cm, and the relative error is 55%. Even though the relative error is high when ground settlement is small, it does not harm the whole performance of the neural network because in small settlements even with large relative error, the neural network error is still small. The typical relative error ranges from 1% to 6.5%.

Test data 1: In Figure 5.17 the input data is: Radius 1.0275 meter, depth 16.65 meter, ground water depth 23.86 meter, ground loss 9.55%, soil unit weight 2045 kg/m,^{3} bulk modulus 9.92 kPa, shear modulus 4.78 kPa, cohesion 5 MPa, friction angle 27.5,° dilation angle 0.° The ground settlement predicted by FLAC^{3D} is listed in the first column of Table 5.3, and the ground settlement predicted by the neural network is listed in the second column.

Table 5.3 Ground Settlement Data of FLAC^{3D} and Neural Networks (Test Data 1)

Distance from center line (m)	Result of FLAC^{3D} (cm)	Result of neural network (cm)
0	1.203	1.24
1	1.203	1.262
2	1.194	1.228
3	1.178	1.220
4	1.155	1.205
5	1.128	1.154
6	1.096	1.117
7	1.062	1.062
8	1.026	1.013
9	0.988	0.967

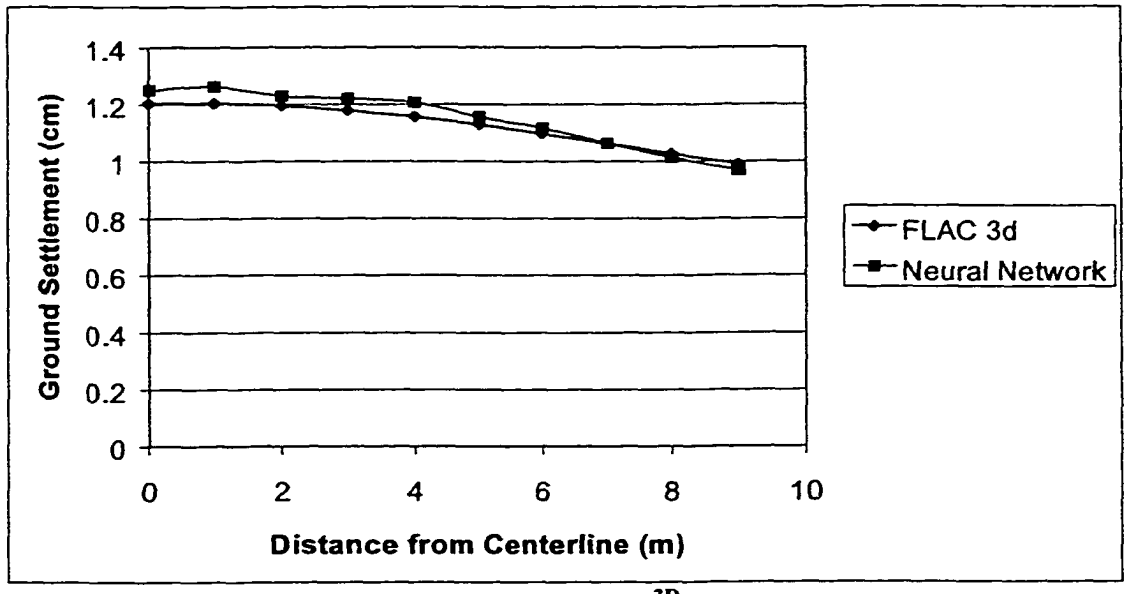

Figure 5.17 Ground Settlement Result of FLAC^{3D} and Neural Network (Test Data 1)

Test data 2: In Figure 5.18, the input data is: Radius 1.0275 meter, depth 19.85 meter, ground water depth 20.44 meter, ground loss 9.1%, soil unit weight 1687.5 kg/m,^{3} bulk modulus 5.38 MPa, shear modulus 3.39 MPa, cohesion 5 MPa, friction angle 32.5,° dilation angle 10.° The ground settlement predicted by FLAC^{3D} is listed in the first column of Table 5.4, and the ground settlement predicted by the neural network is listed in the second column.

Table 5.4 Ground Settlement Data of FLAC^{3D} and Neural Networks (Test Data 2)

Distance from center line (m)	Result of FLAC^{3D} (cm)	Result of neural network (cm)
0	1.103	1.058
1	1.103	1.065
2	1.098	1.073
3	1.087	1.064
4	1.072	1.053
5	1.053	1.035
6	1.031	1.013
7	1.006	0.975
8	0.980	0.945
9	0.952	0.906

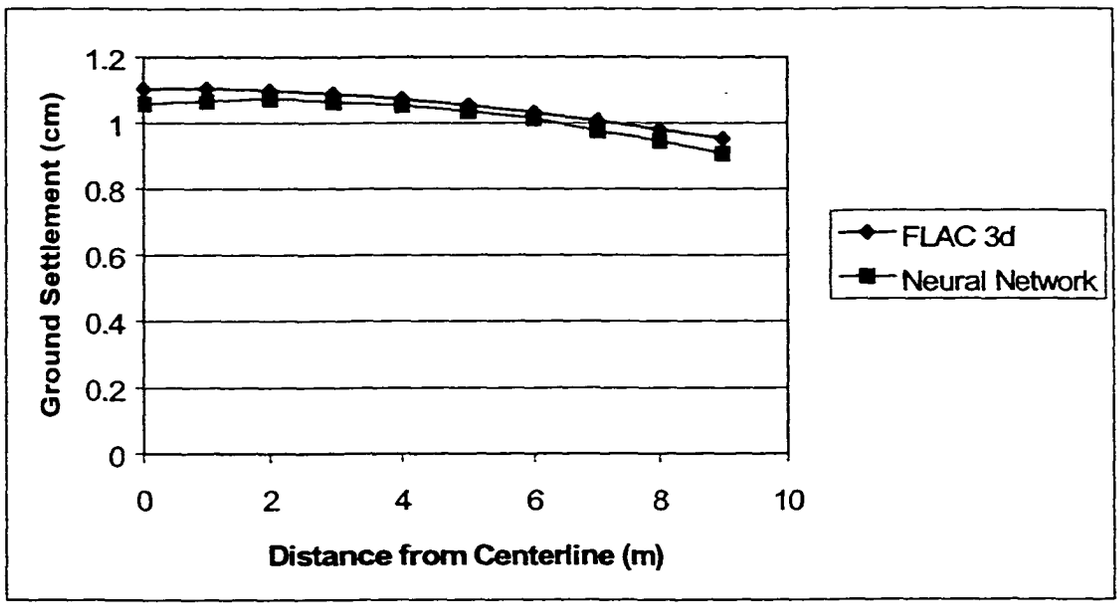

Figure 5.18 Ground Settlement Result of FLAC^{3D} and Neural Network (Test Data 2)

Test data 3: Radius 1.095 meter, depth 20.85 meter, ground water depth 1.82 meter ground loss 6.4%, soil unit weight 1660 kg/m^3, bulk modulus 14.53 MPa, shear modulus 9.897 MPa, cohesion 1 MPa, friction angle 15,° dilation angle 0.° The ground settlement predicted by FLAC^{3D} is listed in the first column of Table 5.5, and the ground settlement of predicted by the neural network is listed in the second column.

Table 5.5 Ground Settlement Data of FLAC^{3D} and Neural Networks (Test Data 3)

Distance from center line (m)	Result of FLAC^{3D} (cm)	Result of neural network (cm)
0	0.219	0.233
1	0.219	0.233
2	0.218	0.227
3	0.216	0.232
4	0.213	0.224
5	0.209	0.214
6	0.204	0.211
7	0.199	0.206
8	0.193	0.190
9	0.188	0.185

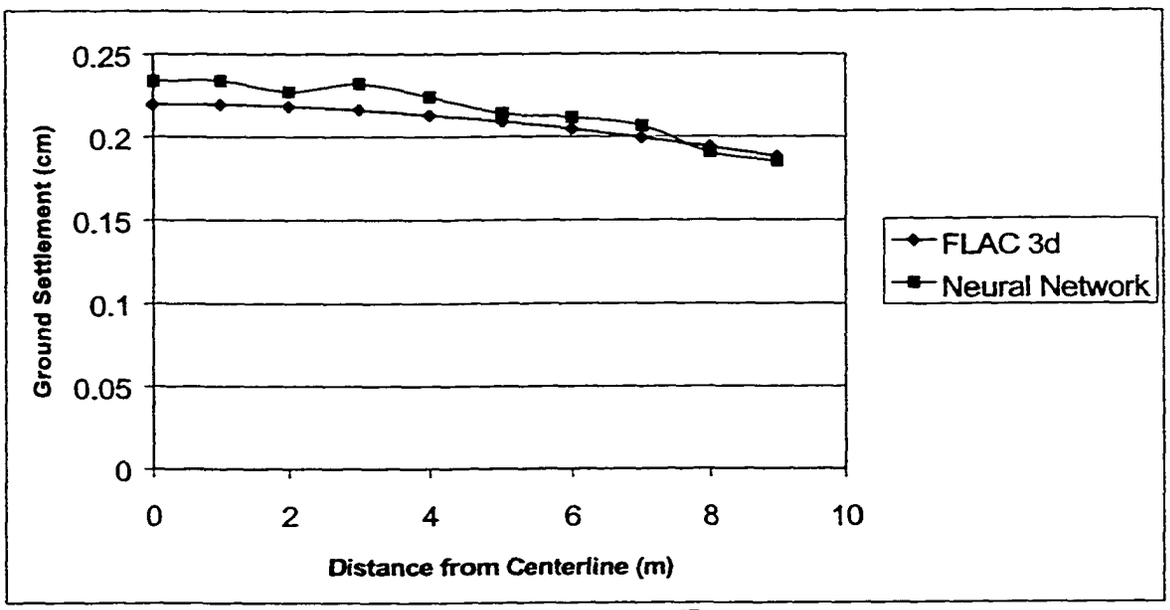

Figure 5.19 Ground Settlement Result of FLAC^{3D} and Neural Network (Test Data 3)

Test data 4: Radius 0.555 meter, depth 20.85 meter, ground water depth 5.55 meter, ground loss 1%, soil density 1632.5 kg/m,^{3} bulk modulus 32.93 MPa, shear modulus 7.25 MPa, cohesion 8 MPa, friction angle 31.25,° dilation angle 10.° The ground settlement predicted by FLAC^{3D} is listed in the first column of Table 5.4, and the ground settlement predicted by the neural network is listed in the second column.

Table 5.6 Ground Settlement Data of FLAC^{3D} and Neural Networks (Test Data 4)

Distance from center line (m)	Result of FLAC^{3D} (cm)	Result of neural network (cm)
0	0.052	0.080
1	0.050	0.079
2	0.046	0.073
3	0.041	0.060
4	0.036	0.053
5	0.031	0.041
6	0.027	0.033
7	0.023	0.033
8	0.020	0.023
9	0.017	0.025

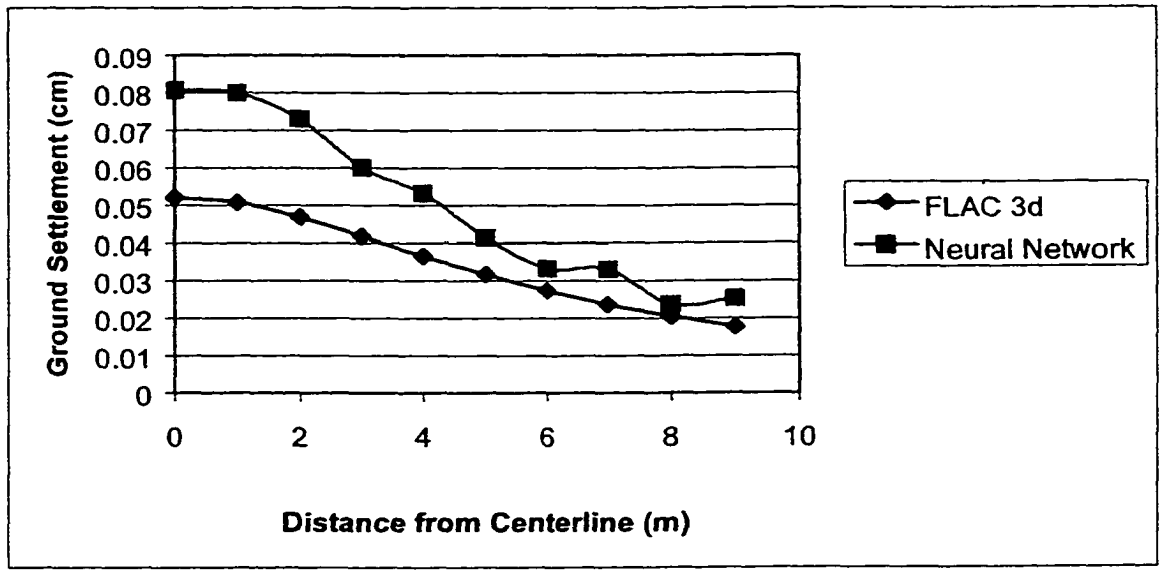

Figure 5.20 Ground Settlement Result of FLAC^{3D} and Neural Network (Test Data 4)

Test data 5: Radius 1.0275 meter, depth 20.85 meter, ground water depth 20.757 meter, ground loss 4.15%, soil density 1770 kg/m,^{3} bulk modulus 28.15 MPa, shear modulus 12.25 MPa, cohesion 5.5 MPa, friction angle 25,° dilation angle 0.° The ground settlement predicted by FLAC^{3D} is listed in the first column of Table 5.7, and the ground settlement predicted by the neural network is listed in the second column.

Table 5.7 Ground Settlement Data of FLAC^{3D} and Neural Networks (Test Data 5)

Distance from center line (m)	Result of FLAC^{3D} (cm)	Result of neural network (cm)
0	0.522	0.534
1	0.523	0.533
2	0.521	0.529
3	0.517	0.524
4	0.511	0.517
5	0.503	0.504
6	0.494	0.493
7	0.484	0.476
8	0.473	0.461
9	0.462	0.444

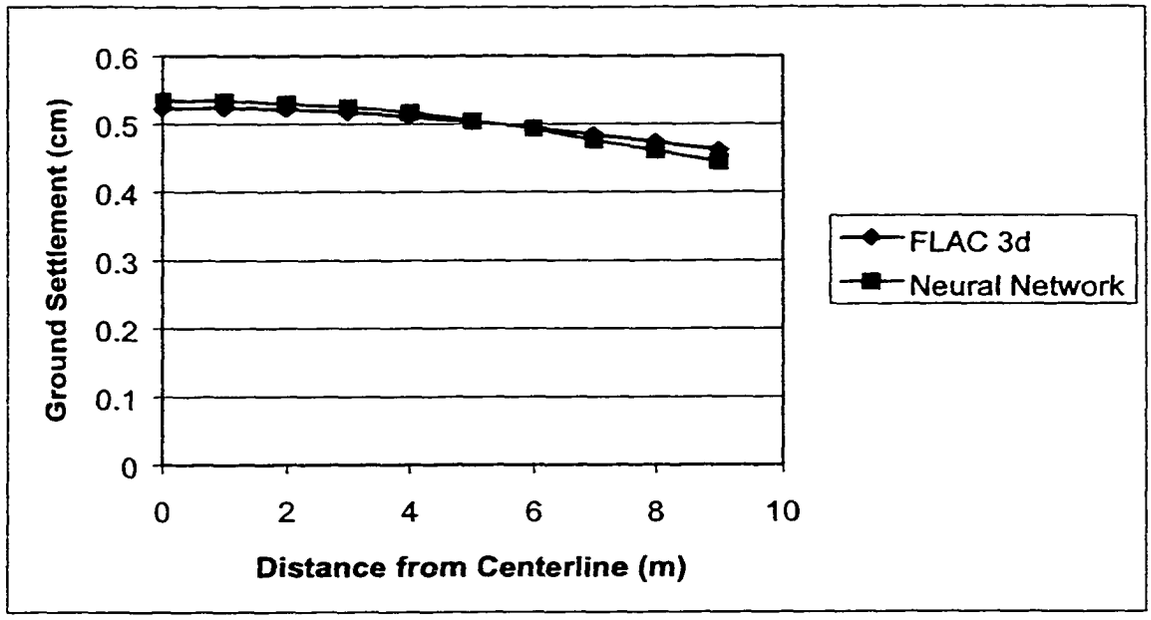

Figure 5.21 Ground Settlement Result of FLAC^{3D} and Neural Network (Test Data 5)

Test data 6: Radius 0.42 meter, depth 15.6 meter, ground water depth 13.14 meter, ground loss 5.95%, soil density 1550 kg/m,^{3} bulk modulus 34.52 MPa, shear modulus 11.93 MPa, cohesion 9.5 MPa, friction angle 18.75,° dilation angle 10.° The ground settlement predicted by FLAC^{3D} is listed in the first column of Table 5.8, and the ground settlement predicted by neural network is listed in the second column.

Table 5.8 Ground Settlement Data of FLAC^{3D} and Neural Networks (Test Data 6)

Distance from center line (m)	Result of FLAC^{3D} (cm)	Result of neural network (cm)
0	0.205	0.187
1	0.205	0.191
2	0.203	0.193
3	0.200	0.193
4	0.196	0.194
5	0.191	0.196
6	0.186	0.190
7	0.180	0.187
8	0.174	0.182
9	0.168	0.170

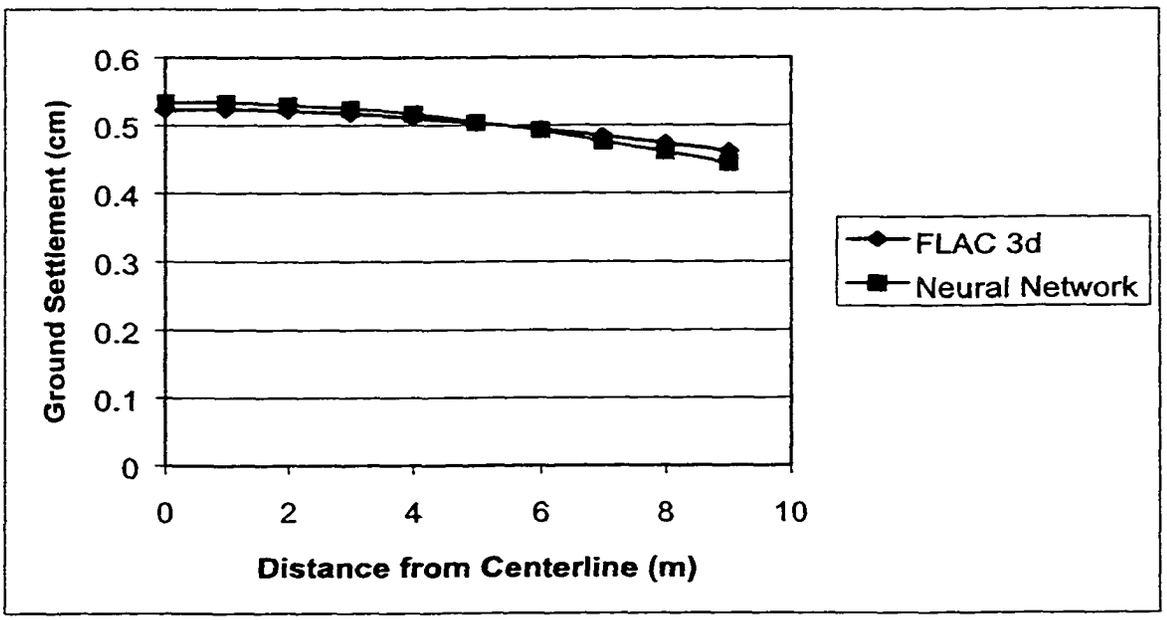

Figure 5.22 Ground Settlement Result of FLAC^{3D} and Neural Network (Test Data 6)

Test data 7: Radius 0.8925 meter, depth 12.45 meter, ground water depth 6.56 meter, ground loss 4.15%, soil density 1935 kg/m,^{3} bulk modulus 23.78 MPa, shear modulus 12.59 MPa, cohesion 8 MPa, friction angle 32.25,° dilation angle 0.° The ground settlement predicted by FLAC^{3D} is listed in the first column of Table 5.9, and the ground settlement predicted by the neural network is listed in the second column.

Table 5.9 Ground Settlement Data of FLAC^{3D} and Neural Networks (Test Data 7)

Distance from center line (m)	Result of FLAC^{3D} (cm)	Result of neural network (cm).
0	0.410	0.427
1	0.409	0.425
2	0.402	0.411
3	0.392	0.394
4	0.378	0.378
5	0.362	0.354
6	0.345	0.337
7	0.327	0.320
8	0.309	0.293
9	0.292	0.279

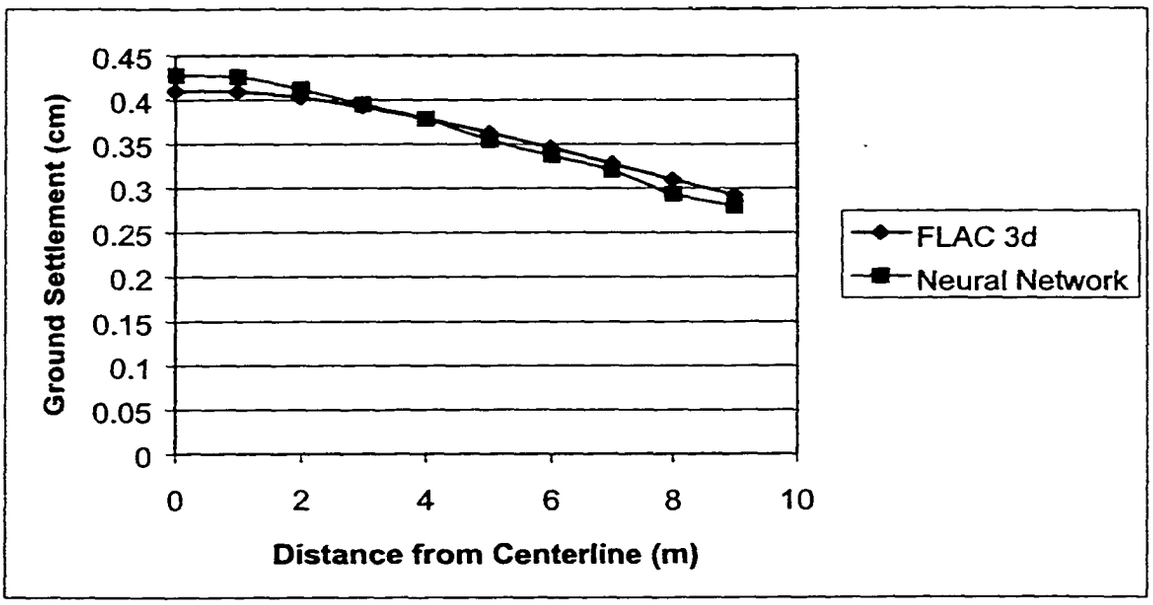

Figure 5.23 Ground Settlement Result of FLAC^{3D} and Neural Network (Test Data 7)

Test data 8: Radius 1.43 meter, depth 15.60 meter, ground water depth 22.45 meter, ground loss 7.75%, soil density 2017.5 kg/m,^{3} bulk modulus 16.27 MPa, shear modulus 7.83 MPa, cohesion 2 MPa, friction angle 23.75,° dilation angle 10.° The ground settlement predicted by FLAC^{3D} is listed in the first column of Table 5.10, and the ground settlement of neural network is listed in the second column.

Table 5.10 Ground Settlement Data of FLAC^{3D} and Neural Networks (Test Data 8)

Distance from center line (m)	Result of FLAC^{3D} (cm)	Result of neural network (cm)
0	0.986	0.973
1	0.986	0.978
2	0.977	0.958
3	0.961	0.941
4	0.939	0.919
5	0.913	0.883
6	0.882	0.856
7	0.850	0.816
8	0.815	0.780
9	0.780	0.748

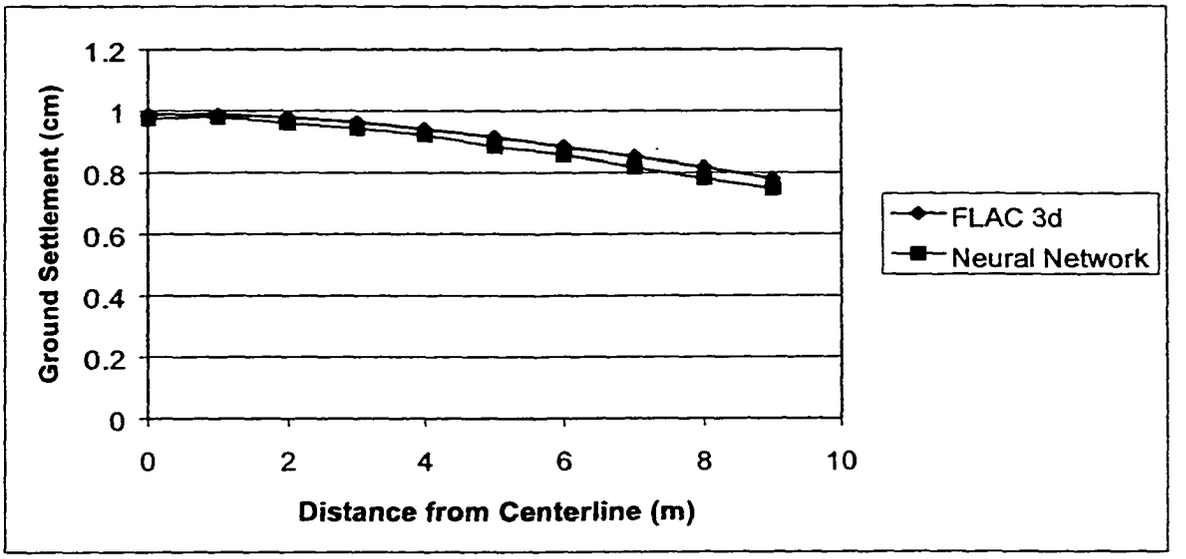

Figure 5.24 Ground Settlement Result of FLAC^{3D} and Neural Network (Test Data 8)

After comparing the FLAC^{3D} result and neural network result, the neural network can represent the FLAC^{3D} ground settlement predictions accurately. The maximum absolute error is less than 0.1 cm. This error is acceptable in engineering practice. Compared to theoretical method, empirical method and numerical method, the neural network approach has several advantages over other method:

- Includes more soil and project parameters than the theoretical method
- Much faster than the numerical method

- Easy to use. User does not need to understand neural networks
- Suitable for a larger range of soil types

5.7 Case Histories

The microtunneling experiments carried out at Waterways Experment Station provided some ground settlement data [Bennett, 1997]. The experimental data, FLAC^{3D} result, neural network result and calculation result provide by Bennett [1997] are shown in Figures 5.25, 5.26, and 5.27. The method used by Bennett to calculate the ground settlement was the emperical method.

Case 1: The soil type is sand, microtunneling depth is 2.7405 meter, pipe diameter is 66.04 cm and ground loss is 5.8% of microtunneling cutting face. Ground water table is below the pipe, soil unit weight is 1630 kg/m^3, bulk modulus is 16.0 Mpa, shear modulus is 12.5 Mpa, cohesion is 0, friction angle is 37°, dilation angle is 0°.

Case 2: The soil type is clay, microtunneling depth is 2.436 meter, pipe diameter is 66.04 cm and ground loss is 5.8% of microtunneling cutting face. Ground water table is below the pipe, soil unit weight is 1401 kg/m^3, bulk modulus is 0.833 Mpa, shear modulus is 0.384 Mpa, cohesion is 8kPa, friction angle is 0°, dilation angle is 0°.

Case 3: The soil type is clay gravel, microtunneling depth is 2.436 meter, pipe diameter is 66.04 cm and ground loss is 5.8% of microtunneling cutting face. Ground water table is below the pipe, soil unit weight is 1868 kg/m^3, bulk modulus is 0.8 Mpa, shear modulus is 0.384 Mpa, cohesion is 0, friction angle is 37°, dilation angle is 0°.

The comparison of the results of FLAC^{3D}, neural network, measured settlement and calculated settlement (empirical method) shows that the FLAC^{3D} and neural network

can predict the ground settlement associated with microtunneling reasonably well overall and to a better degree than the empirical method

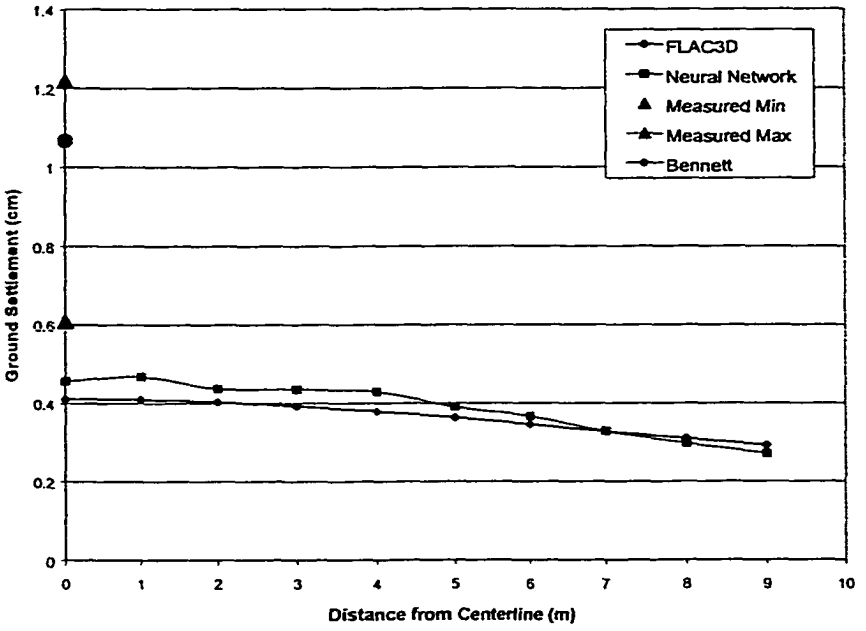

Figure 5.25 Ground Settlement in Sand

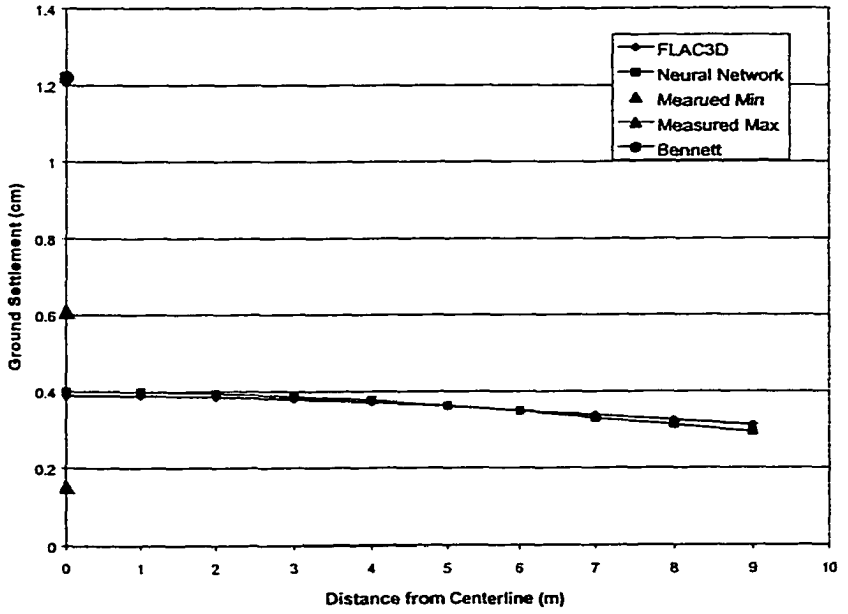

Figure 5.26 Ground Settlement in Clay

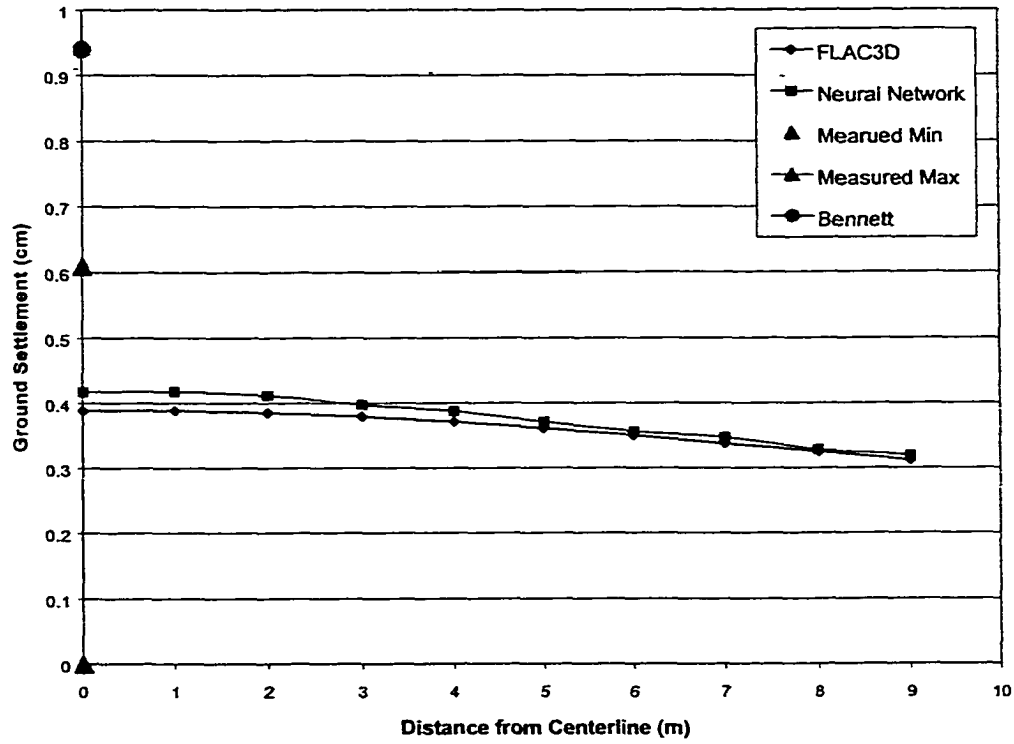

Figure 5.27 Ground Settlement in Clay Gravel

CHAPTER 6

CONCLUSIONS & RECOMMENDATIONS

In this research, the ground settlement associated with microtunneling is studied using a theoretical approach, an empirical approach, numerical simulation, and an artificial intelligence approach to reproduce quickly the result of numerical simulation.

The theoretical approach is based on the equivalent ground loss [Lee, 1989] and point ground loss [Sagaseta, 1987] concept. It can predict the ground settlement with one simple equation, but it does not consider the effect of varying soil properties. Because of its limitations, it is principally a good method to check against the other methods.

The empirical approach is based on large diameter tunneling case histories, and it is widely used in predicting the ground settlement associated with large diameter tunneling. This approach appears to provide satisfactory results in normally consolidated clays but tends to be misleading in granular soils [New and O'Reilly, 1991] and also in overconsolidated clays [Eisenstein et al., 1981]. Although some aspects of microtunneling are similar to large diameter tunneling, microtunneling is a significantly different technique in terms of its pipe jacking procedure and remote control steering. No information was found in the literature indicating the accuracy of the empirical method for predicting the ground settlement associated with microtunneling.

The numerical simulation approach in this thesis uses the finite difference method to predict the ground settlement associated with microtunneling. Numerical methods can provide results that agree reasonably with the results from field data provided the ground loss data is known but, in general, the simulated ground settlement trough appears to be wider than the results observed in the field. The drawbacks of numerical methods include the problems that, firstly, the user must at least have some knowledge about the simulation process and have spent some time in learning how to use the numerical method software; and, secondly, the user has to wait for a long time for the result of a single numerical simulation.

Using numerical simulation coupled with an artificial intelligence approach, a feed forward neural network that can provide the ground settlement profile was developed to predict the ground settlement associated with microtunneling. Input data required for the neural network are the soil and project parameters plus the equivalent ground loss parameter that can be calculated with method provided in chapter 2. The training of the neural network used a back propagation learning algorithm on training data developed from the numerical simulation. After 26 hours of training, the neural network can predict the settlement very closely. The neural network developed was tested on the same problem against a commercial neural network software and the neural network developed in this research had much lower errors than the commercial software because it is specifically optimized for this particular problem.

The neural network method has several advantages. Firstly, the neural network developed can provide an estimate derived from a wide range of site and project parameters. Secondly, the neural network can provide results immediately. Thirdly, the

neural network method is easy to use. The user does not need to understand how the neural network works and/or prepare complicated input data files. The method can be used to understand the extent of ground loss that may cause damaging surface settlement under particular site conditions by varying the unknown or critical parameters. This, in turn, can be used to guide operational practice on critical microtunneling projects.

CHAPTER 7

FURTHER WORK

7.1 Measurement of Ground Loss

Although we can predict the ground movement from the soil loss parameter with reasonable accuracy, the estimation of a soil loss, especially that includes the most damaging condition of extensive soil loss at the face, is very difficult. The soil loss is affected by many factors such as soil characteristics, ground water level, microtunneling machine advance speed, tail void, and the presence and position of other underground structures. Nevertheless, because of its speed of prediction, the neural network approach developed in this thesis could be used effectively in the on-site prevention of damaging ground movements – if we can measure the soil loss at the face in real time in the microtunneling machine.

In order to measure the soil loss in microtunneling machine, we need to measure the difference in mass per unit volume between the incoming slurry and the outcoming slurry. For income slurry weight we have:

$$W_i = \gamma_i v_i \tag{7.1}$$

where W_i is the incoming slurry weight during microtunneling machine advance of one unit length, γ_i is the incoming slurry density, and v_i is incoming slurry volume in one unit time.

For outgoing slurry weight we have:

$$W_o = \gamma_o v_o \tag{7.2}$$

where W_o is outgoing slurry weight, γ_o is the outgoing slurry density, v_o is outgoing slurry volume in one unit time, and v_m is the advance speed of microtunneling machine.

W_o-W_i is the weight of soil lost in the microtunneling process. So the volume of the soil lost in microtunneling machine is:

$$V_{loss} = (W_o - W_i)/\gamma_{soil} - \pi R^2 v_m \tag{7.3}$$

where V_{loss} is the volume of soil lost in the microtunneling process. In order to get the volume of soil loss, we must add in the soil loss cause by the tail void, which is:

$$V_{tv} = \pi(R^2 - r^2)v_m \tag{7.4}$$

The R and r are the outside diameter of the microtunneling machine and the permanent pipe respectively, and v_m is the advance speed of microtunneling machine. So the V_s is:

$$V_s = V_{ioss} + V_{tv} = (W_o - W_i) - \pi r^2 v_m \tag{7.5}$$

7.2 Prediction of Ground Settlement in Real Time

If a flow meter can be developed, as indicated above, that can measure the density and velocity of the slurry flow in real time, a control system can be used to provide feedback to the microtunneling machine. The density and velocity of the income and outcome slurry flow provide data on the ground mass removed by microtunneling machine. This can be compared with the volume represented by the physical machine advanc provided that the density of soil around the microtunneling can be estimated before the microtunneling work. Adding the volume changes caused by the annular space, machine attitude, etc, the short-term ground settlement prediction for a microtunneling project could be updated in real time as site data was collected. This

would provide a means of initial prediction of ground movements prior to the project and updating of these projections in real time based on machine performance data and soil conditions obtained on site.

REFERENCES

Anagnostou, G. and Kovari, K (1994) " The Face Stability of Slurry-Shield-Driven Tunnels" Tunnelling and Underground Space Technology Vol. 9 No.2 April. 1994

Attewell, P. B. 1978. " Ground movements caused by tunnelling in soil" Proc. Conf. On Large Ground Movements and Structures, Cardiff 1977. P812-948. London: Pentech Press.

Attewell, P. B. and Selby, A. R. (1989) " Tunnelling in Compressible Soils: Large Ground Movements and Structural Implications" Tunnelling and Underground Space Technology Vol. 4 No. 4

Bennett, R. D., and Taylor, P. (1993). "Construction of Microtunneling test facility at WES and preliminary Test Results" Construction Productivity Advancement Research (CPAR) program, Trenchless Technology Center, Louisiana Tech University, Ruston, LA

Bennett, R. D., and Staheli, K. (1997) "Controlled Field Tests of Retrievable Microtunneling System with Reaming Capabilities" Construction Productivity Advancement Research (CPAR) Program, CPAR-GL 97-1, May 1997

Bennett, R. D. (1998) "Jacking Loads and Ground Deformations Associated with Microtunneling" Ph.D. Thesis Univeristy of Illinois at Urbana-Champaign

Bennett, R. D., Guice L. K., Khan, S. and Staheli, K. (1995) "Guidelines for Trenchless Technology: Cured-in Place Pipe (CIPP), Fold and Formed Pipe (FFP) Mini-Hoaizontal Directional Drilling (mini-HDD) Microtunneling" TTC Technical Report #400

Cording, E. J., and Hansmire, W. H. (1975) "Displacement around soft ground tunnels, General Report: Session IV, Tunnels in soil." Proceeding 5th Panamerican Congr. on soil Mechanics and Foundation Engineering

Eisenstein, Z., El-Nahhas, F., and Thomson, S. (1981). "Strain field around a tunnel in stiff soil" Proc. 10th Int. Conf. on Soil Mech. and Found. Engineering. Vol. 1, A. A. Balkema, Rotterdam, The Netherlands

Freeman, J. A., and Skapura, D. M. (1991) "Neural networks: algorithm, applications, and programming techniques." Reading, MA: Addison-Wesley

Hertz, J., Krogh, A. and Palmer, R. G. (1991) "Introduction to the theory of neural computation", New York, Addison-Wesley

Hornik, K., Stinchcommbe, M. "Multilayer feedforward networks are universal approximators." Neural Networks 2:359-366

Hurrell, M.R. (1985). " The empirical prediction of long-term surface settlements above shield-driven tunnels in soil" Ground Movements and Structures: Proc. 3rd Int. Conf., Cardiff 1984. P161-170. London: Pentech Press

Jacobs, R. A. (1988) "Increased rates of convergence through learning rate adapation." Neural Networks 1: 295-307

Klein, S. J. (1995) "Design Aspects of Microtunneling Projects" NO-DIG Engineering Vol. 2, No. 2 summer 1995 p.9-12

Lee, K. M. 1989. "Prediction of ground deformations resulting from shield tunneling in soft clays." Ph.D. thesis, The University of Western Ontario, London, Ont.

Lee, K. M., and Rowe, R. K. (1990a) "Finite element modeling of the three-dimensional ground deformations due to tunneling in soft cohesive soils. Part I. Methods of analysis." Computers and Geotechnics. 10(2): 87-110

Lee, K. M. and Rowe, R. K. (1990b) "Finite element modeling of the three-dimensional ground deformations due to tunneling in soft cohesive soils. Part II. Results." Computers and Geotechnics. 10(2): 87-110

Lo, K. Y., and Rowe, R. K. (1982) "Prediction of ground subsidence due to tunneling in clays" Research Report GEOT-10-82, Faculty of Engineering Science, The University of Western Ontario, London, Ont.

Lin, C. T. and Lee, C. S. G. (1996) "Nural Fuzzy Systems" Prentice-Hall, Inc. Upper Saddle River, NJ

Loganathan, N. and Poulos, H. G. (1998) " Analytical Prediction for Tunneling-Induced Ground Movements in Caly" Journal of Geotechnical and Geoenvironmental Engineering, Vol 124 No. 9

New, B. M. and O'Reilly, M. P. (1991). "Tunneling induced ground movements, predicting their magnitude and effects." Proceeding 4th Conference on Ground Movements and Structures.

O'Reilly, M. P. and New, B. M. (1982) "Settlements above tunnels in the United Kingdom – their magnitude and prediction." Proceeding, Tunneling'82 pp.137-181. London: Institution of Mining and Metallurgy

Peck, R. B., (1969) "Deep excavations and tunneling in soft ground." Proceeding, 7th International Conference on Soil Mechanics and Foundation Engineering, Mexico City, pp. 225-290

Peck, R. B. Hendron, A. J., Jr., and Mohraz, B. (1972). "State of the art of soft ground tunneling" Proceedings, 1st Rapid Excavation Tunneling Conference, Chicago, vol. 1, pp. 259-286

Post, R. G. (1997) "Run Silent, Run Deep: Three Deep River Crossings by Microtunneling in The Seattle Area" Proceedingof North American NO-DIG '97. Seattle, Washington p.299-312

Raines, G. L. (1996) "Nimitz Highway Relief Sewer: A Value Engineered Microtunnel Alternative" NO_DIG Engineering Vol. 3, No. 3 p.2-6

Rowe, R. K. and Kack, G. J. (1983) "A theoretical examination of the settlements induced by tunneling: four case histories" Canadian Geotechnical Journal, 20: 299-314

Sagaseta, C. (1988)"Analysis of undrained soil deformation due to ground loss" Geotechnique DEC 1988 v38 n4 p647.

Stallebrass, S. E., Grant, R. J., and Taylor, R. N. (1996) " A finite element study of ground movement measured in centrifuge model tests of tunnels." Proceeding, Int. symp. on Geotech Aspects of Underground constr. in Soft Ground, The Netherlands.

Vogl, T. P., Mangis, J. K., Rigler, A. K., Zink, W. T. and Alkon, D. L. (1988) "Accelerating the convergence of the back-propagation method" Biol. Cybern. 59:257-263

Ward, W. H. 1969 Panel discussion. Proceedings, 7th International Conference on Soil Mechanics and Foundation Engineering, Mexico City, Vol. 3, pp. 320-325.

APPENDIX A

GENDATA.JAVA

APPENDIX A

GENDATA.JAVA

```
import java.io.*;
import java.sql.*;
import javax.swing.*;
import java.awt.*;
import java.awt.event.*;
import java.util.*;

public class GenData {

   private Connection connection;
   private JTable table;
   private DataInputStream input;


   public GenData()
   {
      // The URL specifying the Books database to which
      // this program connects using JDBC to connect to a
      // Microsoft ODBC database.
      String url = "jdbc:odbc:thesis";
      String username = "anonymous";
      String password = "guest";

          // Load the driver to allow connection to the database
      try {
         Class.forName( "sun.jdbc.odbc.JdbcOdbcDriver" );
         connection = DriverManager.getConnection(
            url, username, password );
      }
      catch ( ClassNotFoundException cnfex ) {
         System.err.println(
            "Failed to load JDBC/ODBC driver." );
         cnfex.printStackTrace();
         System.exit( 1 );  // terminate program
      }
      catch ( SQLException sqlex ) {
         System.err.println( "Unable to connect" );
         sqlex.printStackTrace();
      }

          readData();
          shutDown();
   }

   private void readData(){
       int array_size =20;
    int counter = 0;
    double radius[], depth[], ground_lose[], density[], e[], cohension[],
friction[],p_ratio[];
    double dialation;
    double radius_low = 0.15, radius_high = 1.5;
    double depth_low = 3.0, depth_high = 24;
    double ground_lose_low = 1, ground_lose_high = 10;
```

```
    double density_low = 1550, density_high = 2100;
    double e_low = 0.5, e_high = 40;
    double cohension_low = 0, cohension_high = 10;
    double friction_low = 10, friction_high = 35;
    double p_ratio_low = 0.1, p_ratio_high = 0.45;
    int r[] = new int [8];
    double bulk, shear;
    String s = new String("DELETE * from soil_proper ");

    radius = new double [array_size];
    depth = new double [array_size];
    ground_lose = new double [array_size];
    density = new double [array_size];
    e = new double [array_size];
    cohension = new double [array_size];
    friction = new double [array_size];
    p_ratio = new double[array_size];

    execute_query (s);

    for ( int i = 0 ; i < array_size; i++)
    {
      radius[i] = radius_low + (radius_high - radius_low) * i / 20.0;
      depth[i] = depth_low + ( depth_high - depth_low ) * i / 20.0;
      ground_lose[i] = ground_lose_low + (ground_lose_high - ground_lose_low ) * i /
20.0;
      density[i] = density_low + ( density_high - density_low )* i / 20.0;
      e[i] = e_low + ( e_high - e_low) * i / 20.0;
      cohension[i] = cohension_low + ( cohension_high - cohension_low) * i / 20.0;
      friction[i] = friction_low + (friction_high - friction_low) * i / 20.0;
      p_ratio[i] = p_ratio_low + (p_ratio_high - p_ratio_low) * i / 20.0;
    }

    for( int i = 0 ; i < 1000 ; i ++)
    {
      for(int j = 0; j < 8; j++)
        r[j] = (int) (20. * Math.random());

      dialation = (double) ( 10 * (int) (2. * Math.random()));


      if(depth[ r[1] ]/radius[ r[0] ] < 6)
      {
                i --;
                if(i < 0) i = 0;
                continue;
          }

          shear = e[ r[4] ] / (2.0 * (1.0 + p_ratio[ r[5] ]));
          bulk = e[ r[4] ] / (3.0 * (1.0 - 2.0 * p_ratio[ r[5] ]));


      String query = new String();
      query = "INSERT INTO soil_proper VALUES( " + i + ", "
              + radius[ r[0] ] + ", " + depth[ r[1] ] + ", " + ( depth [r[1]] -
Math.random() * (depth[ r[1]] + 10) ) + ", " +
              + ground_lose[ r[2] ] + ", " + density[ r[3] ] + ", "
              + bulk + ", " + shear + ", " + cohension[ r[6] ] + ", "
              + friction[ r[7] ] + ", " + dialation  + ");";

      execute_query( query );
    }
   }

   private void execute_query(String s){
   Statement statement;


   try {
    statement = connection.createStatement();
    statement.executeUpdate( s );
```

```
        statement.close();
        }
       catch (SQLException sqlex) {
         sqlex.printStackTrace();
       }
     }


     public void shutDown()
     {
        try {
           connection.close();
        }
        catch ( SQLException sqlex ) {
           System.err.println( "Unable to disconnect" );
           sqlex.printStackTrace();
        }
     }

     public static void main( String args[] )
     {
        final GenData app = new GenData();
     }

}
```

APPENDIX B

DATAFILEGEN.JAVA

APPENDIX B

DATAFILEGEN.JAVA

```
import java.io.*;
import java.sql.*;
import javax.swing.*;
import java.awt.*;
import java.awt.event.*;
import java.util.*;
import java.text.DecimalFormat;

public class DatafileGen {

   private Connection connection;
   private JTable table;
   private ObjectOutputStream output;
   private RandomAccessFile raf;
   private File fileName;


   public DatafileGen()
   {
      // The URL specifying the Books database to which
      // this program connects using JDBC to connect to a
      // Microsoft ODBC database.
      String url = "jdbc:odbc:thesis";
      String username = "anonymous";
      String password = "guest";

          // Load the driver to allow connection to the database
      try {
         Class.forName( "sun.jdbc.odbc.JdbcOdbcDriver" );
         connection = DriverManager.getConnection(
            url, username, password );
      }
      catch ( ClassNotFoundException cnfex ) {
         System.err.println(
            "Failed to load JDBC/ODBC driver." );
         cnfex.printStackTrace();
         System.exit( 1 );  // terminate program
      }
      catch ( SQLException sqlex ) {
         System.err.println( "Unable to connect" );
         sqlex.printStackTrace();
      }
      getData();
          //createTable();

   }       .


/*   private void createTable(){
          Statement statement;
       ResultSet resultSet;
          String xi, yi;
```

```
      StringBuffer queryBuffer = new StringBuffer("CREATE TABLE calculate_settlement ( ID
number");

          for (int i = 0; i< 100; i++)
           {
                  if (i < 10)
                  {
                         xi = new String("x0" + i);
                         yi = new String("y0" + i);
                  }
                  else
                  {
                         xi = new String("x" + i);
                         yi = new String("y" + i);
                  }

                  queryBuffer.append( ",\n " + xi + " double, " + yi + " double");
          }
          queryBuffer.append(");");
          String query = new String(queryBuffer.toString());
          System.out.println(query);

      try {
         statement = connection.createStatement();
         resultSet = statement.executeQuery( query );
         displayResultSet( resultSet );
         statement.close();
      }
      catch ( SQLException sqlex ) {
         sqlex.printStackTrace();
      }
   }
*/


   private void getData()
   {
      Statement statement;
      ResultSet resultSet;
      try {
         String query = "SELECT * FROM soil_proper";
         statement = connection.createStatement();
         resultSet = statement.executeQuery( query );
         displayResultSet( resultSet );
         statement.close();
      }
      catch ( SQLException sqlex ) {
         sqlex.printStackTrace();
      }
   }

   private void displayResultSet( ResultSet rs )
      throws SQLException
   {

          // position to first record
      boolean moreRecords = rs.next();

          // If there are no records, display a message
      if ( ! moreRecords ) {
         System.out.println( "ResultSet contained no records" );
         return;
      }
          Vector rows = new Vector();
      try {
         // get column heads
         ResultSetMetaData rsmd = rs.getMetaData();
         // get row data
         do {
                        rows = getNextRow( rs, rsmd );
```

```
                        WriteFile(rows);
                        rows.clear();
            } while ( rs.next() );
            // display table with ResultSet contents
         }
         catch ( SQLException sqlex ) {
            sqlex.printStackTrace();
         }
      }

      private void WriteFile(Vector rows)
      {
            int n;
            int n3,n4;
            double
radius,depth,water_table,ground_loss,density,bulk,shear,cohension,friction,dilation;
            double tunnel_r;
            int l_nl = 0;
         double a;
         double total_width = 0.0;
            String name;
         String file = new String("");

         DecimalFormat precisionFour = new DecimalFormat( "0.0000" );


            n = Integer.parseInt(rows.get(0).toString());
            radius = Double.parseDouble(rows.get(1).toString());
            depth = Double.parseDouble(rows.get(2).toString());
            water_table = Double.parseDouble(rows.get(3).toString());
            ground_loss = Double.parseDouble(rows.get(4).toString());
            density = Double.parseDouble(rows.get(5).toString());
            bulk = Double.parseDouble(rows.get(6).toString());
            shear = Double.parseDouble(rows.get(7).toString());
            cohension = Double.parseDouble(rows.get(8).toString());
            friction = Double.parseDouble(rows.get(9).toString());
         dilation = Double.parseDouble (rows.get(10).toString());



            tunnel_r = Math.sqrt( radius * radius * (1 + ground_loss/100.0));

              if(depth <= 10.0)
              {
                     n3 = 10;
                     n4 = 10;
              }
              else
              {
                     n3 = 2 * ( (int)(depth/2.0));
                     n4 = 2 * ( (int)(depth/2.0));
              }

         a = 2.0 * depth / n4;
         //System.out.println("\n" + a + "\n");
         while(total_width < 6 * depth){
          total_width += a * Math.pow ( (1+ 0.1), (double) l_nl);
          //System.out.println(" ln_l " + l_nl + " total_width " + total_width);
          l_nl++;
         }
               if (n<10)
                     name = new String("00" + n);
               else
                     if (n<100)
                           name = new String("0" + n);
               else
                     name = new String(""+ n);

               try{
                     //output = new ObjectOutputStream( new FileOutputStream(name +
```

```
".dat"));
                    fileName = new File(name + ".dat");
                    raf = new RandomAccessFile(fileName, "rw");
            }
            catch(IOException exp)
            {
                    System.out.println("Can not Open file");
                    System.out.println(exp.toString());
            }
      System.out.print("Creating Data file " + name + ".dat.....");
      try{
                file = new String("new\n" +
                                                "title\n" +
                                                "pipe depth is "+ depth +
                                                "density = " + density + "bulk =" +
precisionFour.format(bulk) + "Shear = " + precisionFour.format(shear) + "M coh = " +
cohension +
                                                "k fric = " + friction + " g_l =" +
ground_loss + " r = " + radius + "\n" +
                                                ";\n" +
                                                ";set the parameter\n" +
                                                ";*************************************\n"
+
                                                "define set_parameter\n" +
                                                "   depth = " + depth + "\n" +
                                                "   width = 7 * depth\n" +
                                                "   rock_depth = - width\n" +
                                                "   thickness = 16\n" +
                                                "   inter_width = width\n" +
                                                "   inter_depth = rock_depth\n" +
                                                "\n" +
                                                "   n1 = 5\n" +
                                                "   n2 = 4\n" +
                                                "   n3 = " + n3 + "\n" +
                                                "   n4 = " + n4 + "\n" +
                                                "\n" +
                                                "   r1 = 1\n" +
                                                "   r2 = 1\n" +
                                                "   r3 = 1\n" +
                                                "   r4 = 1.1\n" +
                                                "\n" +
                                                "   b_mod= " + precisionFour.format(bulk) +
"e6\n" +
                                                "   s_mod = " + precisionFour.format(shear)
+ "e6\n" +
                                                "   fric_ang = " + friction + "\n" +
                                                "   coh_mod = " + cohension + "e3\n" +
                                                "   dil_ang = " + dilation + "\n" +
                                                "   den_num = " + density + "\n" +
                                                "   grav_num = -9.81\n" +
                                                "   k = 1\n" +
                                                "\n" +
                                                "   tunnel_r = " +
precisionFour.format(tunnel_r) + "\n" +
                                                "   pipe_r = " +
precisionFour.format(radius) + "\n" +
                                                "end\n" +
                                                "set_parameter\n" +
                                                "\n" +
                                                ";generate soil zon\n" +
                                                ";*************************************\n"
+
                                                "gen zone radcyl p0 0 0 0 p1 depth 0 0 p2 0
thickness 0 p3 0 0 depth &\n" +
                                                "      size n1 n2 n3 n4 dim tunnel_r
tunnel_r tunnel_r tunnel_r &\n" +
                                                "      rat r1 r2 r3 r4 fill\n" +
                                                "gen zone reflect dip 0 dd 90 ori 0 0 0\n"
+
                                                "\n" +
                                                "define var1\n" +
```

```
"   p0_x = depth\n" +
"   p0_y = 0\n" +
"   p0_z = - depth\n" +
"\n" +
"   p1_x = inter_width\n" +
"   p1_z = -depth\n" +
"   p1_y = 0\n" +
"\n" +
"   p2_x = p0_x\n" +
"   p2_y = thickness\n" +
"   p2_z = p0_z\n" +
"\n" +
"   p3_x = depth\n" +
"   p3_z = depth\n" +
"   p3_y = 0\n" +
"\n" +
"   l_n3 = n3\n" +
"   l_n1 = " + l_n1 + "\n" +
"   l_n2 = n2\n" +
"   l_r1 = r4\n" +
"   l_r2 = 1\n" +
"   l_r3 = 1\n" +
"end\n" +
"var1\n" +
"gen zon brick p0 p0_x p0_y p0_z p1 p1_x
p1_y p1_z p2 p2_x p2_y p2_z &\n" +
"     p3 p3_x p3_y p3_z  &\n" +
"     size l_n1 l_n2 l_n3 rat l_r1 l_r2
l_r3\n" +
"\n" +
"define var2\n" +
"   p0_x = 0\n" +
"   p0_y = 0\n" +
"   p0_z = inter_depth\n" +
"\n" +
"   p1_x = depth\n" +
"   p1_y = 0\n" +
"   p1_z = p0_z\n" +
"\n" +
"   p2_x = p0_x\n" +
"   p2_y = thickness\n" +
"   p2_z = p0_z\n" +
"\n" +
"   p3_x = 0\n" +
"   p3_y = 0\n" +
"   p3_z = - depth\n" +
"\n" +
"   b_n1 = int (n3/2)\n" +
"   b_n2 = n2\n" +
"   b_n3 = l_n1\n" +
"   b_r1 = 1\n" +
"   b_r2 = 1\n" +
"   b_r3 = 1/l_r1\n" +
"   \n" +
"end\n" +
"var2\n" +
"gen zon brick p0 p0_x p0_y p0_z p1 p1_x
p1_y p1_z p2 p2_x p2_y p2_z &\n" +
"     p3 p3_x p3_y p3_z &\n" +
"     size b_n1 b_n2 b_n3 rat b_r1 b_r2
b_r3\n" +
"\n" +
"define var3\n" +
"   p0_x = depth\n" +
"   p0_y = 0\n" +
"   p0_z = inter_depth\n" +
"\n" +
"   p1_x = inter_width\n" +
"   p1_y = 0\n" +
"   p1_z = p0_z\n" +
"\n" +
```

```
                                        "   p2_x = p0_x\n" +
                                        "   p2_y = thickness\n" +
                                        "   p2_z = p0_z\n" +
                                        "\n" +
                                        "   p3_x = depth\n" +
                                        "   p3_y = 0 \n" +
                                        "   p3_z = - depth\n" +
                                        "\n" +
                                        "   lb_n1 = l_n1\n" +
                                        "   lb_n2 = n2\n" +
                                        "   lb_n3 = b_n3\n" +
                                        "   lb_r1 = l_r1\n" +
                                        "   lb_r2 = 1\n" +
                                        "   lb_r3 = b_r3\n" +
                                        "end\n" +
                                        "var3\n" +
                                        "gen zon brick p0 p0_x p0_y p0_z p1 p1_x
p1_y p1_z p2 p2_x p2_y p2_z &\n" +
                                        "      p3 p3_x p3_y p3_z &\n" +
                                        "      size lb_n1 lb_n2 lb_n3 rat lb_r1
lb_r2 lb_r3\n" +
                                        "\n" +
                                        ";material (soil) property calculation and
setup\n" +
";*****************************************\n" +
                                        "def property_cal\n" +
                                        "end\n" +
                                        "property_cal\n" +
                                        "model mohr\n" +
                                        "prop b b_mod sh s_mod coh coh_mod fric
fric_ang dil dil_ang\n" +
                                        "\n" +
                                        ";initial stress calcualtion FISH\n" +
                                        ";*************************************\n"
+
                                        "def gravity_cal\n" +
                                        "szz_number = depth * den_num * grav_num\n"
+  "sxx_number = szz_number * k\n" +
                                        "syy_number = sxx_number\n" +
                                        "z_grad = - den_num * grav_num\n" +
                                        "x_grad = - den_num * grav_num * k\n" +
                                        "y_grad = x_grad\n" +
                                        "end\n" +
                                        "gravity_cal\n" +
                                        ";setup initial stress condition\n" +
";*************************************\n" +
                                        "ini density den_num\n" +
                                        "set gravity 0 0 grav_num\n" +
                                        "ini szz szz_number grad 0 0 z_grad \n" +
                                        "ini sxx sxx_number grad 0 0 x_grad \n" +
                                        "ini syy syy_number grad 0 0 y_grad \n" +
                                        "\n" +
                                        "water density = 1000\n" +
                                        "water table origin 0 0 " +
precisionFour.format(water_table) + " normal 0 0 -1\n" +
                                        ";boundary condition calculation\n" +
";*************************************\n" +
                                        "def boundary_cal\n" +
                                        "x_right_low = width - 0.1\n" +
                                        "x_right_high = width + 0.1\n" +
                                        "z_low = rock_depth - 0.1\n" +
                                        "z_high = rock_depth +0.1\n" +
                                        "y_b_low = thickness - 0.1\n" +
                                        "y_b_high = thickness + 0.1\n" +
                                        "z_top_high = depth + 0.1\n" +
                                        "z_top_low_h = depth - 0.0001\n" +
                                        "z_top_low_l = depth - 1\n" +
```

```
                                        "end\n" +
                                        "boundary_cal\n" +
                                        "\n" +
                                        "set log on\n" +
                                        "set logfile ..\\log\\" + name + ".log\n" +
                                        "print gp p range z z_top_low_h z_top_high
y -.1 .1\n" +
                                        "set log off\n" +
                                        "\n" +
                                        ";setup boundary condtion\n" +

";*****************************************\n" +
                                        "apply xvel 0 range x -.1 .1\n" +
                                        "fix x z range x x_right_low
x_right_high\n" +
                                        "fix z range z z_low z_high\n" +
                                        "apply yvel 0 range y -.1 .1\n" +
                                        "apply yvel 0 range y y_b_low y_b_high\n" +
                                        "\n" +
                                        "set mechanical force 50\n" +
                                        "solve\n" +
                                        "\n" +
                                        ";setup excavation tunnel and excavate\n" +

";*****************************************\n" +
                                        "group tunnel range cyl end1 0 0 0 end2 0
thickness 0 rad tunnel_r\n" +
                                        "del range group tunnel\n" +
                                        "set large\n" +
                                        "ini zdisp = 0 xdisp = 0 ydisp = 0\n" +
                                        "\n" +
                                        ";define the monitor FISH function\n" +

";*****************************************\n" +
                                        "define xxx\n" +
                                        "p_gp = gp_head\n" +
                                        "loop while p_gp # null\n" +
                                        "   x = gp_xpos(p_gp)\n" +
                                        "   z = gp_zpos(p_gp)\n" +
                                        "   z_vel= gp_zvel(p_gp)\n" +
                                        "\n" +
                                        "   gap = tunnel_r - pipe_r\n" +
                                        "   p = x * x + (z + gap) * ( z + gap)\n" +
                                        "   id_number = gp_id(p_gp)\n" +
                                        "\n" +
                                        "   r = pipe_r * pipe_r\n" +
                                        "   if z_vel # 0\n" +
                                        "      if p < r\n" +
                                        "      command\n" +
                                        "      apply xvel 0 range id id_number
id_number\n" +
                                        "      apply yvel 0 range id id_number
id_number\n" +
                                        "  apply zvel 0 range id id_number
id_number\n" +
                                        "      endcommand\n" +
                                        "      endif\n" +
                                        "   endif\n" +
                                        "   p_gp = gp_next(p_gp)\n" +
                                        "endloop\n" +
                                        "end  \n" +
                                        "\n" +
                                        ";run the program\n" +

";*****************************************\n" +
                                        "hist unbal\n" +
                                        "\n" +
                                        "define run_able\n" +
                                        " loop n (1,150)\n" +
                                        "  command\n" +
                                        "   step 1\n" +
```

```
                                                    "   xxx\n" +
                                                    "  endcommand\n" +
                                                    "  endloop\n" +
                                                    "end\n" +
                                                    "run_able\n" +
                                                    "\n" +
                                                    "set fishcall = xxx\n" +
                                                    "solve\n" +
                                                    "save ..\\result\\" + name + ".sav\n" +
                                                    "set pagelength 200\n" +
                                                    "set log on\n"  +
                                                    "print gp disp  range z z_top_low_l
z_top_high y -.1 .1\n" +
                                                    "quit\n");
                System.out.print("Working....");
                }
                catch(ArrayIndexOutOfBoundsException aibe)
                {
                   System.out.println(aibe.toString());
                }

             try{
                    //output.writeObject("");
                    raf.writeUTF(file);
             }
             catch(IOException excp)
             {
                    System.out.println("Error in writing file");
             }
       file = new String("");
       System.out.print("Done\n");
     }
     private Vector getNextRow( ResultSet rs,
                                ResultSetMetaData rsmd )
         throws SQLException
     {
        Vector currentRow = new Vector();
        for ( int i = 1; i <= rsmd.getColumnCount(); ++i )
           switch( rsmd.getColumnType( i ) ) {
              case Types.DOUBLE:
                    currentRow.addElement(new Double(rs.getDouble( i )) );
                 break;
              case Types.INTEGER:
                    currentRow.addElement(
                       new Long( rs.getLong( i ) ) );
                 break;
              default:
                 System.out.println( "Type was: " +
                    rsmd.getColumnTypeName( i ) );
           }
       return currentRow;
     }

     public void shutDown()
     {
        try {
           connection.close();
        }
        catch ( SQLException sqlex ) {
           System.err.println( "Unable to disconnect" );
           sqlex.printStackTrace();
        }
     }

     public static void main( String args[] )
     {
        final DatafileGen app = new DatafileGen();
     }

}
```

APPENDIX C

READLOG.JAVA

APPENDIX C

READLOG.JAVA

```
import java.io.*;
import java.sql.*;
import javax.swing.*;
import java.awt.*;
import java.awt.event.*;
import java.util.*;

public class ReadLog {

   private Connection connection;
   private JTable table;
   private DataInputStream input;


   public ReadLog()
   {
      // The URL specifying the Books database to which
      // this program connects using JDBC to connect to a
      // Microsoft ODBC database.
      String url = "jdbc:odbc:thesis";
      String username = "anonymous";
      String password = "guest";

          // Load the driver to allow connection to the database
      try {
         Class.forName( "sun.jdbc.odbc.JdbcOdbcDriver" );
         connection = DriverManager.getConnection(
            url, username, password );
      }
      catch ( ClassNotFoundException cnfex ) {
         System.err.println(
            "Failed to load JDBC/ODBC driver." );
         cnfex.printStackTrace();
         System.exit( 1 );  // terminate program
      }
      catch ( SQLException sqlex ) {
         System.err.println( "Unable to connect" );
         sqlex.printStackTrace();
      }

          readData();
          shutDown();
   }

   private void readData(){

          int n = 503;        //n define how many dat files will be read
          String line = new String();
          String filename;
          for( int i = 0; i < n ; i++)
          {
                 if (i < 10)
                 {
```

```
                        filename = new String("00" + i + ".log");
                }
                else
                        if (i< 100)
                        {
                                filename = new String("0" + i + ".log");
                        }
                        else
                        {
                                filename = new String(i + ".log");
                        }

                try{
                        input = new DataInputStream( new FileInputStream(filename));
                        BufferedReader d = new BufferedReader(new
InputStreamReader(input));
                        System.out.print("Analysis data file " + filename +
".............");
                        analyse(d,i);
                        System.out.print("Done\n");

                }
                catch(IOException excep)
                {
                        System.out.println(filename + " can not open");
                }

        }
   }

   private void analyse(BufferedReader d, int k){
        String line = new String();
        int n = 100;
        int id1[] = new int[n];
        int id2[] = new int[2*n];
        double x[] = new double [n];
        double zDisp[] = new double [2*n];
        double surfaceDisp[] = new double [n];
        int out = 1;
        for (int i = 0 ; i < n; i++)
        {
                id1[i] = 0;
                x[i] = 0.0;
                surfaceDisp[i] = 0.0;
        }

        for (int i = 0; i< 2 * n; i++)
        {
                id2[i] = 0;
                zDisp[i] = 0.0;
        }
        try{
            do {
                    //System.out.println(line);
                    line = d.readLine();
                    //StringTokenizer strtoken = new StringTokenizer(line);

                    //if(strtoken.countTokens() == 1) continue;
                    if ( line.startsWith("Gridpoint Position"))
                    {
                            //System.out.println("Gridpoint Position");
                            position(d,id1,x);
                    }
                    //System.out.println(line);

                    if ( line.startsWith("Gridpoint Displacement"))
                    {
                            //System.out.println("Gridpoint Displacement");
                            displacement(d,id2,zDisp);
                            out = 0;
                    }
```

```
                }while(out == 1);
            }

            catch(IOException excep){
                    System.out.println(" Error in reading file");
            }

            getSurfDisp(id1,id2,zDisp,surfaceDisp,n);
            sortData(n,id1,x,surfaceDisp);
            writeData(k,n,x,surfaceDisp);

    }

    private void sortData(int n,int id[], double x[], double surfaceDisp[]){
            int total = 0;
            for (int i =0; i< n ; i++)
            {
                    if(id[i] == 0)
                    {
                            total = i;
                            break;
                    }
            }
            int min = 0;
            double temp = 0.0;
            for(int i = 0; i< total; i++)
            {
                    min = i;
                    for(int j = i + 1; j < total; j++)
                    {
                            if(x[j] < x[min]) min = j;
                    }

                    temp = x[i];
                    x[i] = x[min];
                    x[min] = temp;

                    temp =surfaceDisp[i];
                    surfaceDisp[i] = surfaceDisp[min];
                    surfaceDisp[min] = temp;
            }

    }

    private void writeData(int k, int n, double x[], double surfaceDisp[])
    {
       Statement statement;
           StringBuffer queryBuffer = new StringBuffer("INSERT INTO ground_settlement
Values(" + k);
            for (int i = 0; i< n; i++)
            {
                    queryBuffer.append(", " + x[i] + ", " + surfaceDisp[i]);
            }

            queryBuffer.append(");");

            String query = new String(queryBuffer.toString());

       try {
          statement = connection.createStatement();
          statement.executeUpdate( query );
          statement.close();
       }
       catch ( SQLException sqlex ) {
          sqlex.printStackTrace();
       }
    }
```

```
    private void getSurfDisp(int id[], int id2[],double zDisp[], double surfaceDisp[],int
n){
        for(int i =0; i<n; i++)
        {
            if(id[i] == 0) break;
            for(int j =0; j<2*n; j++)
            {
                if(id2[j] == 0) continue;
                if(id[i] == id2[j])
                {
                    surfaceDisp[i] = - 100. * zDisp[j];
                    continue;
                }
            }
        }
    }

    private void displacement(BufferedReader d, int id[], double zDisp[]){
        String line = new String();
        String s0 = new String();
        String s1 = new String();
        String s2 = new String();
        String s3 = new String();

        int i =0;
        StringTokenizer token = new StringTokenizer("");
        do{
            try{
                line = d.readLine();
                line = line.replace(',', ' ');
                line = line.replace(')', ' ');
                line = line.replace('(', ' ');
                token = new StringTokenizer(line);
                s0 = token.nextToken();
                if ( Character.isDigit( s0.charAt(0)))
                {
                    s1 = token.nextToken();
                    s2 = token.nextToken();
                    s3 = token.nextToken();
                    id[i] = Integer.parseInt(s0);
                    zDisp[i] = Double.parseDouble(s3);
                    i++;
                }
            }
            catch(IOException excep){
                System.out.println(" Error in reading files");
            }
        }while( !line.startsWith("Flac3D>") );


    }

    private void position(BufferedReader d, int id[], double x[]){
        String line = new String();
        String s0 = new String();
        String s1 = new String();
        String s2 = new String();
        String s3 = new String();

        int i =0;
        StringTokenizer token = new StringTokenizer("");
        do{
            try{
                line = d.readLine();
                line = line.replace(',', ' ');
                line = line.replace(')', ' ');
                line = line.replace('(', ' ');
                token = new StringTokenizer(line);
                s0 = token.nextToken();
                if ( Character.isDigit( s0.charAt(0)))
                {
```

```
                                s1 = token.nextToken();
                                s2 = token.nextToken();
                                s3 = token.nextToken();
                                id[i] = Integer.parseInt(s0);
                                x[i] = Double.parseDouble(s1);
                                i++;
                        }

                }
                catch(IOException excep){
                        System.out.println(" Error in reading files");
                }
        }while( !line.startsWith("Flac3D>"));

    }

    public void shutDown()
    {
       try {
          connection.close();
       }
       catch ( SQLException sqlex ) {
          System.err.println( "Unable to disconnect" );
          sqlex.printStackTrace();
       }
    }

    public static void main( String args[] )
    {
       final ReadLog app = new ReadLog();
    }

}
```

APPENDIX D

LEASTSQUARE.JAVA

APPENDIX D

LEASTSQUARE.JAVA

```
import java.io.*;
import java.sql.*;
import javax.swing.*;
import java.awt.*;
import java.awt.event.*;
import java.util.*;

public class LeastSquare1 {

   private Connection connection;
   private JTable table;
   private ObjectOutputStream output;

   public LeastSquare1()
   {
      // The URL specifying the Books database to which
      // this program connects using JDBC to connect to a
      // Microsoft ODBC database.
      String url = "jdbc:odbc:thesis";
      String username = "";
      String password = "";

         // Load the driver to allow connection to the database
      try {
         Class.forName( "sun.jdbc.odbc.JdbcOdbcDriver" );
         connection = DriverManager.getConnection(
            url, username, password );
      }
      catch ( ClassNotFoundException cnfex ) {
         System.err.println(
            "Failed to load JDBC/ODBC driver." );
         cnfex.printStackTrace();
         System.exit( 1 );  // terminate program
      }
      catch ( SQLException sqlex ) {
         System.err.println( "Unable to connect" );
         sqlex.printStackTrace();
      }
      getData();
   }

   private void getData()
   {
      Statement statement;
      ResultSet resultSet;
      try {
         String query = "SELECT * FROM ground_settlement";
         statement = connection.createStatement();
         resultSet = statement.executeQuery( query );
         getResultSet( resultSet );
         statement.close();
      }
      catch ( SQLException sqlex ) {
         sqlex.printStackTrace();
      }
```

```
}

private void getResultSet( ResultSet rs )
   throws SQLException
{

        // position to first record
   boolean moreRecords = rs.next();

       // If there are no records, display a message
   if ( ! moreRecords ) {
      System.out.println( "ResultSet contained no records" );
      return;
   }
       Vector rows = new Vector();
   try {
      // get column heads
      ResultSetMetaData rsmd = rs.getMetaData();
      // get row data
      do {
                     rows = getNextRow( rs, rsmd );
                     Ls(rows);
                     rows.clear();
      } while ( rs.next() );

            shutDown();

   }
   catch ( SQLException sqlex ) {
      sqlex.printStackTrace();
   }
}

private void Ls (Vector row){
  final int array_size = 10;
      double x[] = new double[100];
      double y[] = new double[100];
  double a[] = new double[ array_size ];
  double xen[] = new double[ 2 * array_size];
  double yen[] = new double[ array_size ];
  double coef[][] = new double[array_size][array_size];
  double temp = 0;

      int n,k=0;



      n = Integer.parseInt(row.get(0).toString());

  System.out.print( " Working on " + n + " item ..............");
        for (int i = 1; i < 200; i += 2)
        {
                    temp = Double.parseDouble(row.get(i).toString());
              x[(int)(i-1)/2] = temp;
              y[(int)(i-1)/2] = Double.parseDouble(row.get(i+1).toString());

              if(i > 1 && temp == 0.0)
              {
                      y[(int)(i-1)/2] = 0.0;
                      k = (int)(i-1)/2;
                      break;
              }

        }
  int m ;
  m = k - 1;

  for (int i = 0; i < 2 * array_size ; i++)
  {
     for(int j = 0; j < m; j++)
     {
```

```
            xen[i] += Math.pow (x[j], (double) i);
          }
        }

        for ( int i = 0; i < array_size; i ++)
        {
           for(int j = 0; j < m; j++)
           {
             yen[i] += y[j] * Math.pow (x[j], (double) i);

           }
        }

        for(int i = 0; i < array_size; i ++)
        {
         for(int j = 0; j < array_size; j++)
         {
           coef[i][j] = xen[ i + j ];
         }
        }

        solve(a, coef, yen, array_size);
        WriteCoef( a, n );
        WriteSettlement(a,n,x[m]);
        WriteSettlement(a,x,n,m);
        System.out.println("Done");
      }

      private void WriteSettlement(double a[], int n, double x)
      {
         Statement statement;
         String query = new String("INSERT INTO cal_at_point VALUES( ");
         query += n ;
         boolean out_boundary = false;

         for(int i = 0; i < 50; i ++)
         {
                  if( (double) i > x) out_boundary = true;
                  double temp = CalculationSettlementAtX(a, (double) i );

                  if(temp < 0)
                         query += ", 0";
                  else
                  query += ("," + temp);
         }

         query += ");";

         try{
            statement = connection.createStatement();
            statement.executeUpdate( query );
            statement.close();
         }
         catch ( SQLException sqlex ) {
            System.out.println(sqlex.toString());
         }
      }


      private void WriteSettlement(double a[],double x[], int n, int k)
      {
         Statement statement;
         String query = new String("INSERT INTO calculation VALUES( ");
         query += n ;

         for(int i = 0; i < 50; i ++)
         {
                  if(i > k)
                  {
                         query += ", 0";
                         continue;
```

```
                }
            query += "," + CalculationSettlementAtX(a, x[i]);
        }

        query += ");";

        try{
            statement = connection.createStatement();
            statement.executeUpdate( query );
            statement.close();
        }
        catch ( SQLException sqlex ) {
            System.out.println(sqlex.toString());
        }
    }

    private double CalculationSettlementAtX(double a[], double x)
    {
        double temp = 0.0;
        for(int i = a.length -1; i >= 0 ; i --)
        {
          temp =  a[i] + temp * x ;
          //System.out.println(i);
        }

        return temp;
    }

    private void solve(double a[], double coef[][], double yen[], int n)
    {
        double temp;
        for(int j = 0 ; j < n ; j ++)
        {
          for (int i = j + 1 ; i < n; i ++)
          {
              temp = coef[i][j] / coef[j][j];
              for(int k = j + 1; k < n; k++)
              {
                coef[i][k] -= coef[j][k] * temp;
              }
              coef[i][j] = 0;
              yen[i] -= yen[j] * temp;
          }
          //show_matrix(coef, yen, n);
        }
        BackCalculation(a,coef,yen,n);
    }

   private void show_matrix(double coef[][],double y[], int n)
   {
        System.out.println("\n\n");
        for(int i = 0; i < n ; i ++)
        {
          for(int j = 0; j < n ; j++)
          {
            System.out.print(coef[i][j] + ",    ");
          }
          System.out.print(y[i]);
          System.out.print("\n");
        }

    }

    private void BackCalculation(double a[], double coef[][],double yen[], int n)
    {
        double temp;

        for(int i = n - 1 ; i >= 0; i --)
        {
          for(int j = i + 1 ; j < n; j ++)
          {
```

```
            yen[i] -= a[j] * coef[i][j];
          }
          a[i] = yen[i] / coef[i][i];
        }
      }

      private void WriteCoef(double a[], int k)
      {
         Statement statement;
         String query = new String("INSERT INTO appro_coef VALUES(");
         query += k ;

         for(int i = 0; i < a.length; i ++)
         {
           query += ", " + a[i];
         }

         query += ");";

              try{
            statement = connection.createStatement();
            statement.executeUpdate( query );
            statement.close();
         }
         catch ( SQLException sqlex ) {
            System.out.println(sqlex.toString());
         }
      }

      private Vector getNextRow( ResultSet rs,
                                 ResultSetMetaData rsmd )
          throws SQLException
      {
         Vector currentRow = new Vector();
         for ( int i = 1; i <= rsmd.getColumnCount(); ++i )
            switch( rsmd.getColumnType( i ) ) {
               case Types.DOUBLE:
                     currentRow.addElement(new Double(rs.getDouble( i )) );
                  break;
               case Types.INTEGER:
                     currentRow.addElement(
                        new Long( rs.getLong( i ) ) );
                  break;
               default:
                  System.out.println( "Type was: " +
                     rsmd.getColumnTypeName( i ) );
            }
        return currentRow;
      }

      public void shutDown()
      {
         try {
            connection.close();
         }
         catch ( SQLException sqlex ) {
            System.err.println( "Unable to disconnect" );
            sqlex.printStackTrace();
         }
      }

      public static void main( String args[] )
      {
         final LeastSquare1 app = new LeastSquare1();
      }
   }
```

APPENDIX E

ANN.JAVA

APPENDIX E

ANN.JAVA

```
import java.math.*;
import java.io.*;
import java.sql.*;
import java.util.*;

public class Ann  extends Connect{

  private int input_number;
  private int hidden_number;
  private int output_number;
  private int training_size;
  private double  lamda;
  private double  mom;
  private double  l_rate;
  private double  epsi;
  private double  bias;
  private double  v[][]; //weight array between input layer and hidden layer
  private double  w[][]; //weight array between hidden layer and output layer
  private double  vBias[];
  private double  wBias[];
  public double  training_input[][];
  private double  input[];
  private double  OutputMax[];
  private double  OutputMin[];
  private double  hidden[];
  private double  differential_hidden[];
  private double  h_theta[];
  private double  output[];
  private double  differential_output[];
  private double  o_theta[];
  public double  desire_output[][];
  private double  delta_w[];
  private double  delta_v[];
  private double  hidden_mom[][];
  private double  output_mom[][];
  private String  del;

  Ann (int in, int h, int o, int t, double rate, double l, double e, double b, double
mom){

  super("thesis");

  // in : input  node number;
  // o  : output node number;
  // h  : hidden layer number;
  // t  : training size, the number of training event;
  // rate:  learning rate;
  // epsi:  error tolerent;
  // bias:  learing bias;

  input_number  = in;
  //System.out.println("Input_number is  " + input_number);
  hidden_number = h;
  //System.out.println("Hidden_number is  " + hidden_number);
  output_number = o;
```

```
//System.out.println("output_number is  " + output_number);
training_size = t;
//System.out.println("training_size is  " + training_size);
l_rate = rate;
epsi = e;
bias = b;
lamda = l;
double start_temperature = 100;
double end_temperature = 0.01;
int number_temperature = 30;
int steps = 1000;

v = new double[input_number][hidden_number];
delta_v = new double[hidden_number];
w = new double[hidden_number][output_number];
delta_w = new double[output_number];
vBias = new double[hidden_number];
wBias = new double[output_number];

input = new double[input_number];
OutputMax = new double[output_number];
OutputMin = new double[output_number];
hidden = new double[hidden_number];
differential_hidden = new double[hidden_number];
h_theta = new double[hidden_number];
o_theta = new double[output_number];
output = new double[output_number];
differential_output = new double[output_number];
training_input = new double[input_number][training_size];
desire_output = new double[output_number][training_size];
hidden_mom = new double [input_number][hidden_number];
output_mom = new double [hidden_number][output_number];
}

public void show_v()
{
        for(int i = 0; i < input_number; i ++)
        {
                System.out.print("id " + i );
                for(int j = 0; j < hidden_number; j++)
                System.out.print(v[i][j] + ", ");
                System.out.println();
        }

        for( int i = 0; i < hidden_number; i ++)
        {
                System.out.print("id " + i + "   ");
                System.out.println(h_theta[i]);
        }
        System.out.println();
}

public void show_w()
{
        for(int i = 0; i < hidden_number; i ++)
        {
                System.out.print("id " + i + "   ");
                for(int j = 0; j < output_number; j++)
                System.out.print(w[i][j] + ", ");
                System.out.println();
        }

        for(int i = 0; i < output_number; i ++)
        {
                System.out.print("id " + i + "   ");
                System.out.println(o_theta[i]);
        }
}

public void initial_weight(){
```

```
Statement statement;
int sign = 0;
double temp =0;

del = new String("DELETE * FROM v; ");
Delete(del);

////////////////////////////////////
//initialize the v weight array;
////////////////////////////////////

for (int i = 0 ; i < input_number + 1; i++)
{
  //System.out.println("i is  " + i);
  StringBuffer queryBuffer = new StringBuffer("INSERT INTO v ( node,");

      for(int j = 0; j < hidden_number ; j ++)
      {
              queryBuffer.append("y");
              if(j < 10) queryBuffer.append("00");
              if(j < 100 && j >=10)queryBuffer.append("0");
              if(j == hidden_number - 1)
              {
                      queryBuffer.append(j + ")");
              }
              else
              {
                      queryBuffer.append(j + ",");
              }
      }

      queryBuffer.append(" VALUES( " + i );


  for(int j = 0 ; j < hidden_number ; j++)
  {
    if(Math.random() > 0.5)
      sign = 1;
    else
      sign = -1;

    temp = sign * (Math.random()/3.0);
       if(i != input_number)
       {
              v[i][j] = temp;
       }
       else
       {
              vBias[j] = temp;
       }

    queryBuffer.append(", " + temp );
  }

  queryBuffer.append(");");
  String query = new String(queryBuffer.toString());
  //System.out.println(query);

  Insert(query);
}

////////////////////////////////////
//
//initialize the w weight array;
//
//
////////////////////////////////////


  del = new String("DELETE * FROM w;");
  Delete(del);
```

```
for ( int i = 0; i < hidden_number + 1; i++)
{

  StringBuffer queryBuffer = new StringBuffer("INSERT INTO w (hidden_node,");

      for(int j = 0; j < output_number; j ++)
      {
              queryBuffer.append("y");
              if(j < 10) queryBuffer.append("0");
              if(j == output_number - 1)
              {
                      queryBuffer.append(j + ")");
              }
              else
              {
                      queryBuffer.append(j + ",");
              }
      }

      queryBuffer.append(" VALUES( " + i );


  for( int j = 0; j < output_number; j++)
  {
    if(Math.random () > 0.5)
      sign = 1;
    else
      sign = -1;

    temp = sign * (Math.random ()/3.0);
       if (i != hidden_number)
       {
              w[i][j] = temp;
       }
       else
       {
              wBias[j] = temp;
       }
    queryBuffer.append(", " + temp);
  }
  queryBuffer.append(");");
  String query = new String (queryBuffer.toString());
  //System.out.println(query);

  Insert(query);

}

//initialize the hidden layer theta array;
del = new String("DELETE * from h_theta;");
Delete(del);

StringBuffer queryBuffer;
String query;
for ( int i = 0 ; i < hidden_number; i++)
{

  queryBuffer = new StringBuffer("INSERT INTO h_theta VALUES (");
  if (Math.random () > 0.5)
    sign = 1;
  else
    sign = -1;

  h_theta[i] = sign * (Math.random () * 3);
  queryBuffer.append( i + ", " + h_theta[i]);

  queryBuffer.append(");");
  query = new String (queryBuffer.toString());
```

```
      //System.out.println(query);

          Insert(query);
    }

          del = new String("DELETE * from o_theta;");
          Delete(del);

    //initialize the output layer theta array;
    for ( int i = 0 ; i < output_number; i++)
    {

      queryBuffer = new StringBuffer("INSERT INTO o_theta VALUES (");
      if ( Math.random () > 0.5)
        sign = 1;
      else
        sign = -1;

      o_theta[i] = sign * (Math.random () * 3);

      queryBuffer.append(i + ", " + o_theta[i]);
      queryBuffer.append(");");
      query = new String (queryBuffer.toString());
      //System.out.println (query);

      Insert(query);
    }
  }

    public void query_v(){
      Statement statement;
      ResultSet resultset;

      String query = new String("SELECT * FROM v");

      try{
        statement = connection.createStatement ();
        resultset = statement.executeQuery(query);
        get_v(resultset);
        statement.close();
      }
      catch(SQLException excep)
      {
        System.out.println(excep.toString ());
      }
    }

    public void query_new_v(){
      Statement statement;
      ResultSet resultset;

      String query = new String("SELECT * FROM v_new");

      try{
        statement = connection.createStatement ();
        resultset = statement.executeQuery(query);
        get_v(resultset);
        statement.close();
      }
      catch(SQLException excep)
      {
        System.out.println(excep.toString ());
      }
    }

    public void get_v( ResultSet rs) throws SQLException {

      boolean moreRecord = rs.next();

      if( ! moreRecord){
        System.out.println ("resultset contained no records");
```

```
      System.out.println ("I can not find v vector");
      return;
    }

    try{

      int line = 0;
      for(int j = 0; j < input_number+1; j++)
      {
        line = (int) rs.getInt(1);
        //System.out.println("Line is " + line + "  and j is " + j + "    ");
              if (line == input_number)
              {
                    for (int i = 0; i < hidden_number; i ++)
                    {
                          vBias[i] = (double) rs.getDouble (i + 2);
                    }
              }
              else
              {
                    for (int i = 0 ; i < hidden_number; i++)
                    {
                          v[line][i] = (double) rs.getDouble(i+2);
                    }
              }
        rs.next();
      }
    }
    catch(SQLException excep)
    {
      System.out.println(excep.toString());
    }
  }

  public void ReadMaxMin(){
        Statement statement;
        ResultSet resultset;

        String query = new String ("SELECT * FROM ground_settlement_max_min");

    try{
      statement = connection.createStatement ();
      resultset = statement.executeQuery(query);
      GetMaxMin(resultset);
      statement.close();
    }
    catch(SQLException excep)
    {
      System.out.println(excep.toString ());
    }

  }

  public void GetMaxMin(ResultSet rs) throws SQLException {
       int line;

    boolean moreRecord = rs.next();

    if( ! moreRecord){
      System.out.println ("resultset contained no records");
      return;
    }

       ////////////////////////////////
       //
       //Read Max and Min output Value and save them into proper arrays.
       //
       ////////////////////////////////

       try{
```

```
          for(int j = 0; j < 2; j++)
      {
        line = (int) rs.getInt(1);
               if(line == 0)
               {
                       for (int i = 0; i < output_number; i ++)
                       {
                               OutputMax[i]= (double) rs.getDouble (i + 2);
                       }
               }
               else
               {
                       for (int i = 0 ; i < output_number; i++)
                       {
                               OutputMin[i] = (double) rs.getDouble(i+2);
                       }
               }
        rs.next();
      }
        }
    catch(SQLException excep)
    {
      System.out.println(excep.toString());
    }
  }

  public void query_w(){
    Statement statement;
    ResultSet resultset;

    String query = new String("SELECT * FROM w");

    try{
      statement = connection.createStatement ();
      resultset = statement.executeQuery(query);
      get_w(resultset);
      statement.close();
    }
    catch(SQLException excep)
    {
      System.out.println(excep.toString ());
    }

  }

  public void query_new_w(){
    Statement statement;
    ResultSet resultset;

    String query = new String("SELECT * FROM w_new");

    try{
      statement = connection.createStatement ();
      resultset = statement.executeQuery(query);
      get_w(resultset);
      statement.close();
    }
    catch(SQLException excep)
    {
      System.out.println(excep.toString ());
    }

  }

  public void get_w( ResultSet rs) throws SQLException {

    //System.out.println("Now is w time");

    boolean moreRecord = rs.next();

    if( ! moreRecord){
```

```
      System.out.println ("resultset contained no records");
      return;
    }

    try{

      int line = 0;
      for(int j = 0; j < hidden_number + 1; j++)
      {
        line = (int) rs.getInt(1);
        //System.out.print("Line is " + line + "  and j is " + j + "   ");
              if(line == hidden_number)
              {
                    for (int i = 0; i < output_number; i ++)
                    {
                          wBias[i]= (double) rs.getDouble (i + 2);
                    }
              }
              else
              {
                    for (int i = 0 ; i < output_number; i++)
                    {
                          w[line][i] = (double) rs.getDouble(i+2);
                          //if (i < 5) System.out.print(w[line][i] + "   ");
                    }
              }
        //System.out.print("\n");
        rs.next();
      }
    }
    catch(SQLException excep)
    {
      System.out.println(excep.toString());
    }
  }

  public void query_h_theta(){

    Statement statement;
    ResultSet resultset;

    String query = new String("SELECT * FROM h_theta");

    try{
      statement = connection.createStatement ();
      resultset = statement.executeQuery(query);
      get_h_theta(resultset);
      statement.close();
    }
    catch(SQLException excep)
    {
      System.out.println(excep.toString ());
    }
  }

  public void get_h_theta(ResultSet rs) throws SQLException {

    //System.out.println("Now is h_theta time");
    boolean moreRecord = rs.next();

    if( ! moreRecord){
      System.out.println ("resultset contained no records");
      return;
    }

    try{

      int line = 0;
      for(int j = 0; j < hidden_number; j++)
      {
        line = (int) rs.getInt(1);
```

```
            //System.out.print("Line is " + line + "  and j is " + j + "    ");
            h_theta[line] = (double) rs.getDouble(2);
            //System.out.print(h_theta[line] + "    ");
            //System.out.print("\n");
            rs.next();
          }
        }
        catch(SQLException excep)
        {
          System.out.println(excep.toString());
        }
      }

      public void query_o_theta(){

        Statement statement;
        ResultSet resultset;

        String query = new String("SELECT * FROM o_theta");

        try{
          statement = connection.createStatement ();
          resultset = statement.executeQuery(query);
          get_o_theta(resultset);
          statement.close();
        }
        catch(SQLException excep)
        {
          System.out.println(excep.toString ());
        }
      }

      public void get_o_theta(ResultSet rs) throws SQLException {

        //System.out.println("Now is o_theat time");
        boolean moreRecord = rs.next();

        if( ! moreRecord){
          System.out.println ("resultset contained no records");
          return;
        }

        try{

          int line = 0;
          for(int j = 0; j < output_number; j++)
          {
            line = (int) rs.getInt(1);
            //System.out.print("Line is " + line + "  and j is " + j + "    ");
            o_theta[line] = (double) rs.getDouble(2);
            //System.out.print(o_theta[line] + "    ");
            //System.out.print("\n");
            rs.next();
          }
        }
        catch(SQLException excep)
        {
          System.out.println(excep.toString());
        }
      }
    //
    //

      public void init_trainingset(){

        Statement statement;
        ResultSet resultSet1, resultSet2;

        String query = new String("SELECT * FROM soil_proper");

        try{
```

```
      statement = connection.createStatement ();
      resultSet1 = statement.executeQuery(query);
      get_training_data(resultSet1);
      statement.close();
    }
    catch(SQLException excep){
      System.out.println( excep.toString());
    }

    query = new String("SELECT * FROM cal_at_point");

    try{
      statement = connection.createStatement();
      resultSet2 = statement.executeQuery(query);
      get_desire_output(resultSet2);
      statement.close();
    }
    catch(SQLException excep){
      System.out.println(excep.toString ());
    }
  }

  ////////////////////////////////
  //get training input data
  ////////////////////////////////

public void get_training_data(ResultSet rs) throws SQLException {

    boolean moreRecord = rs.next();
    System.out.println("I am in get training_data");

    if ( ! moreRecord ) {
        System.out.println( "ResultSet contained no records" );
        System.out.println( " I can not find anything");
        return;
    }

    try{

      int line = 0;

      for(int j = 0 ; j < training_size; j++)
      {
        line = (int) rs.getInt (1);
        if( line > training_size )
        {
          j --;
          rs.next();
          continue;
        }

        for(int i =0; i < input_number; i++)
        {
          training_input[i][line] = (double) rs.getDouble (i+2);
                  //pre doing for depth
                  //if(i == 1)
                        //  training_input[i][line] = training_input[i][line]/10;
                  //pre doing for water table
                  //if(i == 2)
                        //  training_input[i][line] = training_input[i][line]/10;
                  //pre process soil density
                  if(i ==4)
                          training_input[i][line] = training_input[i][line]/1000;
                  //pre process bulk
                  //if(i ==5)
                        //  training_input[i][line] = training_input[i][line]/10;
                  //pre procee shear
                 //  if(i ==6)
                 //        training_input[i][line] = training_input[i][line]/10;
                    //pre process cohesion
                    //if(i ==6)
```

```
                //        training_input[i][line] = training_input[i][line]/10;
                  //pre process friction angle
                  //if(i ==8)
                        //  training_input[i][line] = training_input[i][line]/10;
                  //pre process dilation angle
                  //if(i ==9)
                        //  training_input[i][line] = training_input[i][line]/10;


        }
        rs.next();
       }
    }
    catch(SQLException excep)
    {
         System.out.println("There are some problems here");
      System.out.println(excep.toString());
      excep.getMessage();
    }
  }


////////////////////////////////
//Get desired output from database
////////////////////////////////

 public void get_desire_output(ResultSet rs) throws SQLException {

   boolean moreRecord = rs.next();

   if( ! moreRecord){
     System.out.println ("resultset contained no records");
     return;
   }

   try{

     int line = 0;
     for(int j = 0; j < training_size; j++)
     {
       line = (int) rs.getInt(1);

       if(line > training_size)
       {
                     j--;
                     rs.next();
                     continue;
              }

       for (int i = 0 ; i < output_number; i++)
       {
         desire_output[i][line] = (double)  rs.getDouble(i+2);
                if(line == 0 )
                {
                       OutputMax[i] = desire_output[i][line];
                       OutputMin[i] = desire_output[i][line];
                }

                if( desire_output[i][line] > OutputMax[i])
                       OutputMax[i] = desire_output[i][line];

                if(desire_output[i][line] < OutputMin[i])
                       OutputMin[i] = desire_output[i][line];


                //System.out.println(line + "    " + desire_output[i][line]);
       }
       rs.next();
     }
```

```
            ////////////////////////////
            //
            //Normalize the output data
            //
            ////////////////////////////

            for(int j = 0; j < training_size; j ++)
            {
                    for(int i = 0; i < output_number; i ++)
                    {
                            desire_output[i][j] = ( desire_output[i][j] - OutputMin[i] ) / (
OutputMax[i] - OutputMin[i] );
                            desire_output[i][j] = ( 0.5 + desire_output[i][j] ) / 1.5;
                    }
            }


        }
        catch(SQLException excep)
        {
          System.out.println(excep.toString());
        }
      }


      public double anneal(double start_temperature,
                      double end_temperature,
                      int number_temperature,
                      int steps){

      double center_v[][] = new double[input_number][hidden_number];
      double center_w[][] = new double[hidden_number][output_number];
      double best_v[][] = new double[input_number][hidden_number];
      double best_w[][] = new double[hidden_number][output_number];

      double best_error;
      double temperature;
      double temp_mult;
      int improved = 0;
      double learning_error;
      int n_iter = 5;
      int setback = 3;


      //set the initial center value
      //copy the v w value to the center value
      for(int i = 0 ; i < input_number; i++)
        for(int j = 0; j < hidden_number; j++)
          center_v[i][j] = v[i][j];

      for(int i = 0 ; i < hidden_number; i++)
        for(int j = 0 ; j < output_number; j++)
          center_w[i][j] = w[i][j];

      best_error = 1000; //learning(v,w,input_number,hidden_number,output_number,steps);

      temperature = start_temperature;
      temp_mult = Math.exp( Math.log ( end_temperature / start_temperature ) /
(number_temperature - 1) );

      for (int itemp = 0; itemp < number_temperature; itemp ++)
      {

        //System.out.println("Temp iteration is  " + itemp);

        for( int i = 0; i < n_iter; i++)
        {
          System.out.println("Temp iteration is  " + itemp + " n_iter is " + i + " Improved?
" + improved);
          System.out.println("Temperature is " + temperature);
          improved = 0;
```

```
        shake(center_v, center_w, temperature);
        learning_error = learning(steps);

        if( /* Math.abs(best_error - learning_error) / best_error > 0.01 && */best_error >
learning_error )
        {
          best_error = learning_error;
          improved = 1;

          for(int m = 0; m < input_number; m++)
            for(int n = 0; n < hidden_number; n++)
              best_v[m][n] = v[m][n];

          for(int m = 0; m < hidden_number; m++)
            for(int n = 0; n < output_number; n ++)
              best_w[m][n] = w[m][n];

          if(best_error < epsi) break;

          i -= setback;
          if(i < 0 ) i = 0;
        }
      }

        if ( improved == 1 )
        {
          for(int m = 0 ; m < input_number; m++)
            for(int n = 0; n < hidden_number; n++)
              center_v [m][n] = best_v[m][n];

          for(int m = 0 ; m < hidden_number; m++)
            for(int n = 0 ; n < output_number; n++)
              center_w[m][n] = best_w[m][n];
        }

        if(best_error < epsi) break;

      temperature *= temp_mult;
   }

      for( int i = 0 ; i < input_number; i ++)
        for(int j = 0; j < hidden_number; j++)
          v[i][j] = center_v[i][j];

      for(int i = 0 ; i <hidden_number; i++)
        for(int j = 0; j < output_number; j++)
          w[i][j] = center_w[i][j];

      //learning(2000);
      //write_vw();
          //shutDown();


      return best_error;
  }
    public void WriteMaxMin(){
          Statement statement;

          ////////////////////////////////////
          //
          //Delete previous saved Max and Min Settlement value
          //
          ////////////////////////////////////
          del = new String("DELETE * FROM ground_settlement_max_min; ");
          Delete(del);

          ////////////////////////////////////
          //
          //Write OuputMax Value into database
```

```
        //
        ////////////////////////////////

            String query = new String("INSERT INTO ground_settlement_max_min (id, ");
            for (int j = 0; j < output_number; j ++)
            {
                    query += "y";
                    if(j < 10) query += "0";
                    if( j == (output_number - 1) )
                            query += j ;
                    else query += j + ",";
            }

            query += ") VALUES (0,";

            for(int j = 0; j <output_number; j ++)
            {
                    if( j == output_number - 1)
                            query += OutputMax[j] + ");";
                    else
                            query += OutputMax[j] + ", ";
            }


            Insert(query);
            System.out.println(query);


        ////////////////////////////////////////
        //
        //Write Output Min Value in to database
        //
        ////////////////////////////////////////


            query = new String("INSERT INTO ground_settlement_max_min (id, ");
            for (int j = 0; j < output_number; j ++)
            {
                    query += "y";
                    if(j < 10) query += "0";
                    if( j == output_number - 1)
                            query += j ;
                    else query += j + ",";
            }

            query += ") VALUES ( 1, ";

            for(int j = 0; j <output_number; j ++)
            {
                    if( j == output_number - 1)
                            query += OutputMin[j] + ");";
                    else
                            query += OutputMin[j] + ", ";
            }

            Insert(query);
            System.out.println(query);


    }

    public void write_vw(){
    Statement statement ;

    del = new String("DELETE * FROM v_new; ");
    Delete(del);

    ////////////////////////////////////////
    //
```

```
//    Write new v weight back in database
//
//////////////////////////////////////

for (int i = 0 ; i < input_number + 1; i++)
{
  StringBuffer queryBuffer = new StringBuffer("INSERT INTO v_new ( node,");

      for(int j = 0; j < hidden_number; j ++)
      {
              queryBuffer.append("y");
              if(j < 10) queryBuffer.append("00");
              if(j < 100 && j >=10)queryBuffer.append("0");
              if(j == hidden_number - 1)
              {
                      queryBuffer.append(j + ")");
              }
              else
              {
                      queryBuffer.append(j + ",");
              }
      }

      queryBuffer.append(" VALUES( " + i );

      if( i == input_number)
      {
              for(int j = 0 ; j < hidden_number; j++)
              {
                      queryBuffer.append(", " + vBias[j] );
              }
      }
      else
      {
              for(int j = 0 ; j < hidden_number; j++)
              {
                      queryBuffer.append(", " + v[i][j] );
              }
      }

  queryBuffer.append(");");
  String query = new String(queryBuffer.toString());
  //System.out.println(query);

  Insert(query);
}


del = new String("DELETE * FROM w_new; ");
Delete(del);

//////////////////////////////////////////
//
//
// Write new w weight back to database
//
//
//////////////////////////////////////////

for ( int i = 0; i < hidden_number + 1; i++)
{

  StringBuffer queryBuffer = new StringBuffer("INSERT INTO w_new (hidden_node,");

      for(int j = 0; j < output_number; j ++)
      {
              queryBuffer.append("y");
              if(j < 10) queryBuffer.append("0");
              if(j == output_number - 1)
              {
                      queryBuffer.append(j + ")");
```

```
                }
                else
                {
                        queryBuffer.append(j + ",");
                }
        }

        queryBuffer.append(" VALUES( " + i );
        if ( i == hidden_number)
        {
                for( int j = 0; j < output_number; j++)
                {
                        queryBuffer.append(", " + wBias[j]);
                }
        }
        else
        {
                for( int j = 0; j < output_number; j++)
                {
                        queryBuffer.append(", " + w[i][j]);
                }
        }


    queryBuffer.append(");");
    String query = new String (queryBuffer.toString());
        //System.out.println(query);
    //System.out.println(query);
    Insert(query);

        }

  }


  private void shake(double center_v[][],
                     double center_w[][],
                     double temperature){

    int RANDMAX = 1;
    double r;
    //The variance of a uniform deviate on 0-1 is 1/12
    //Adding four random variance multiplies the variance by 4
    //while dividing by 2 divides teh variance by 4
    //and sqrt(12) = 3.464101615
    temperature *= 3.464101615 / ( 2. * (double) RANDMAX );
    int counter = 0;

    for(int i = 0 ; i < input_number; i++)
      for(int j = 0; j < hidden_number; j++)
      {
        r = 250.0 * Math.random() ;
        v[i][j] = center_v[i][j] + temperature * r;
        if(Math.abs(v[i][j]) > 5.0)
        {
          v[i][j] = 5.0 * Math.abs(v[i][j]) / v[i][j];
          counter ++;
        }
      }

    System.out.println (" IN v there are " + counter + "  exceed 5 ");
    counter = 0;

    for (int i = 0; i < hidden_number; i++)
      for(int j = 0 ; j < output_number; j++)
      {
        //r = 250.0 * ( Math.random () + Math.random () - Math.random () - Math.random
()};
                r = 250.0 * Math.random();
        w[i][j] = center_w[i][j] + temperature * r;
        if(Math.abs(w[i][j]) > 5.0)
```

```
        {
          w[i][j] = 5.0 * Math.abs(w[i][j]) / w[i][j];
          counter ++;
        }
      }

    System.out.println(" In w there are " + counter + " exceed 5 " );
  }


  public double learning (int steps){

   double maxerror = 0.1;
   double average_error = 100.0;
   double old_error = 100.0;
   double delta_learning_rate = 0.0;
   double err;
   double old_rate = l_rate;
   int mark = 0;
   int decreased_step = 0;

   init_momentum();

   for( int iter = 0; iter < steps; iter ++)
   {
          if(iter%100 == 0)
                System.out.print(" loops " + iter + " maxerror node is " + mark + "    "
+ maxerror + " average_error is " + average_error/training_size + "\n");

      if(average_error < old_error || average_error - old_error == 0)
                decreased_step ++;
          if(old_error < average_error)
                decreased_step = -1;

          if(decreased_step >= 100)
          {
                delta_learning_rate =  0.01 * l_rate;
                System.out.println("Increased Learning Rate to " + (l_rate +
delta_learning_rate));
                decreased_step = 0;
          }

          if(decreased_step < 0)
          {
                delta_learning_rate = - 0.05 *l_rate;
                System.out.println("Decreased Learning Rate to " + (l_rate +
delta_learning_rate));
                decreased_step = 0;
          }

          l_rate += delta_learning_rate;
          delta_learning_rate = 0;

      if( maxerror  < 0.000000000001 ) break;
      old_error = average_error;

      maxerror = 0.0;
      average_error = 0.0;

      for( int i = 0; i < training_size; i++)
      {
        feed_forward(i);
        err = error(i);
        average_error += err;
        if( maxerror < err)
        {
          maxerror = err;
          mark = i;
        }
        if( err >= epsi)
        {
```

```
        back_propagation(i);
      }
    }
  }

 l_rate = old_rate;
  return average_error/training_size;
}

private void init_momentum()
{
  for(int i = 0 ; i < input_number; i++)
    for(int j = 0; j < hidden_number; j++)
      hidden_mom[i][j] = 0.0;

  for(int i = 0 ; i < hidden_number; i++)
    for(int j = 0 ; j < output_number; j++)
      output_mom[i][j] = 0.0;
}


//////////////////////////////////////////
//
//Feed forward function to calculate the output
//
//////////////////////////////////////////

public void feed_forward(int k){

        ////////////////////////////////////
        // Get the kth training pattern
        ////////////////////////////////////

        for( int i = 0; i < input_number; i++)
             input[i] = training_input[i][k];

        ////////////////////////////////////////
        //Make sure all the hidden node value to be 0
        ////////////////////////////////////////

        for (int i = 0 ; i < hidden_number; i++)
        {
             hidden[i] = 0.0;
             differential_hidden[i] = 0.0;
        }

        ////////////////////////////////////
        //
        //Calculate feed forward fro input layer to hidden layer
        //
        ////////////////////////////////////

        for( int j = 0 ; j < hidden_number; j++)
        {
                for( int i = 0 ; i < input_number; i++)
                        hidden[j] += v[i][j] * input[i];

                hidden[j] += vBias[j];
                hidden[j] = active_function( hidden[j],h_theta[j]);
        }

        ////////////////////////////////////////
        //
        // Make sure all the output node initialed to be 0
        //
        ////////////////////////////////////////

        for( int i = 0; i < output_number; i++)
        {
                output[i] = 0.0;
```

```
                differential_output[i] = 0.0;
        }

        ////////////////////////////////////////
        //
        // Calculate feed forwar from hidden layer to output layer
        //
        ////////////////////////////////////////

        for (int j= 0 ; j < output_number; j ++)
        {
                for( int i = 0 ; i < hidden_number; i++)
                        output[j] += w[i][j] * hidden[i];

                output[j] += wBias[j];
                output[j] = active_function( output[j],o_theta[j]);
        }
        /*
        for(int i = 0; i < output_number; i ++)
              // System.out.println("output[ " + i + " ][" + k + "] = " + ((output[i]
*1.5 - 0.5)*(OutputMax[i] - OutputMin[i]) + OutputMin[i]));
                System.out.println( ((desire_output[i][k] *1.5 - 0.5)*(OutputMax[i] -
OutputMin[i]) + OutputMin[i])  + "            " + ( (output[i] *1.5 - 0.5)*(OutputMax[i]
- OutputMin[i]) + OutputMin[i])  );
        System.out.println();
        */

  }

  ////////////////////////////////////////////////
  //Back propagation error
  ////////////////////////////////////////////////

  private void back_propagation(int k)
  {
    delta_weight_calculation(k);
    update_weight();
  }


  ////////////////////////////////////////////////
  //Function Calculate error signal
  ////////////////////////////////////////////////

  private void delta_weight_calculation(int k)
  {

    for (int i = 0 ; i < output_number; i++)
    {
              delta_w[i] = 0.0;
              delta_w[i] = (desire_output[i][k] - output[i]) * lamda * output[i] * ( 1 -
output[i]);
    }

    for (int i = 0 ; i < hidden_number; i++)
    {
              delta_v[i] = 0.0;
              for (int j = 0; j < output_number; j++)
                      delta_v[i] +=  delta_w[j] * w [i][j];

              delta_v[i] = delta_v[i] * lamda * hidden[i] * ( 1 - hidden[i] ) ;
    }
  }

  ////////////////////////
  //Update the delta weight
  ////////////////////////

  private void update_weight(){

    double temp;
```

```
    for (int i = 0 ; i < input_number; i++)
        {
                temp = 0.0;
                for( int j = 0 ; j < hidden_number; j++)
                {
                        temp = l_rate * delta_v[j] * input[i] + mom * hidden_mom[i][j];
                        v[i][j] += temp ;
                        hidden_mom[i][j] = temp;
                }

        }

        for(int i = 0; i < hidden_number; i ++)
        {
                vBias[i] += l_rate * delta_v[i];
        }

    for (int i = 0; i < hidden_number; i++)
        {
                for (int j = 0; j < output_number; j++)
                {
                        temp = l_rate * delta_w[j] * hidden[i] + mom * output_mom[i][j];
                        w[i][j] += temp;
                        output_mom[i][j] = temp;
                }

        }

        for(int i = 0; i < output_number; i ++)
        {
                wBias[i] += l_rate * delta_w[i];
        }

}




////////////////////////////////
//function used to test input tuple.
////////////////////////////////

public void feed_forward(double input[]){


        ////////////////////////////////////////
        //Make sure all the hidden node value to be 0
        ////////////////////////////////////////

        for (int i = 0 ; i < hidden_number; i++)
        {
             hidden[i] = 0.0;
             differential_hidden[i] = 0.0;
        }

        ////////////////////////////////////
        //
        //Calculate feed forward fro input layer to hidden layer
        //
        ////////////////////////////////////

        for( int j = 0 ; j < hidden_number; j++)
        {
                for( int i = 0 ; i < input_number; i++)
                        hidden[j] += v[i][j] * input[i];

                hidden[j] += vBias[j];
                //differential_hidden[j] = differential_active_function( hidden[j]);
```

```
                hidden[j] = active_function( hidden[j],h_theta[j]);
        }

        ////////////////////////////////////////
        //
        // Make sure all the output node initialed to be 0
        //
        ////////////////////////////////////////

        for( int i = 0; i < output_number; i++)
        {
                output[i] = 0.0;
                differential_output[i] = 0.0;
        }


        ////////////////////////////////////////
        //
        // Calculate feed forwar from hidden layer to output layer
        //
        ////////////////////////////////////////

        for (int j = 0 ; j < output_number; j ++)
        {
                for( int i = 0 ; i < hidden_number; i ++)
                        output[j] += w[i][j] * hidden[i];

                output[j] += wBias[j];
                //differential_output[j] = differential_active_function( output[j]);
                output[j] = active_function( output[j],o_theta[j]);
        }

        ////////////////////////////////////
        //Print test output on screen
        ////////////////////////////////////

        for(int i = 0; i < output_number; i ++)
                System.out.println("output[ " + i + " ] = " + output[i]);
  }




  private double active_function(double x,double y)
  {
        return 1.0 / ( 1.0 + Math.exp( - (lamda * x - y) ));
  }

//  private double differential_active_function (double x)
//  {
//        return active_function(x) * ( 1.0 - active_function(x));
//  }

/*
  private double active_function(double x, double y){
    double result;
    result = ( 2.0 / ( 1 + Math.exp( - (x -y) ) ) - 1.0 );
    return result;
  }
/*
  private double differential_active_function(double x){
    double result;
    result = 4.0 * 0.5 * ( 1 + active_function(x) / 4.0 ) * ( 1 - active_function(x) /
4.0 );
    return result;
  }
*/
```

```
    //////////////////////
    //Calculate the error of one training tuple
    //////////////////////
    private double error(int k){

      double e = 0.0;

          for( int i = 0; i < output_number; i ++)
      {
        e += ( (desire_output[i][k] - output[i]) * (desire_output[i][k] - output[i]));
      }

      e = e/2.0;
      return e;
    }

    private void initial_delta_vw(){
      for (int i = 0 ; i < hidden_number; i++)
        delta_v[i] = 0.0;

      for (int i = 0; i < output_number; i++)
        delta_w[i] = 0.0;
    }

    public void shutDown()
     {
        try {
           connection.close();
        }
        catch ( SQLException sqlex ) {
           System.err.println( "Unable to disconnect" );
           sqlex.printStackTrace();
        }
     }
}
```

APPENDIX F

CONNECT.JAVA

APPENDIX F

CONNECT.JAVA

```
import java.io.*;
import java.sql.*;
import java.util.*;

public class Connect{

        Connection connection;

        public Connect(String s){
                // The URL specifying the Books database to which
                // this program connects using JDBC to connect to a
        // Microsoft ODBC database.

                String url = "jdbc:odbc:";
                String username = "anonymous";
                String password = "guest";
                                // Load the driver to allow connection to the database

                url += s;
                try {
                        Class.forName( "sun.jdbc.odbc.JdbcOdbcDriver" );
                        connection = DriverManager.getConnection(url, username, password );
                }
                catch ( ClassNotFoundException cnfex ) {
                        System.err.println("Failed to load JDBC/ODBC driver." );
                        cnfex.printStackTrace();
                        System.exit( 1 );  // terminate program
                }
                catch ( SQLException sqlex ) {
                        System.err.println( "Unable to connect" );
                        sqlex.printStackTrace();
                }
        }

        public ResultSet Select(String query){
                Statement statement;
                ResultSet resultset = null;

            try{
              statement = connection.createStatement ();
              resultset = statement.executeQuery(query);
              statement.close();
            }
            catch(SQLException excep)
            {
              System.out.println(excep.toString ());
        }

        return resultset;
        }

        private void UpdateDatabase(String query)
        {
                Statement statement;
```

```
            try{
              statement = connection.createStatement ();
              statement.executeUpdate(query);
              statement.close();
            }
            catch(SQLException excep)
            {
              System.out.println(excep.toString ());
        }
        }


        public void Insert(String query)
        {
                UpdateDatabase(query);
        }

        public void Delete(String query)
        {
                UpdateDatabase(query);
        }

    public void shutDown()
    {
       try {
          connection.close();
       }
       catch ( SQLException sqlex ) {
          System.err.println( "Unable to disconnect" );
          sqlex.printStackTrace();
       }
    }

}
```

APPENDIX G

FLAC^{3D} INPUT DATA FILE

APPENDIX G

FLAC^{3D} INPUT DATA FILE

```
new
title
pipe depth is 4.0and soil density = 1899.0E =2.0M coh = 6.4k fric = 24.0 ground_loss =3.5
r = 1.0
;
;set the parameter
;************************************
define set_parameter
   depth = 4.0
   width = 7 * depth
   rock_depth = - width
   thickness = 16
   inter_width = width
   inter_depth = rock_depth

   n1 = 5
   n2 = 4
   n3 = 10
   n4 = 10

   r1 = 1
   r2 = 1
   r3 = 1
   r4 = 1.1

   e= 2.0e6
   p_ratio = 0.3
   fric_ang = 24.0
   coh_mod = 6.4e3
   dil_ang = 0
   den_num = 1899.0
   grav_num = -9.81
   k = 1

   tunnel_r = 1.0149
   pipe_r = 1
end
set_parameter

;generate soil zon
;************************************
gen zone radcyl p0 0 0 0 p1 depth 0 0 p2 0 thickness 0 p3 0 0 depth &
        size n1 n2 n3 n4 dim tunnel_r tunnel_r tunnel_r tunnel_r &
        rat r1 r2 r3 r4 fill
gen zone reflect dip 0 dd 90 ori 0 0 0

define var1
   p0_x = depth
   p0_y = 0
   p0_z = - depth

   p1_x = inter_width
```

```
    p1_z = -depth
    p1_y = 0

    p2_x = p0_x
    p2_y = thickness
    p2_z = p0_z

    p3_x = depth
    p3_z = depth
    p3_y = 0

    l_n3 = n3
    l_n1 = int ((n3*(inter_width-depth))/(3.5*depth))
    l_n2 = n2
    l_r1 = 1.2
    l_r2 = 1
    l_r3 = 1
end
var1
gen zon brick p0 p0_x p0_y p0_z p1 p1_x p1_y p1_z p2 p2_x p2_y p2_z &
        p3 p3_x p3_y p3_z  &
        size l_n1 l_n2 l_n3 rat l_r1 l_r2 l_r3
plot surface

define var2
    p0_x = 0
    p0_y = 0
    p0_z = inter_depth

    p1_x = depth
    p1_y = 0
    p1_z = p0_z

    p2_x = p0_x
    p2_y = thickness
    p2_z = p0_z

    p3_x = 0
    p3_y = 0
    p3_z = - depth

    b_n1 = int (n3/2)
    b_n2 = n2
    b_n3 = l_n1
    b_r1 = 1
    b_r2 = 1
    b_r3 = 1/1.2

end
var2
gen zon brick p0 p0_x p0_y p0_z p1 p1_x p1_y p1_z p2 p2_x p2_y p2_z &
        p3 p3_x p3_y p3_z &
        size b_n1 b_n2 b_n3 rat b_r1 b_r2 b_r3

define var3
    p0_x = depth
    p0_y = 0
    p0_z = inter_depth

    p1_x = inter_width
    p1_y = 0
    p1_z = p0_z

    p2_x = p0_x
    p2_y = thickness
    p2_z = p0_z

    p3_x = depth
    p3_y = 0
    p3_z = - depth
```

```
    lb_n1 = l_n1
    lb_n2 = n2
    lb_n3 = b_n3
    lb_r1 = l_r1
    lb_r2 = l
    lb_r3 = b_r3
end
var3
gen zon brick p0 p0_x p0_y p0_z p1 p1_x p1_y p1_z p2 p2_x p2_y p2_z &
       p3 p3_x p3_y p3_z &
       size lb_n1 lb_n2 lb_n3 rat lb_r1 lb_r2 lb_r3

;material (soil) property calculation and setup
;*****************************************
def property_cal
s_mod = e / (2.0*(1.0+p_ratio))
b_mod = e / (3.0*(1.0-2.0*p_ratio))
end
property_cal
model mohr
prop b b_mod sh s_mod coh 8e4 fric fric_ang dil dil_ang

;initial stress calcualtion FISH
;*************************************
def gravity_cal
szz_number = depth * den_num * grav_num
sxx_number = szz_number * k
syy_number = sxx_number
z_grad = - den_num * grav_num
x_grad = - den_num * grav_num * k
y_grad = x_grad
end
gravity_cal
;setup initial stress condition
;*************************************
ini density den_num
set gravity 0 0 grav_num
ini szz szz_number grad 0 0 z_grad
ini sxx sxx_number grad 0 0 x_grad
ini syy syy_number grad 0 0 y_grad

;boundary condition calculation
;*****************************************
def boundary_cal
x_right_low = width - 0.1
x_right_high = width + 0.1
z_low = rock_depth - 0.1
z_high = rock_depth +0.1
y_b_low = thickness - 0.1
y_b_high = thickness + 0.1
z_top_high = depth + 0.1
z_top_low_h = depth - 0.0001
z_top_low_l = depth - 1
end
boundary_cal

set log on
set logfile ..\log\001.log
print gp p range z z_top_low_h z_top_high y -.1 .1
set log off

;setup boundary condtion
;*************************************
apply xvel 0 range x -.1 .1
fix x range x x_right_low x_right_high
fix z range z z_low z_high
apply yvel 0 range y -.1 .1
apply yvel 0 range y y_b_low y_b_high

set mechanical force 50
solve
```

```
plot cont zdisp

;setup excavation tunnel and excavate
;*****************************************
group tunnel range cyl end1 0 0 0 end2 0 thickness 0 rad tunnel_r
del range group tunnel
set large
ini zdisp = 0 xdisp = 0 ydisp = 0

;define the monitor FISH function
;*****************************************
define xxx
p_gp = gp_head
loop while p_gp # null
   x = gp_xpos(p_gp)
   z = gp_zpos(p_gp)
   z_vel= gp_zvel(p_gp)

   gap = tunnel_r - pipe_r
   p = x * x + (z + gap) * ( z + gap)
   id_number = gp_id(p_gp)

   r = pipe_r * pipe_r
   if z_vel # 0
      if p < r
        command
        apply xvel 0 range id id_number id_number
        apply yvel 0 range id id_number id_number
  apply zvel 0 range id id_number id_number
        endcommand
      endif
   endif
   p_gp = gp_next(p_gp)
endloop
end

;run the program
;*********************************************
hist unbal

define run_able
 loop n (1,150)
  command
   step 1
   xxx
  endcommand
  endloop
end
run_able

set fishcall 1 xxx
solve
save ..\result\001.sav
set pagelength 200
set log on
print gp disp range z z_top_low_l z_top_high y -.1 .1
quit
```